**GUILHERME NUNES LUCENA**

# Enzyme modified magnetic nanoparticles: an approach for biomass conversion processes

Thesis presented to Institute of Chemistry, São Paulo State University, in partial fulfillment of the requirements for the degree of Doctor in Chemistry

Supervisor: Prof. Dr. Rodrigo Fernando Costa Marques

Araraquara
2020

**CATALOGUING DATA**

Lucena, Guilherme Nunes
L935e Enzyme modified magnetic nanoparticles: an approach for biomass conversion processes / Guilherme Nunes Lucena. – Araraquara: [s.n.], 2020
116 p.: il.

Thesis (doctor) – Universidade Estadual Paulista, Instituto de Química
Advisor: Rodrigo Fernando Costa Marques

1. Nanoparticles. 2. Enzymes. 3. Immobilized enzymes. 4. Cellulase. 5. Biomass. I. Title.

Bibliotecária Responsável: Ana Carolina Gonçalves Bet – CRB8/8315

**GUILHERME NUNES LUCENA**

# Nanopartículas magnéticas modificadas com enzimas: uma abordagem para processos de conversão de biomassa

Tese apresentada ao Instituto de Química, Universidade Estadual Paulista, como parte dos requisitos para obtenção do título de Doutor em Química

Orientador: Prof. Dr. Rodrigo Fernando Costa Marques

Araraquara
2020

UNIVERSIDADE ESTADUAL PAULISTA

**Câmpus de Araraquara**

## CERTIFICADO DE APROVAÇÃO

TÍTULO DA TESE: "Enzyme modified magnetic nanoparticles: an approach for biomass conversion processes"

**AUTOR: GUILHERME NUNES LUCENA**
**ORIENTADOR: RODRIGO FERNANDO COSTA MARQUES**

Aprovado como parte das exigências para obtenção do Título de Doutor em QUÍMICA, pela Comissão Examinadora:

Prof. Dr. RODRIGO FERNANDO COSTA MARQUES
Departamento de Físico-Química / Instituto de Química - UNESP - Araraquara

Prof. Dr. ARNALDO SARTI
Departamento de Bioquímica e Tecnologia Química / Instituto de Química - UNESP - Araraquara

Prof. Dr. JONAS CONTIERO
Departamento de Bioquimica e Microbiologia / Instituto de Biociências - UNESP - Rio Claro

Prof.ª Dr.ª LARISSA DE FREITAS
Departamento de Engenharia Química / Escola de Engenharia de Lorena - USP - Lorena

Prof. Dr. RAFAEL FIRMANI PERNA
Instituto de Ciência e Tecnologia / UNIFAL / Poços de Caldas

Araraquara, 20 de março de 2020

# CURRICULUM VITAE

## IDENTIFICATION

Full name: Guilherme Nunes Lucena

Name in scientific citations: Lucena, G. N.

## PROFESSIONAL ADDRESS

Institute for Research in Bioenergy, Institute of Chemistry, São Paulo State University "Júlio de Mesquita Filho" – UNESP. Rua Prof. Francisco Degni, 55, Bairro Quitandinha, ZIP: 14.800-060, Araraquara, SP, Brazil.

## ACADEMIC EDUCATION

**Bachelor's degree in Environmental Chemistry (2010-2014)**

Federal University of Tocantins, Gurupi, TO, Brazil

**Graduation in Chemistry (2018-2019)**

University of Franca, Franca, SP, Brazil

**Master's degree in Chemistry (2014-2016)**

Institute of Chemistry, São Paulo State University, Araraquara, SP, Brazil

**Doctor's degree in Chemistry (2016-2020)**

Institute of Chemistry, São Paulo State University, Araraquara, SP, Brazil

## PUBLICATIONS IN SCIENTIFIC JOURNALS

Farias, A. J. G. et al. Potential of limestone tailings for correction and fertilization of an Oxisol in the Brazilian savanna. **Commun. Soil Sci. Plant Anal.**, 2020. DOI: 10.1080/00103624.2020.1744629.

Guedes, W. N. et al. Easy estimation of endoglucanase activity using a free software app for mobile devices. **Br. J. Anal. Chem.**, 7, 2020.

Lucena, G. N. et al. Magnetic cross-linked enzyme aggregates (MCLEAs) applied to biomass conversion. **J. Solid. State Chem.**, 270, 58-70, 2019.

Frem, R. C. G. et al. MOFs (Metal-Organic Frameworks): uma fascinante classe de materiais inorgânicos porosos. **Quim. Nova**, 41, 1178-1191, 2018.

Lucena, G. N. et al. Zn-based porous coordination solid as diclofenac sodium carrier. **J. Solid. State Chem.**, 260, 67-72, 2018.

Silva, R. R. et al. Spectroscopic and elementary characterization of humic substances in organic substrates. **Comum. Sci.**, 9, 264-274, 2018.

Silva, R. R. et al. Over-liming in the chemical attributes in a Red Latosol of texture medium. **Tecnol. & Cien. Agropec.**, 12, 53-58, 2018.

Silva, M. E. C. et al. Synthesis of whey peptide-iron complexes: Influence of using different iron precursor compounds. **Food Res. Int.**, 101, 73-81, 2017.

## BOOK CHAPTERS

Silva, R. R. Rejeitos da mineração de calcário na melhoria dos atributos químicos do solo e nas características agronômicas do capim Mombaça. In: Silva & Freitas, Eds. Capim Mombaça: correção da acidez, gessagem, adubação, bioestimulante, morfofisiologia, qualidade e manejo da pastagem. 1ª ed. Editora UFT, 2018. ISBN: 978-8560487530.

Frem, R. C. G. et al. Design and applications of metal-organic frameworks. In: Longo & La Porta, Eds. Recent advances in complex functional materials: from design to application. 1ª ed. Springer. p. 339-369. 2017. ISBN: 978-3319538976.

## PROFESSIONAL ACTUATION

Teacher: Fundamentals of laboratory practice and fundaments of chemical processes
Course: Chemical Technician
School: Education and technology center, SENAI, Palmas, TO, Brazil
Date: 02/2020 – present

Professor: Experimental physical chemistry
Course: Chemical Engineering
University: Institute of Chemistry, São Paulo State University, Araraquara, SP, Brazil
Date: 02/2019 – 07/2019

Dedico este trabalho à minha família, pais e irmãos, grandes incentivadores e razão de tudo isso.

## AGRADECIMENTOS

Aos meus pais, Leopoldino e Maria, e irmãos, Ananda e Danillo, por todo apoio, carinho e paciência, pois sem eles nada disso teria acontecido.

Àquelas que sempre foram mais que amigas, Brenda, Camila e Mayra, por todo o companheirismo e amizade durante essa jornada que teve início em 2010. Ao lado de vocês me tornei um ser humano melhor. De coração, obrigado por tudo.

Ao Professor Rodrigo, orientador deste trabalho, por todos os ensinamentos, amizade, confiança e pelo auxílio no meu crescimento como pessoa e pesquisador. Comigo, cinco anos de futebol e quatro gols (porque deixei).

À Professora Ariela Veloso de Paula, sempre atenciosa, prestativa e na prática a coorientadora desta tese, por sua atenção, carinho, confiança, amizade e colaboração científica. Me deve um vinho chileno.

Aos amigos do laboratório do IPBEN, Amanda, Bruna e Professor Arnaldo Sarti, por toda amizade, parceria e gratificantes conversas durante os inúmeros cafés desse doutorado. Vou sentir saudade desse trio de palmeirenses sem mundial.

Aos amigos do laboratório de Materiais Magnéticos e Coloides, Caio, Carol, Chico, Gabriel, Luísa e Pelé, pela ajuda na condução desse trabalho e por proporcionarem um excelente ambiente de trabalho. Obrigado, bebemos bem.

À Renata, Crica, pela amizade sincera, parceria e boas conversas. Depois que deixei de trabalhar com você meus resultados nunca mais foram os mesmos.

Aos amigos do futebol (IQ e Ascar) por toda resenha, parceria, cerveja, churrasco e inúmeros gols perdidos. Eu sei, na minha frente o gol fica realmente pequeno.

Ao Instituto de Química e sua equipe de colaboradores (professores, técnicos, biblioteca, manutenção, limpeza e terceirizados) por todo suporte e solicitude.

Ao Sci-Hub e sua criadora, Alexandra Elbakyan, por removerem as barreiras no caminho da ciência.

Por fim, ao FINEP, pelo apoio financeiro (processo 01.14.0151.00) e CNPq, pela bolsa concedida (processo 142288/2016-0). Passou da hora de um aumento.

To infinity and beyond!

*Buzz Lightyear*


Olha, a química não é ciência. É religião...
Religião?
Claro. Veja as coisas. Você tem 2 moléculas e de repente eles viram uma só! É milagre, não dá pra explicar. Ou você acredita nisso ou não...
Esse livro todo está cheio de coisas que dependem de fé!
E agora, Calvin?
Descobri que sou ateu em Química

**ABSTRACT**

Lignocellulosic biomass has highlighted as an essential renewable raw material for production of many value-added chemicals of industrial interest in field as energy production, food, pharmaceutical, agriculture, environment and so on. Despite it, many applications have wrought with a series of difficulties in regarding enzymatic conversion processes, as enzyme operational instability, high production and purification cost, inhibition reactions, and issues of recovery and recycle. To overcome these issues, many enzyme immobilization methods have emerged, among which highlights the obtention of magnetic-cross linked enzyme aggregates (MCLEAs). This materials class is obtained from cross-linking reaction between enzyme physical aggregates and magnetic supports, which can gather the important catalytic properties of the physical aggregates (as a result of enzyme native structure maintenance) to recovery and recycle capacity of magnetic nanoparticles (as result of its intrinsic magnetic properties). Faced it, this work reports the synthesis, characterization and potential application of different cellulases MCLEAs in the cellulose enzymatic conversion process. Sectioned in three chapters, firstly is presented a review about the state of art in concern to obtention of value-added chemicals from lignocellulosic biomass using MCLEAs. In the second chapter, different MCLEAs were prepared in the presence of quitosana-coated magnetic nanoparticles with three different precipitation agents (ammonium sulfate, ethanol and polyethylene glycol). Highlighted the obtention of a MCLEA using ethanol as precipitant agent, which showed highest enzymatic activity (193.42 U $g^{-1}$) and activity recovery (43.53 %), and other MCLEA, obtained by use of polyethylene glycol as precipitation agent, with the highest reusability capacity (80% of initial relative activity after five cycles of reaction). In addition, for the first time, the colloidal properties of MCLEAs and free cellulases were characterized by dynamic light scattering (DLS) and zeta potential analyses, which were correlated with the activity of MCLEAs and free cellulases. As result, was demonstrated that increasing in colloidal stability with changes in temperature has improved the thermal stability of the MCLEAs. The hydrolysis of cellulose-derived from sugarcane bagasse and straw using MCLEAs showed a higher capacity of obtention of cello-oligosaccharides with value-added than the free cellulases. Lastly, final chapter engaged to further investigate the effects of an alternating magnetic field (AMF) in the activity of a MCLEA based on aminosilane-coated magnetic nanoparticles. For this purpose, it was used a factorial design (2x2) with two variables at two levels, frequency (203-420 kHz) and amplitude (3-6 kA $m^{-1}$). Independently of condition, AMF application decrease MCLEA activity when compared to field free condition. In addition, frequency variable implied in more significant effects in the MCLEA activity when compared to AMF amplitude and suggest that

further studies should carried out in conditions of lower AMF frequency. However, although this last result has not been expected, it can help to fill the gap of further study in this growing and essential approach that is the use of magnetic support for enzyme immobilization.

## RESUMO

A biomassa lignocelulósica vem se destacando como uma matéria-prima essencial para a produção de muitos produtos químicos de interesse industrial em áreas como a produção de energia, alimentos, fármacos, agricultura, meio ambiente e assim por diante. Apesar disso, muitas aplicações vêm esbarrando em uma série de dificuldades encontradas nos processos de conversão enzimática, como instabilidade operação das enzimas, alto custo de produção e purificação, reações de inibição e problemas de recuperação e reciclo. Para contornar esses problemas, muitos métodos de imobilização enzimática têm surgido, entre os quais, destaca-se a obtenção de agregados enzimáticos reticulados magnéticos (MCLEAs). Esta classe de materiais é obtida a partir da reação de reticulação entre agregados físicos de enzimas e suportes magnéticos, o qual pode unir as importantes propriedades catalíticas dos agregados físicos (como resultado da manutenção da estrutura nativa da enzima) à capacidade de recuperação e reciclo do suporte magnético (devido suas propriedades magnéticas intrínsecas). Frente a isso, esse trabalho relata a síntese, caracterização e potencial aplicação de MCLEAs de enzimas celulases em processos de conversão de celulose. Dividido em três capítulos, primeiramente é apresentado um review sobre o estado da arte no que diz respeito a obtenção de produtos de valor agregado a partir da biomassa lignocelulósica utilizando MCLEAs. No segundo capítulo, diferentes MCLEAs foram preparados na presença de nanopartículas magnéticas modificadas com quitosana, utilizando três agentes precipitantes diferentes (sulfato de amônio, etanol e polietileno glicol-PEG). Destacou-se a obtenção de um MCLEA utilizando etanol como agente de precipitação, o qual apresentou a maior atividade enzimática (193,42 U $g^{-1}$) e atividade recuperada (43,53 %); e outro MCLEA obtido com polietileno glicol, com a maior capacidade de reciclo (80 % da atividade inicial após cinco ciclos de reação). Adicionalmente, pela primeira vez, as propriedades coloidais dos MCLEAs e celulases livres foram caracterizadas por medidas de espalhamento dinâmico de luz (DLS) e potencial zeta, as quais foram correlacionadas com suas respectivas atividades enzimáticas. Foi demonstrado que o aumento na estabilidade coloidal frente às mudanças de temperatura incrementaram a estabilidade térmica dos MCLEAs. Quando aplicados na hidrólise de celulose obtida a partir de uma mistura de bagaço e palha de cana-de-açúcar, os MCLEAs mostraram a uma maior capacidade de obtenção de celooligosacarídeos de valor agregado do que as celulases livres. Por fim, o último capítulo focou na investigação mais profunda dos efeitos da aplicação de um campo magnético alternado (AMF) na atividade de um MCLEA contendo nanopartículas magnéticas modificadas com aminosilano. Para isto, foi utilizado um planejamento fatorial (2x2) com duas variáveis em dois níveis, frequência (203-420 kHz) e amplitude (3-6 kA $m^{-1}$). Independentemente da condição, a

aplicação do AMF diminuiu a atividade enzimática do MCLEA em comparação à condição sem campo. Adicionalmente, a frequência do AMF mostrou efeitos mais significante na atividade do MCLEA quando comparada à amplitude e sugere-se que estudos posteriores devam ser realizados em condições de frequências mais baixas. No entanto, embora este último resultado não tenha sido o esperado, ele pode ajudar a preencher a lacuna de estudos mais aprofundados desta crescente e essencial abordagem que é o uso de nanopartículas magnéticas como suporte para enzimas.

# RESUMO EXPANDIDO EM PORTUGUÊS

## INTRODUÇÃO

Celulases são um complexo enzimático constituído pelas enzimas endoglucanase, exoglucanase e β-glicosidase. Estas três enzimas agem sinergicamente para produzir glicose a partir da celulose, o polímero carboidrato de baixo custo mais abundante na natureza. As enzimas endoglucanases hidrolisam as ligações β-1,4-glicosídicas na região amorfa da fibra de celulose, produzindo oligômeros de cadeia longa, enquanto as exoglucanases agem nas extremidades da fibra de celulose, produzindo celooligosacarídeos (COS). Posteriormente, os COS são hidrolisados à glicose por ação da enzima β-glicosidase. A hidrólise enzimática da celulose vem sendo extensivamente estudada para a produção de etanol de segunda geração e outros produtos de maior valor agregado. No entanto, embora as enzimas sejam biocatalizadores sustentáveis reconhecidos por sua alta especificidade, eficiência e baixa geração de resíduos, sendo empregadas em uma variedade de processo de interesse industrial, elas apresentam algumas limitações como instabilidade estrutural frente à variações de condições operacionais como pH e temperatura, alto custo de produção e purificação, reações de inibição, dificuldade de recuperação e reciclo, desvantagens estas que acabam onerando o custo de muitos processos. Visando a redução desse custo, o aumento da estabilidade, recuperação e o reciclo das enzimas cellulases, por meio de diversos métodos de imobilização, vem surgindo como uma importante estratégia.

Frente a isso, a obtenção de agregados enzimáticos reticulados (CLEA, *cross-linked enzyme aggregates*) é uma tecnologia robusta, pois a sua capacidade de manutenção da superestrutura organizada na formação dos CLEAs leva a uma boa estabilidade mecânica e à alta atividade enzimática. Os CLEAs consistem em agregados físicos de moléculas de enzimas obtidas pelo uso de agentes precipitantes (por exemplo, solventes, sais ou polímeros), os quais mantêm a estrutura terciária nativa da enzima, interligados entre si, através de agentes reticulantes como o glutaraldeído. Quando a precipitação é realizada na superfície de um suporte sólido, os CLEAs podem ser ligados covalentemente a ele, por exemplo, pelo próprio agente de reticulação, permitindo, desta forma, aliar as vantagens dos CLEAs às propriedades

intrínsecas do suporte, estratégia que pode levar a obtenção de biocatalisadores únicos. Entre os muitos suportes possíveis, as nanopartículas magnéticas (MNP, *magnetic nanoparticles*), tais como a magnetita ($Fe_3O_4$), vem ganhando destaque devido a sua alta área de superfície e capacidade de adsorção, baixa toxicidade, fácil modificação de superfície e, principalmente, suas propriedades magnéticas, as quais a permite ser recuperada a partir do meio reacional pela simples aplicação de campo magnético externo. Neste contexto, muitos trabalhos vêm relatando o uso de MNP como suporte para imobilização de CLEAs de diferentes enzimas. Em resumo, esses CLEAs magnéticos (MCLEAs) vêm apresentando incrementos na estabilidade frente às variações no pH e temperatura, decréscimos em reações inibitórias, alta atividade e, principalmente, uma excepcional capacidade de recuperação e reciclo, fazendo deles uma estratégia essencial na melhoria de muitos processos enzimáticos.

Desta forma, é nesse conjunto de ideias centrais que estão baseados os dois primeiros capítulos da presente tese de doutorado. O primeiro capítulo, intitulado "*Magnetic cross-linked enzyme aggregates (MCLEAs) applied to biomass conversion*", consiste em artigo de revisão já publicado na Journal of Solid State Chemistry (doi: 10.1016/j.jssc.2018.11.003) que trata especificamente da aplicação de MCLEAs nos mais variados processos de conversão de biomassa lignocelulósica, além de aspectos como metodologias de síntese e caracterização dessa importante classe de materiais. O segundo capítulo, intitulado "*Synthesis and characterization of magnetic cross-linked enzyme aggregates of cellulases for the potential application in producing cello-oligosaccharides*" relata a síntese e caracterização de três MCLEAs sintetizados pelo autor utilizado diferentes agentes de precipitação (etanol, sulfato de amônio e polietilenoglicol), além de sua potencial aplicação para produção de celooligosacarídeos, uma classe de compostos com importantes propriedades prebióticas de interesse da indústria farmacêutica e alimentícia. Além disso, no segundo capítulo é apresentado um estudo ainda não relatado na literatura sobre como as propriedades coloidais dos MCLEAs e de enzimas celulases não imobilizadas atuam na estabilidade de ambos frente às variações de pH e temperatura do meio reacional.

Por fim, embora muitos resultados positivos venham sendo observados na aplicação de MCLEAs em processos de conversão de biomassa lignocelulósica, avanços ainda são necessários, principalmente no que diz respeito ao melhor aproveitamento de suas propriedades

magnéticas. E este é o foco do terceiro capítulo, intitulado "*Synthesis, characterization and evaluation of the alternating magnetic field effects in the catalytic activity of a magnetic cross-linked enzyme aggregate*". As propriedades magnéticas das MNP não estão restritas à recuperação e reciclo magnético. Na presença de um campo magnético alternado (AMF, *alternating magnetic field*), como resultado das relaxações de Néel e Brown, as MNP rotacionam e colidem entrem si produzindo calor, um fenômeno chamado hipertermia magnética. O campo magnético alternado pode alterar a cinética enzimática aumentando o número de colisões entre o MCLEA e o substrato, mudar o estado de agregação do MCLEA e disparar mudanças conformacionais na estrutura da enzima, processos estes que podem levar a melhorias na atividade enzimática do MCLEA. Frente a isto, o terceiro capítulo foca na avaliação dos efeitos de campo magnético alternado, sob diferentes condições de frequência e amplitude, na atividade enzimática de um MCLEA. Neste estudo foi observado que incrementos na frequência e na intensidade do campo levaram à diminuição da atividade enzimática do MCLEA. Além disso, a frequência apresentou efeitos estatisticamente mais significativos na atividade catalítica do MCLEA quando comparada à amplitude do campo.

A seguir são apresentados alguns pontos e resultados importantes dos capítulos 1, 2 e 3.

## RESUMO DO CAPÍTULO 1

O incremento na atual demanda energética e por matérias-primas sustentáveis têm requerido o desenvolvimento de novas tecnologias e uso de fontes renováveis. Certamente, o progresso rumo a um desenvolvimento mais sustentável passará pelo de matérias-primas renováveis e versáteis, como a biomassa lignocelulósica, em termos de aplicações em energia, ciência dos materiais, meio ambiente e indústria farmacêutica e alimentícia. Como mostrado na Figura 1, a ideia no uso da biomassa lignocelulósica como matéria-prima renovável consiste em sua conversão em açúcares $C_6$ e $C_5$, as quais podem, posteriormente em diversos produtos químicos de maior valor agregado por diferentes rotas químicas, biológicas e, principalmente, enzimáticas. Embora a natureza recalcitrante e o alto custo dos processos enzimáticos, a obtenção de agregados enzimáticos reticulados magnéticos (MCLEA, da sigla em inglês), vem surgindo como uma tecnologia verde e sustentável para superar tais problemas. Essa classe de

nanomateriais híbridos pode melhorar significativamente a estabilidade enzimática, eficiência e recuperação, diminuindo os custos dos processos de conversão da biomassa lignocelulósica. Frente a isto, o capítulo resume o potencial e os recentes avanços no uso de MCLEAs aplicados em processos de conversão da biomassa lignocelulósica à diversos produtos de maior valor agregado e de interesse industrial.

**Figura 1:** Processos de conversão da biomassa lignocelulósica a produtos de interesse industrial.

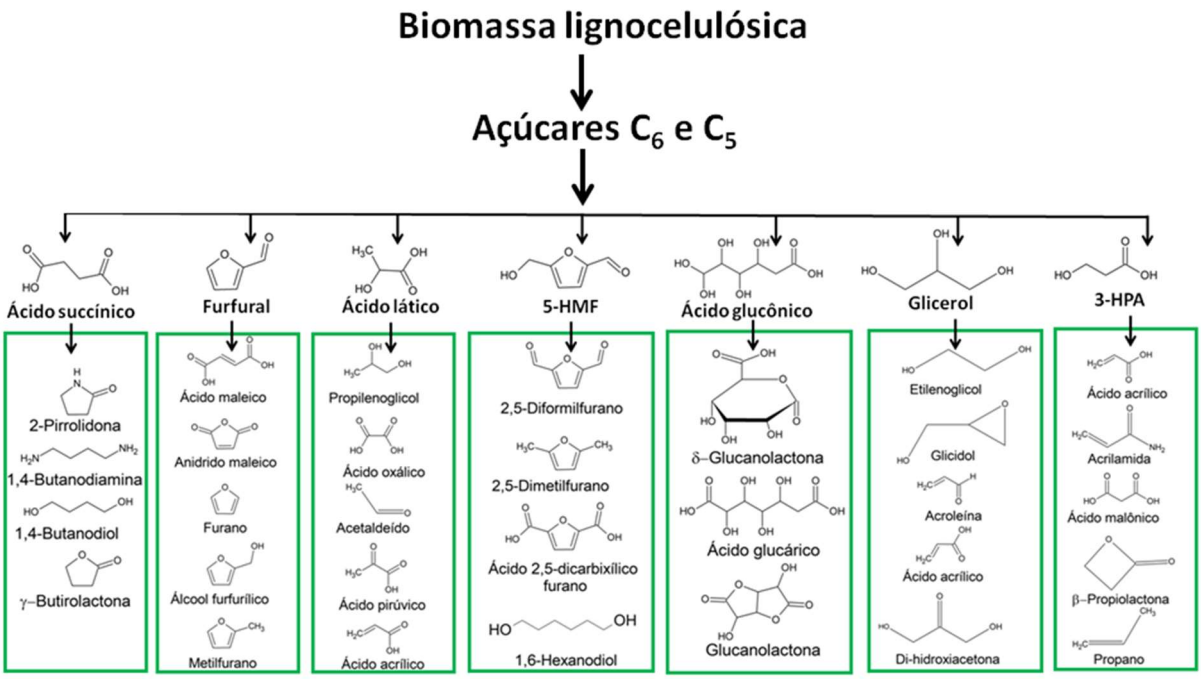


## RESUMO DO CAPÍTULO 2

Foram sintetizados MCLEAs utilizando diferentes agentes de precipitação, sendo eles: etanol (MCLEA-ET), sulfato de amônio (MCLEA-AS) e polietilenoglicol (MCLEA-PEG). Esses MCLEAs foram obtidos pela precipitação das celulases na superfície de nanopartículas magnéticas modificadas com quitosana e utilizando glutaraldeído como agente de reticulação.

A Figura 2 apresenta o efeito da temperatura na atividade enzimática das celulases livres e dos MCLEAs obtidos. Variações na temperatura influenciaram significativamente a atividade enzimática das celulases livres, sendo observadas diminuições na atividade na ordem de 50%

em torno da temperatura ótima de 50 °C. No entanto, a temperatura mostrou efeitos menos significativos na atividade catalítica dos MCLEAs, indicando que o método de imobilização proposto foi efetivo no aumento da estabilidade térmica das celulases.

**Figura 2:** Efeito da temperatura na atividade enzimáticas das celulases livres e de seus respectivos MCLEAs obtidos utilizando como agentes precipitantes etanol (MCLEA-ET), sulfato de amônio (MCLEA-AS) e polietilenoglicol (MCLEA-PEG).

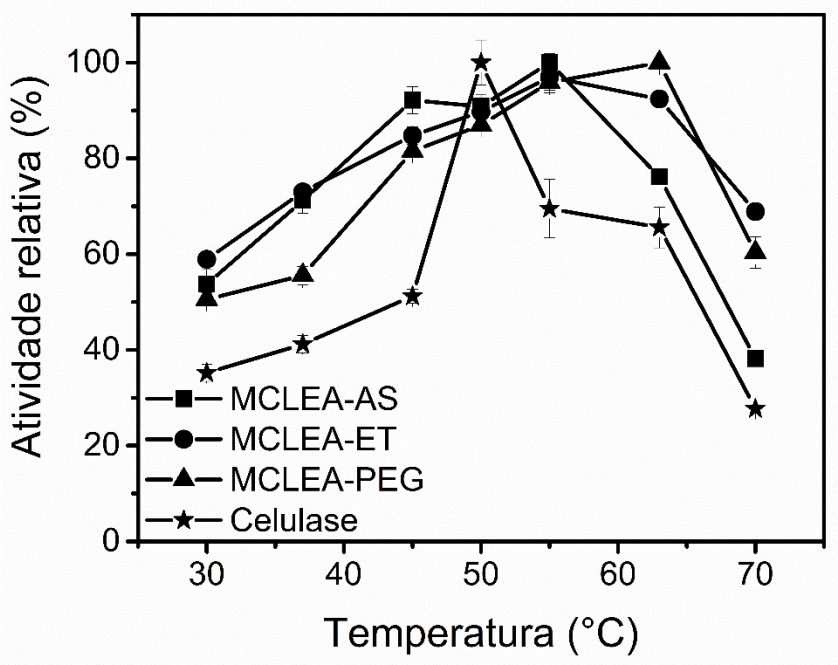


Para melhor entendimento do comportamento térmico das celulases e de seus respectivos MCLEAs, medidas de espalhamento dinâmico de luz (DLS, *dynamic light scattering*) foram realizadas para investigar o comportamento coloidal (estado de agregação) das amostras frente às variações de temperatura. A Figura 3 apresenta os resultados do perfil de distribuição de tamanho de partículas (PSD*, particle-size distribution*) dos MCLEAs e das celulases frente às variações de temperatura obtidos por DLS. Na condição de temperatura ótima (50 °C) e abaixo dela, as celulases mostram-se agregadas em aglomerados da ordem de 7 e 54 nm. Para a celulase livre, incrementos na temperatura a partir de seu valor ótimo alterou seu PSD de forma significativa, sendo observada a formação de agregados enzimáticos da ordem de 100 e 500 nm. Esta mudança no perfil PSD sugere que o mecanismo de desnaturação

das celulases por efeito da temperatura pode ser atrelado à agregação da estrutura proteica, o qual pode estar causando mudanças na estrutura nativa da enzima, como por exemplo, bloqueio do sítio ativo. Em relação aos MCLEAs, independente do agente precipitante utilizado, não foram observadas mudanças em estado de agregação após variações na temperatura. Isto indica uma manutenção de sua estrutura reticulada mesmo em temperaturas muito acima da condição ótima, sugerindo que a alta estabilidade coloidal observada pode ser a responsável por sua estabilidade térmica.

**Figura 3:** Efeito da temperatura no perfil de distribuição de tamanho de partículas das celulases livres e de seus respectivos MCLEAs obtidos utilizando diferentes agentes precipitantes.

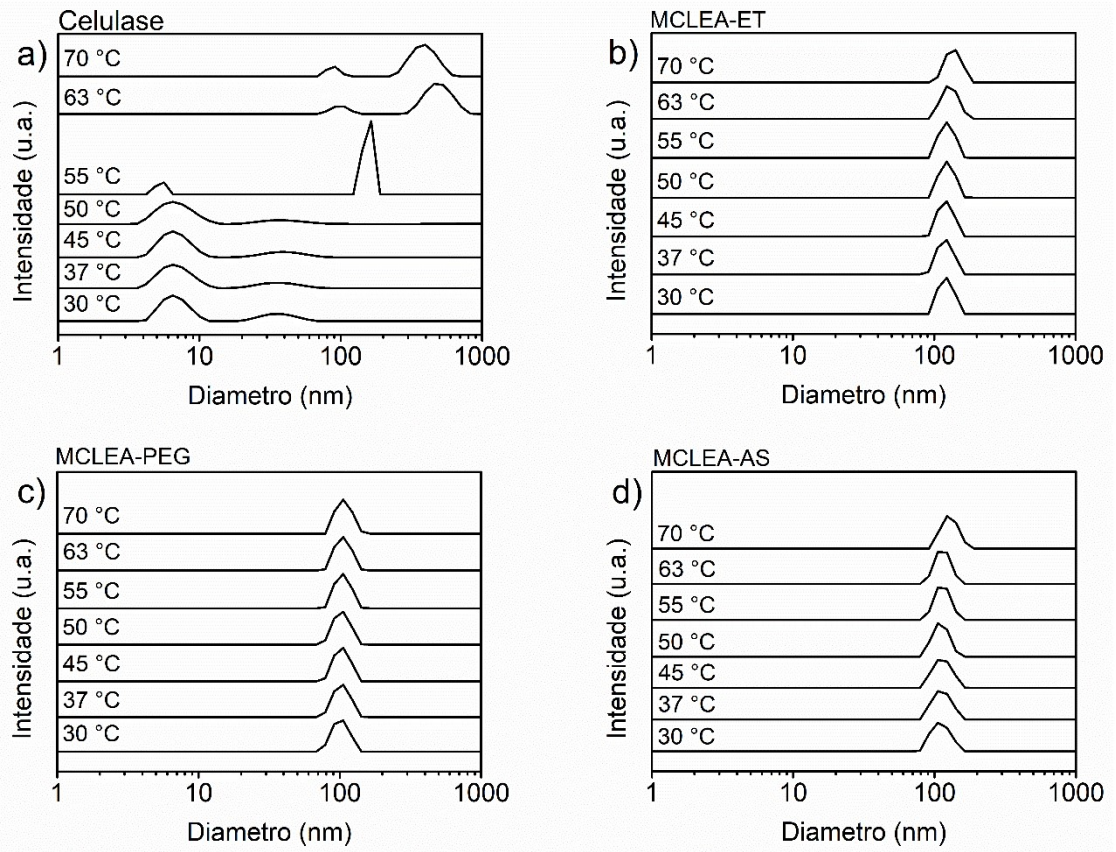


Posteriormente, foi avaliada a capacidade de reciclo dos MCLEAs utilizando um campo magnético, após sucessivos ciclos de hidrólise do substrato carboximetilcelulose. Como

observado na Figura 4, os MCLEAs mostram excelente capacidade de reciclo, destacando-se o MCLEA-PEG, o qual manteve aproximadamente 80% de atividade inicial após 5 ciclos reacionais.

**Figura 4:** Atividade enzimática dos MCLEAs após sucessivas reações de hidrólise de carboximetilcelulose.

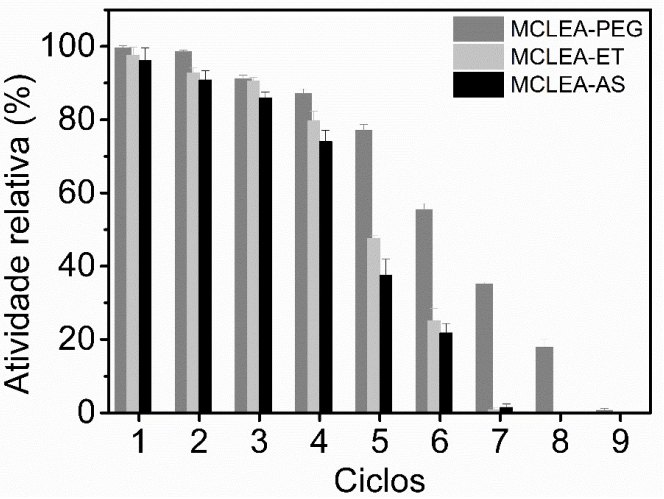


Por fim, os MCLEAs e as celulases livres foram testados na hidrólise de celulose proveniente de uma mistura de bagaço e palha de cana-de-açúcar. Por cromatografia de exclusão de tamanho (ou permeação em gel) os celooligosacarídeos (COS) presentes nos hidrolisados foram caracterizados em termos de massa molar (Mn e Mw), índice de polidispersão (PDI, *polydispersity index*) e grau de polimerização (DP, *degree of polymerization*) baseado na massa molar da glicose (180,15 g $mol^{-1}$), sendo estes resultados apresentados na Tabela 1. Observou-se que, em sua forma livre, as celulases produziram COS com DP iguais a 3 e 6. Por outro lado, além desses, os MCLEAs produziram COS com valores mais elevados de DP (12), resultado importante, uma vez que COS com DP mais elevados são produzidos com um custo operação de até 500 vezes maior que seus análogos de baixo peso molecular. Desta forma, os MCLEAs obtidos mostram-se como uma interessante ferramenta para produção sustentável de produtos de maior valor agregado a partir da biomassa lignocelulósica.

**Tabela 1:** Massa molar dos celooligosacarídeos obtidos na hidrólise da mistura de bagaço e palha de cana de açúcar realizadas pelos MCLEAs e celulases livres. Os picos dos cromatogramas foram analisados pelo software Omini SEC v. (5.1).

| Amostra | Mn (Da) | Mw (Da) | PDI (Mw/Mn) | DP |
|---|---|---|---|---|
| **Celulase** | 1061 | 1104 | 1,04 | 6 |
| | 584 | 609 | 1,04 | 3 |
| **MCLEA-ET** | 2244 | 2350 | 1,05 | 12 |
| | 1104 | 1136 | 1,03 | 6 |
| | 599 | 627 | 1,04 | 3 |
| **MCLEA-AS** | 2203 | 2312 | 1,05 | 12 |
| | 1081 | 1112 | 1,03 | 6 |
| | 597 | 623 | 1,04 | 3 |
| **MCLEA-PEG** | 2122 | 2217 | 1,04 | 12 |
| | 1029 | 1054 | 1,02 | 6 |
| | 568 | 592 | 1,04 | 3 |

## RESUMO DO CAPÍTULO 3

Neste capítulo foi obtido um MCLEA após a reticulação promovida por glutaraldeído entre as celulases e nanopartículas modificadas com aminosilano. Destacam-se os seguintes resultados.

Conforme mostrado na Figura 5, o MCLEA apresenta um incomum comportamento de maior atividade enzimática em temperaturas inferiores à condição ótima da enzima livre. Este resultado mostra-se promissor para abordagens modernas de produção de etanol de segunda geração por processos de hidrólise e fermentação simultâneos (SSF, *simultaneous saccharification and fermentation*) da celulose. Em processos SSF, a fermentação dos açúcares provenientes da hidrólise da celulose é feita de forma simultânea a própria hidrólise. Apesar de apresentar vantagens em relação aos processos tradicionais, como redução de custos operacionais e da inibição da celulase por seus produtos de hidrólise, o SSF apresenta obstáculos em sua implementação como o fato da fermentação feita pela levedura *Saccharomyces cerevisiae* ser realizada a baixas temperaturas (37 °C) e a hidrólise da celulose

a altas temperaturas (50 °C). Assim, a possibilidade de realizar a hidrólise da celulose a baixas temperaturas, como demonstrado pelo MCLEA, torna-se uma ferramenta importante na implementação de processos SSF.

**Figura 5:** Superfície de contorno da atividade enzimática do MCLEA em resposta às variações de pH e temperatura. Superfície obtida por planejamento fatorial composto central.

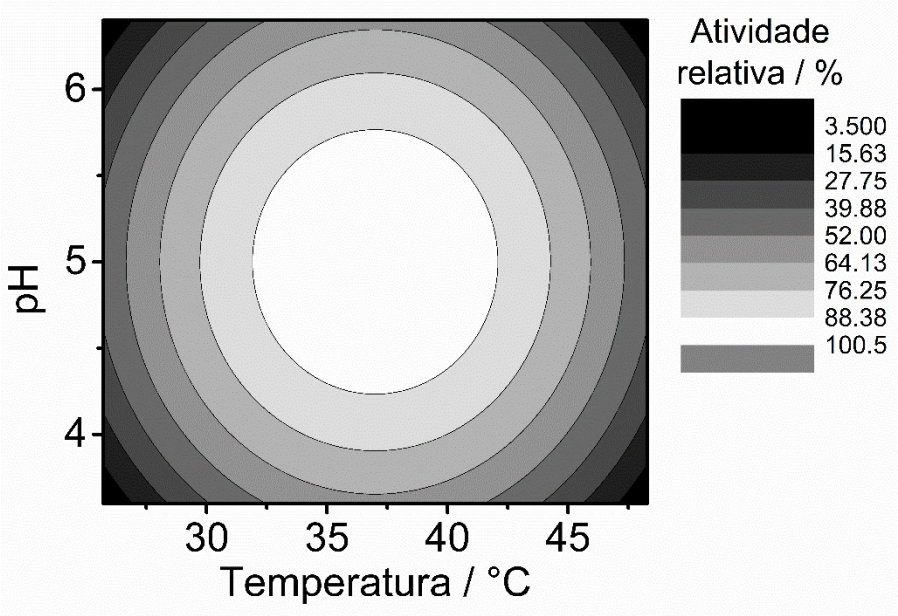


Os demais resultados são referentes a aplicação de um campo magnético externo nos MCLEAs durante a hidrolise de carboximetilcelulose. Um planejamento fatorial (2x2) com duas variáveis, frequência (f) e intensidade (B) de campo magnético, ambas em dois níveis, 203-420 kHz e 3-6 kA $m^{-1}$, respectivamente, foi empregado para melhor entender os efeitos do campo na atividade enzimática do MCLEA. Conforme mostrado na Figura 6, independente das condições avaliadas de intensidade e frequência, a aplicação de um campo magnético alternado levou à uma diminuição na atividade enzimática do MCLEA em relação a condição sem campo magnético (controle).

**Figura 6:** Efeitos aplicação de um campo magnético alternado na atividade enzimática do MCLEA.

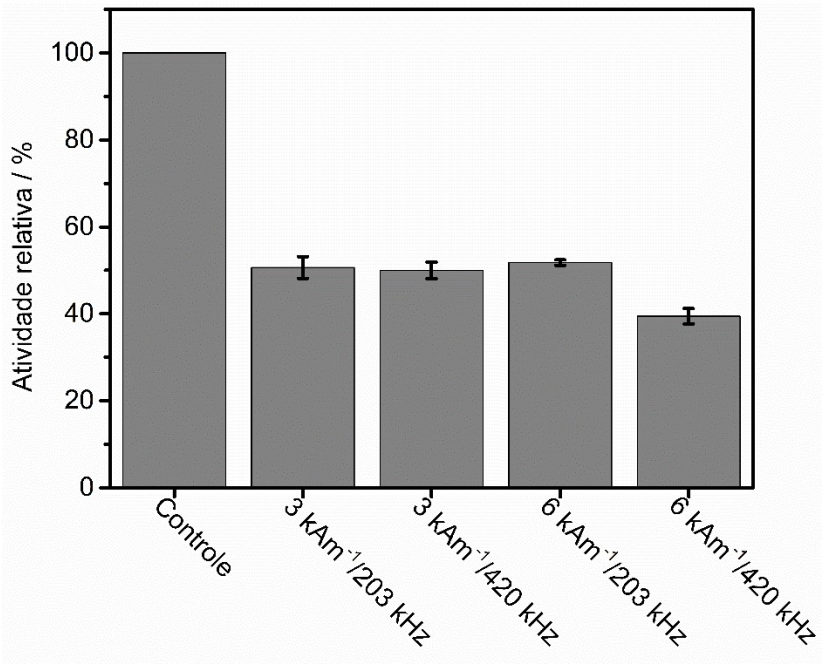


Adicionalmente, conforme mostrado na Figura 7, a frequência apresenta efeito mais significativo na atividade enzimática quando comparada aos efeitos do campo e da interação campo frequência (fb). Alguns resultados da literatura mostram incrementos na atividade enzimática de enzimas imobilizadas em suportes magnéticos, no entanto, utilizando campos magnéticos em condições de frequência bem inferiores as utilizadas neste trabalho (da ordem de 300 vezes menor). Em condições de alta frequência, o torque do movimento rotacional das nanopartículas magnéticas surge em decorrência de uma defasagem de fase entre o campo magnético aplicado e o momento magnético induzido, o que leva à uma magnetização não instantânea das nanopartículas, sugerindo que, em tais condições, a rotação das partículas depende de campo de intensidade mais elevadas. Frente a isso, é preferível que estudos posteriores sejam conduzidos em condições de frequências mais baixas.

**Figura 7:** Efeitos da frequência, intensidade e da interação entre as variáveis na atividade enzimática do MCLEA.

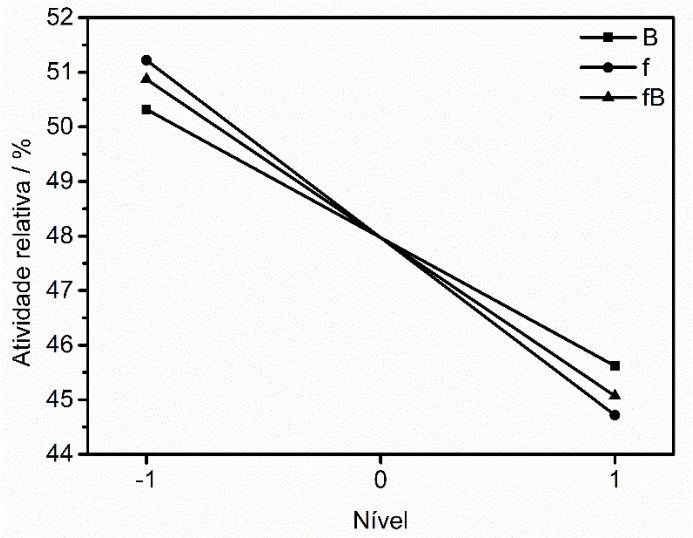


Embora um aumento da atividade enzimática do MCLEA sob um campo magnético alternado não tenha sido obtido, os dados apresentados podem ajudar a preencher a lacuna que consiste a falta de estudos mais efetivos no que diz respeito ao melhor aproveitamento das propriedades magnéticas dos suportes utilizados na imobilização de enzimas.

## TABLE SYMBOL

**APTS:** 3-aminopropyl-triethoxysilane

**B:** amplitude of the alternating magnetic field

**$C_5$:** sugar with 5 carbons

**$C_6$:** sugar with 6 carbons

**CCD:** central composite design

**CLEA:** cross-linked enzyme aggregates

**CMC:** carboxymethylcellulose

**COS:** cello-oligosaccharides

**DLS:** dynamic light scattering

**DNS:** 3,5-dinitrosalicilic acid

**DP:** degree of polymerization

**f:** frequency of the alternating magnetic field

**FT-IR:** Fourier transform infrared

**GPC:** gel permeation chromatography

**MCLEA:** magnetic cross-linked enzyme aggregates

**MCLEA-AS:** magnetic cross-linked enzyme aggregates obtained with ammonium sulfate

**MCLEA-ET:** magnetic cross-linked enzyme aggregates obtained with ethanol

**MCLEA-PEG:** magnetic cross-linked enzyme aggregates obtained with polietilenoglicol 600

**MNP:** magnetic nanoparticles

**NP-APTS:** 3-aminopropyl-triethoxysilane-modified magnetic nanoparticle

**NP-CH:** chitosan-modified magnetic nanoparticle

**PDI:** polydispersity index

**PEG:** polietilenoglicol 600

**PSD:** particle-size distribution

**PXRD:** powder X-ray diffraction

**SEM:** scanning electronic microscopy

**TGA:** thermogravimetric analyses

**ζ-potential:** zeta potential

# TABLE OF CONTENTS

# *Chapter 1*

## *Magnetic cross-linked enzyme aggregates (MCLEAs) applied to biomass conversion*

**ABSTRACT**

The increasing energy and demand for sustainable materials require the development of renewable production technologies to meet current global needs. Certainly, the progress for a sustainable development goes through the use of renewable and versatile raw materials, as the lignocellulosic biomass, in terms of application in energy, materials and environment sciences. The key role in the use of lignocellulosic biomass as renewable raw material has been its conversion to $C_6$ and $C_5$ sugars, which can be converted in different materials by several biological and chemical routes. Although its recalcitrance nature and high cost of the enzyme that promotes such conversions, obtaining a magnetic cross-linked enzyme aggregates (**MCLEAs**) has emerged as a green and sustainable technology to overcome these problems. This class of nanohybrids materials can significantly improve enzyme stability, activity and its recovery, decreasing the cost of process and adverse consequence of use of fossil raw materials. So, this review intends to show the potential and recently advances of **MCLEAs** applied to biomass conversion to value-added materials.

**Keywords:** magnetic nanoparticles, enzyme immobilization, sustainable development

This chapter was previously published as a review article in the Journal of Solid State Chemistry.
Available at https://doi.org/10.1016/j.jssc.2018.11.003
Reproduced with permission from Elsevier (see attached file 1).

## 1.1 Introduction: a look over biomass

The well-being of our society and of the next generations is unpredictable without the recent and futures advances in the fields of energy, environment and materials science. However, it requires a paradigm shift from traditional concepts of industrial process to development of new sustainable technologies that includes aspects as the use of renewable energy and materials, avoiding hazardous chemicals and reducing or eliminating wastes. This point of view is directly linked to green chemistry, basically defined as the prevention of pollution by efficient use of renewable resources of energy and materials, waste minimization and the avoidance of toxic and hazardous substances in the production and application of chemical products [1,2]. Thus, one of the main challenges of society is, therefore, make progress in discovery of new green and sustainable technologies which can be used to attend the sustainable development requirement based on green chemistry principles [3,4].

Certainly, to make any progress in the sustainable development it must goes through use of renewable raw materials and versatile in terms of application in energy, environment and materials science. Thus, the lignocellulosic, the most abundant and bio-renewable biomass on earth, emerge as a solution [5]. Biomass is basically a stored source of solar energy initially collected by plants during the photosynthesis process whereby carbon dioxide is captured and converted to plant materials mainly in the form of cellulose, hemicellulose and lignin. The biomass materials include principally crop residues, forest and wood process residues, animal wastes including human sewage and municipal solid waste food processing wastes, among others [6].

The biomass has a positive impact on Carbon Footprint and has been accepted as a new renewable source for global sustainable development. Basically, the use of biomass started with energy crises brooked out in 70 decade and, more recently, with a wave of interest in new energy sources because of high oil prices [7,8]. A study from European Observatory on Renewable Energy, in 2013 showed that 46% of renewable energy in the European Union comes from solid biomass, and it was accounted for 3% of electricity and 15% of the heat produced in industrial units [9]. According to U.S. Department of Energy [10], 10% of energy in the U.S. is derived from renewable energy sources. Biomass, a renewable and bio-degradable energy resource, provides 50% of renewable energy needs in the U.S. However, on global scale, biomass represents only 10% of the produced renewable energy [11,12]. Consequently, it seems that biomass plays a key role in the energy industry.

Besides that, the researches on energy generation has been growing on biomass applied in the production of cleaner energy, such as second generation ethanol [13-18], hydrogen [19-25] and biogas [26-30], as substitute of fossil fuels to decrease the greenhouse gas emissions. Beyond energy production, biomass can replace all fossil fuels used to produce materials and chemicals [31-36].

The key in the use of biomass as renewable raw material is the use of their derivatives $C_6$ and $C_5$ sugar (e.g., glucose and xylose), which can be converted in new materials by several biological and chemical routes [37]. However, to convert lignocellulosic biomass to value-added materials remains a challenge due to its degradation resistance, energy and cost of process. Firstly, it is necessary a delignification pretreatment to eliminate the lignin and expose the cellulose and hemicellulose to the attack of hydrolytic enzymes as cellulase and xylanase, respectively. Then, the cellulose and hemicellulose should be hydrolyzed to $C_6$ and $C_5$ sugars, respectively [38]. Lastly, $C_6$ and $C_5$ sugars can be converted to a range of chemicals and materials.

Others technical difficulties have been reported to biomass conversion. Among its, cellulase enzymes are strongly inhibited by hydrolysis product [39]; enzymes are easily denatured by changes in the pH and temperature [40]; and finally, beyond of the difficult recovery from reaction medium, to enhanced hydrolysis yield, a large amount of enzyme is consumed, what has become a bottleneck process from financial point of view [41,42]. So, extensive research is currently being undertaken all over the world to address these problems.

With the advance of nanotechnology, the use of nanohybrids materials as Cross-Linked Enzyme Aggregates (**CLEAs**), obtained by enzyme immobilization on supports, is a technological solution when it is desired to increase the enzymatic stability, efficiency and reusability by recovering from reaction medium [43-46]. Among the supports, magnetite nanoparticles ($Fe_3O_4$) has caught attention due to magnetic properties, which allow it selective recovering from reaction by applying an external magnetic field.

Therefore, allied to environment benefits of the use of biomass as renewable resource for chemicals, fuels and materials, these magnetic nanohybrids materials, called Magnetic Cross-Linked Enzyme Aggregates (**MCLEAs**), shows as a promising green and sustainable technology when it thought in the biomass conversion. So, this article reviews the recent advances and the challenges of the biomass and their derived conversion using the **MCLEAs** nanohybrids materials.

## 1.2 Biomass: structure, enzymatic conversion and products

### 1.2.1 Structure

The Fig. 1 shows the typical structure of lignocellulosic biomass. The content of biomass varies depending on the biomass type. Usually, lignin, hemicellulose and cellulose constitute 10-40%, 20-40% and 40-50% wt% of the plant material respectively, which has also a small amount of esters, alcohols, steroids, sulphates, oxalates, carbonates, silicates, among other, called extractives [47-48]. Cellulose is a polymer of glucose molecules in which individual glucose units are connected via 1-4 linked β-d-anhydroglucopyranose units. Hemicellulose is intrinsically linked to cellulose, having branched structure and built by a combination of $C_5$ or $C_6$ sugars, including several polysaccharides, in which xylans are the main constituent. Lignin is the highly branched polymer of the biomass. With a heterogenic nature and formed by phenyl propane units, lignin has been found to serve as the matrix support material along with hemicellulose to embed cellulose fibers [49-51]. These components are strongly intermeshed and bonded through covalent and non-covalent bonds forming the lignocellulosic complex. This typical structure is responsible by the strong native recalcitrance to enzymes and relatively low digestibility of raw biomass materials [52].

**Fig. 1.** Typical structure of lignocellulosic biomass. Reprinted with permission from ref [53]. Copyright 2018, Elsevier.

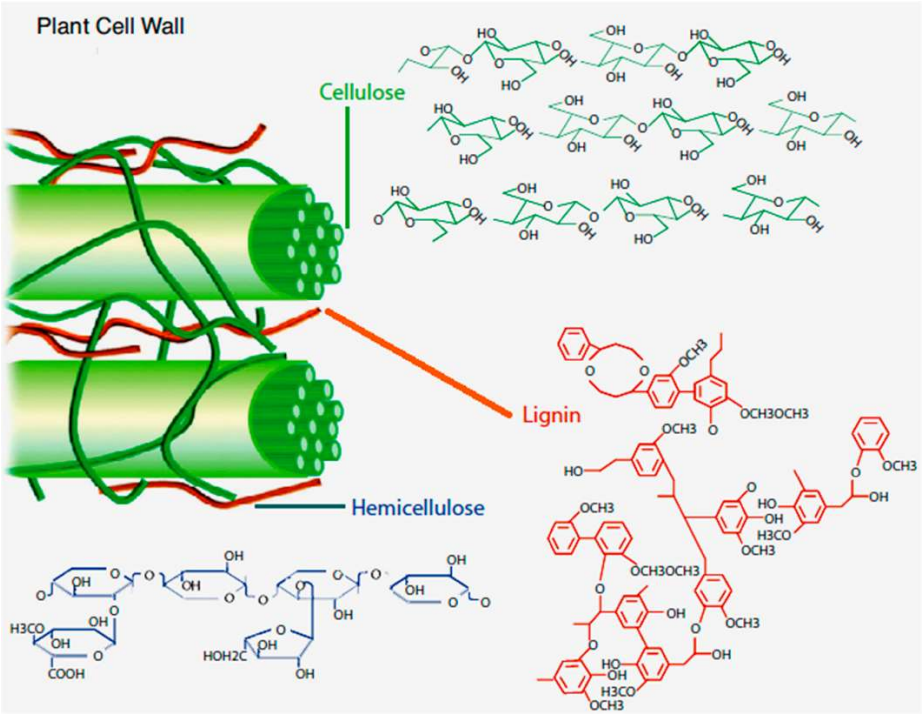

### 1.2.2 Enzymatic conversion

The main enzymes in the biomass conversion processes are cellulase and xylanase. The cellulases are enzymes that hydrolyze β-1,4 linkages in cellulose chains. The cellulose hydrolysis occurs by a combination of three main types of cellulases [54]: endoglucanases (EC 3.2.1.4), exoglucanases (EC 3.2.1.91), and glucosidases (EC 3.2.1.21). Endoglucanases hydrolyze glycosidic bonds at the amorphous regions of the cellulose generating long chain oligomers for the action of exoglucanases or cellobiohydrolases, which cleave the long chain oligosaccharides generated by the action of endoglucanases into short chain oligosaccharides. There are two types of exoglucanases, acting unidirectionally on the long chain oligomers either from the reducing or nonreducing ends liberating cellobiose, which is further hydrolyzed to glucose by β-glucosidases [55]. Synergy between cellulases have been identified between different cellobiohydrolases (with specificity for reducing and non-reducing ends); between endo and exo-glucanases; between endo-glucanases; between cellobiohydrolases, endo-glucanases and β-glucosidases [56-61].

The xylanases (EC 3.2.1.8) are among the xylanolytic enzyme system that include endoxylanase, β-xylosidase, α-glucuronidase, α-arabinofuranosidase, and acetylxylan esterase [55]. Xylanases are a group of glycoside hydrolase enzymes that degrade the linear polysaccharide xylan into xylose by catalyzing the hydrolysis of the glycosidic linkage (β-1,4) of xylosides. Xylanases have been classified in at least three ways: based on the molecular weight and isoelectric point [62], the crystal structure [63] and kinetic properties, or the substrate specificity and product profile [64]. The favorable system for the classification of xylanases is based on the primary structure and comparison of the catalytic domains. Among xylanases, endoxylanases are the most important due to their direct involvement in cleaving the glycosidic bonds and liberating short xylooligosaccharides [65,66].

### 1.2.3 Products from $C_6$ and $C_5$ sugars

The Fig. 2 shows that after cellulose and hemicellulose hydrolysis, the $C_6$ and $C_5$ sugars produced can be converted into a whole range of industrial raw materials, such as 3-hydroxy propionic acid (3-HPA), 5-hydroxymethyl furfural (5-HMF), glycerol, succinic acid, lactic acid, gluconic acid and furfural. These new biomass-derived compounds from $C_6$ and $C_5$ sugars can be used as raw materials to several important chemicals for industry [37,67]. Enzymatic processes are employed in many of these conversions, which open a whole range of **MCLEAs**

applications, making these nanohybrids materials an important tool for a sustainable development based on biomass conversion.

**Fig. 2.** Some value-added chemicals from lignocellulosic biomass.

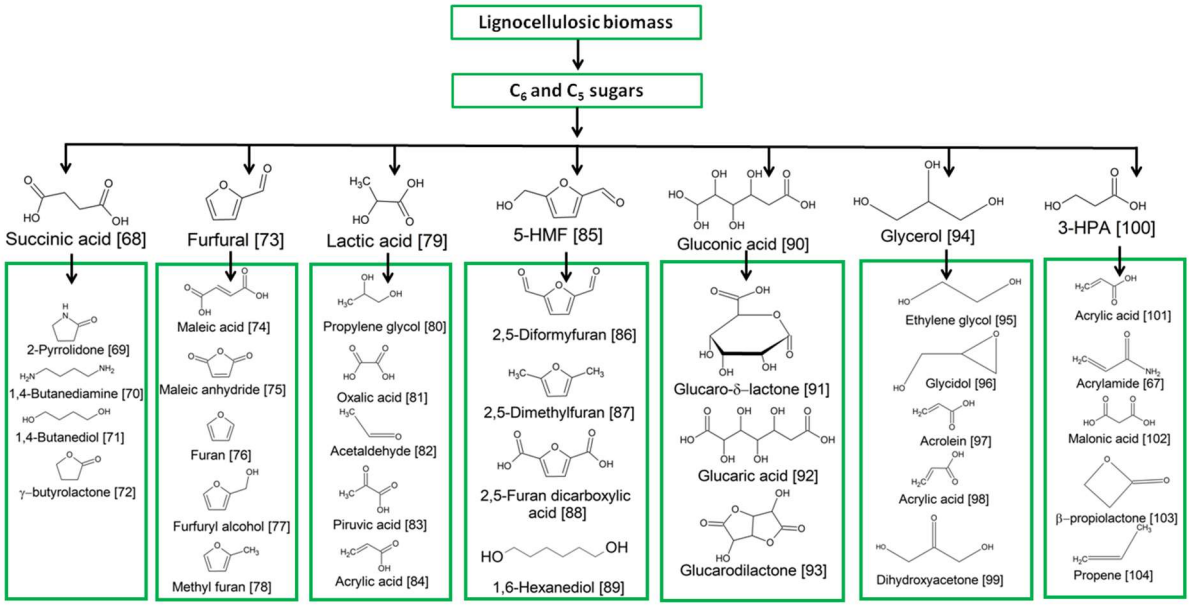


### 1.2.4 Magnetite nanoparticles as enzymes supports

Enzyme immobilization has been recognized as an effective technology to enhance its stability and reusability in industrial process. However, it is highly challenging the maintenance of their structural stability. Consequently, various materials as hydrophobic supports beads [105], macroporous zirconia [106], silica [107], polymer nanofibers [108], zeolite [109], metal-organic frameworks [110] and so forth, have been employed to enzyme immobilization. Advancements in the fields of nanoscience and nanotechnology have resulted in several possibilities for nanomaterials applications in biological and chemical fields. Among the various nanomaterials, the use of magnetic nanoparticles has received considerable attention as new supports for enzyme immobilization [111]. Magnetite ($Fe_3O_4$) is one of the most used magnetic particles due to low toxicity, biocompatibility, high surface area and affinity to proteins; allowing surface functionalization with reactive functional groups for chemical modifications, easy and convenient isolation from reaction mixture and recycling for reuse [112,113]. However, due the anisotropic dipole attraction, hydrophobic nature and high surface energy, uncoated magnetite nanoparticles are generally unstable and tend to aggregate easily,

beyond of to be highly susceptible to oxidation in the presence of oxygen, loosen their specific properties [114-115]. So, a suitable surface functionalization with molecules as chitosan [116], amino-silanes [117] or polymers [118], is necessary to overcome such limitations. Besides that, the enzyme stability and immobilization efficiency can be increased by cross-linking it with magnetic nanoparticles, creating the so called Magnetic Cross-Linked Enzyme Aggregate (**MCLEAs**). This approach allows clear advantages such as high enzyme activity; easy to be produced by inexpensive and effective methods; readily to be reused exhibiting satisfactory stability and performance for selected application. So, aiming to further improve sustainability of process, beyond **MCLEAs** synthesis, different immobilization methods in magnetic supports have been studied and implemented.

### 1.2.5 Enzyme immobilization in magnetic supports and MCLEAs synthesis

Magnetic nanoparticles (MNPs) are well known for their high surface area [119,120] and the possibility of separation from media by using an external magnetic field [121], allowing it to be applied in many areas [122-124]. The use of iron oxide magnetic nanoparticles associated with other materials to produce new composites materials is also known to promote the magnetic character to a material with defined attributes [125]. Among them, graphene oxide (GO), a monolayer of $sp^2$ carbon atoms hexagonally arranged with many oxygen functional groups on its surface is one of materials that MNPs can interact. Because of the decoration of MNPs on the sheets of GO it becomes the magnetic graphene oxide (MGO) which has a high thermal, electric and mechanical characteristic with the addition of the magnetic properties [126-128]. For the same purpose the decoration of polymer matrices with magnetic nanoparticles is also used [129].

To add new appropriate functional groups on the surface of synthesized nanomaterials the functionalization process is necessary. These groups e.g. carboxyl, epoxyl and amino allow high colloidal stability [130] and facilitate the interaction of the nanomaterials in biological applications such as enzyme immobilization. After deciding which nanomaterials well-functionalized will be used as support, it is necessary to choose the best synthetic route for the immobilization process, being the crucial moment for support/enzyme interaction that results in an effective interaction [131], enabling properties such as: good enzymatic activity, high thermal and storage stability, high amount of enzyme loaded, and its reusability.

As shown in Fig. 3, among the enzyme immobilization methods are the physical and chemical methods, varying according to the proposed study [132,133]. The physical adsorption is the oldest method and the enzymes are absorbed through the surface of the support with no further treatment. This proceeding consists in a weaker interaction, it improves a high initial enzymatic activity, being an easier process and can also be used on a large scale, but on the other hand its catalytic activity can drastically decrease over time [134].

The entrapment and the encapsulation are other important physical methods that can be used for immobilization. Enzymes immobilized by entrapment get “trapped” in a limited space inside a polymer matrix and this microenvironment can improve the enzymatic stability [135]. The disadvantage of this process is that substrates with high molecular weight cannot access the entrapped enzyme due the impediment caused by the matrix [136]. The encapsulation is also a method to trap enzymes but, in this case, it is within a semi-permeable shell or membrane, such as hydro-gels, enabling in a high load of enzymes and a great operational stability, however the risks of rupture are high if there is no diffusion of the formed products [137].

**Fig. 3.** Main enzyme immobilization methods.

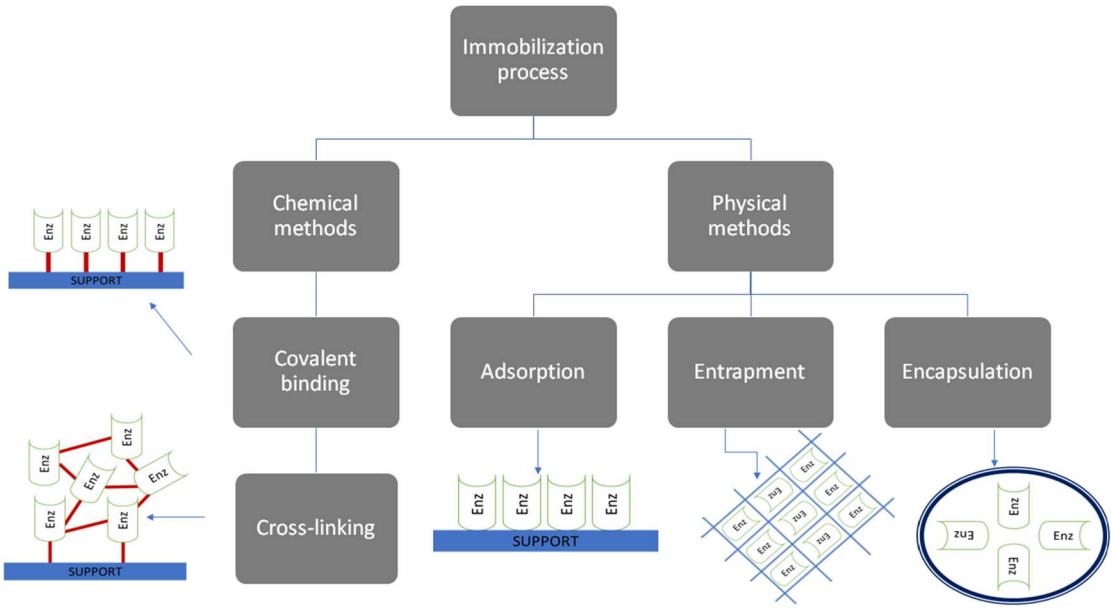


In the chemical procedure, the covalent binding method involves the formation of covalent bonds between the enzyme and the support. The groups usually used in the covalent biding are thiol and amine groups of enzymes [138]. However, it has been shown that the

enzyme might lose its activity during the immobilization procedure if the attachment occurs between support matrix and the active center of the enzyme [139].

A way to solve these problems is to synthesize a cross-link enzyme aggregate using magnetic nanoparticle support, MCLEAs. This procedure involves a precipitation of enzyme and a magnetic nanoparticle support and the subsequent formation of the enzymatic aggregate with a bifunctional cross-linker agent [140]. A **MCLEA** has the advantage of its low cost, easy preparation, high specificity, high enzymatic activity, and stability over a wide pH range [141-144]. The most common cross-linkers agents are bifunctional, which have two similar reactive functional end groups, such as two amines, two thiols or two aldehydes which will interact between identical targets on the enzyme and the support [145]. Among the cross-linker agents, glutaraldehyde (GA) is the most common due to it easy interaction with the amino groups present in the enzymes, the low cost and to be easily handled [146-148]. Table 1 summarizes some data about **MCLEAs** synthesis applied to biomass conversion and its support, enzyme source, cross-linker used and advantages of the **MCLEA** compared to free enzymes, as well o number of recycles studied.

**Tab. 1:** Some data common about MCLEAs synthesis.

| Support/ Functionalization | Enzyme Source | Cross-linker | Advantages | Reuses | Ref |
|---|---|---|---|---|---|
| **Xylanases** | | | | | |
| MNP@HPG | *Thermomyces lanuginosus* | TDI/Citric Acid | High storage stability, high initial activity, high protein loaded | 10 | 149 |
| MNP@$SiO_2$/3-PPA MNP@$SiO_2$/16-PHDA | *Thermomyces lanuginosus* | EDC | High pH and temperature stability | 10 | 150 |
| MNP /Chitosan | *Aspergillus niger* | Glutaraldehyde | High stability, high protein loaded | 7 | 146 |
| MNP@GO | *Thermomyces lanuginosus* | trichlorotriazine | High pH, temperature and storage stability | 10 | 151 |
| **Cellulases** | | | | | |
| MNP@MgO | cellulase cocktail (commercial β-glucosidase and cellulase from *Trichoderma reesei*) | Xylan aldehyde | High pH, temperature stability | 7 | 152 |
| MNP | Cellulase complex | EDC | Good temperature stability | 6 | 153 |
| MNP | *Acinetobacter* | Glutaraldehyde | High pH, temperature and storage stability | 15 | 154 |
| MNP@Chitosan | Not mentioned | Glutaraldehyde | High initial activity | 10 | 155 |
| MNP/MSN | *Trichoderma reesei* | APTMS | Easy separation and storage | 5 | 156 |
| MNP/APTS | Not mentioned | Glutaraldehyde | Good recovery and high temperature stability | 8 | 157 |
| MNP@$SiO_2$ | Not mentioned | - | Good temperature stability, easy separation | 10 | 158 |
| MNP/APTS | Not mentioned | Glutaraldehyde | High enzymatic activity, high stability | 20 | 159 |
| AF-$CoFe_2O_4$ | *Trichoderma reesei* | EDC, NHS | Easy separation | 6 | 160 |
| MNP@$SiO_x$/APTS | *Acremonium cellulolyticus* | Glutaraldehyde | High temperature stability and protein loaded | 10 | 161 |
| MNP@$\beta$-CD/APTES | *Aspergillus niger* | Glutaraldehyde | Easy separation and NP shape control | 16 | 162 |
| MNP | *Trichoderma reesei* | Glutaraldehyde | High storage and pH stability | 10 | 163 |
| MNP@MPS | *Aspergillus* | MBA | High pH, temperature and storage stability | 6 | 164 |
| MNP | *Aspergillus niger* (β-glucosidase) | Glutaraldehyde | High storage stability | 16 | 165 |
| AMNP@ECH | *Sweet almond* (β-glucosidase) | IDA-$Co^{2+}$ | High initial enzymatic activity and temperature stability | 16 | 166 |
| MNP/Polymer/MPS | *Coptotermes formosanus Shiraki* (β-glucosidase) | IDA−$Ni^{2+}$ | High pH, temperature and storage stability | 11 | 167 |

**Notes:** HPG - Hyperbranched polyglycerol; TDI - 2,4-toluene diisocyanate; 3-PPA - 3-phosphonopropionic acid; 16-PHDA - 16- phosphonohexadecanoic acid; EDC - 1-(3-dimethylaminopropyl)-3-ethylcarbodiimide hydrochloride; MSN - Mesoporous Silica nanoparticles; APTMS - 3-aminopropyltrimethoxysilane; NHS - N-hydroxysuccinimide; CD - $\beta$-cyclodextrin; MPS - 3-(trimethoxysilyl)propylmethacrylate; MBA - methylenebis(acrylamide); AMNP - Embedding of MNPs by agarose; ECH – epichlorohydrin; IDA - iminodiacetatic acid; MPS - γ-Methacryloxypropyltrimethoxy-silane.

### 1.2.6 MCLEAs characterization

The structural characterization becomes the state of the art in the enzyme area because it allows obtaining information necessary for understanding the changes in the enzymatic environment and the interactions between the support and the enzyme. Thus, it is possible to evaluate and understand the interactions of protein with the support, and to produce materials more efficient for the use in industrial processes. For this purpose, several techniques can be used to characterize these materials in order to obtain structural, morphological, qualitative and quantitative information to understand the interaction of the enzyme with the support and to evaluate the efficiency of the immobilization and of the biocatalyst produced. Although the system is complex and presents many difficulties, we summarize the main techniques currently used for the characterization and understanding of the properties of the biomaterial.

#### 1.2.6.1 Scanning electron microscopy (SEM) and transmission electron microscopy (TEM)

As shown in Fig. 4, these microscopes can be used to study the surface morphology of the enzyme (topography), the support and the composite and to evaluate the size distribution of the particles. In the case of SEM, a field emission scanning electron microscopy has the advantage of obtaining higher resolution images. Another way of analyzing the samples may be by the technique known as "environmental SEM" in which it is possible to analyze moist samples, however, in this mode, the resolution is decreased. The Cryo-SEM mode has been used and is shown as a promising tool by allowing analysis of the samples close to the native conditions since the samples can be frozen fast which can avoid denaturation and deformations due to agglomeration caused by drying the sample. In addition, Cryo-SEM allows the tomography of the sample which can be a very interesting tool to reveal the actual conformation of the enzyme on the substrate. In general, SEM has been mainly used to prove the enzymatic functionalization on the support, through the photomicrographs of the pure support after the formation of the composite [168-171].

In TEM analysis, the electron beam passes through a thin sample, the greater the electron density of the elements present in the sample the fewer electrons cross sample forming dark contrasts from denser and clearer regions to less dense ones. By using TEM analysis it is possible to elucidate the crystalline structure of a particle by using electron diffraction. In this mode an electron diffraction pattern is generated. As in SEM in general TEM is more used to

show the presence of the enzymes on the substrate by focusing the morphology and size of the substrate particles [172-175].

**Fig. 4.** TEM images of a) pure $Fe_3O_4$; b) $Fe_3O_4$-chitosan; c) cellulase **MCLEA**. Reprinted with permission from ref [155]. Copyright American Chemical Society (2014).

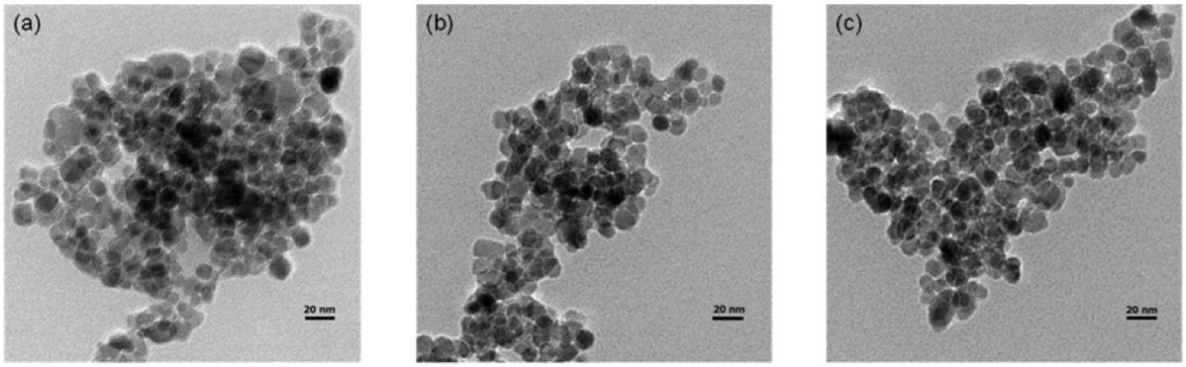


### 1.2.6.2 X-ray photoelectron spectroscopy (XPS)

Another powerful technique for the analysis of enzymatic biocomposites is the surface analysis known as X-ray photoelectron spectroscopy (XPS). The Fig. 5a shows that the XPS spectra give an elementary analysis of the sample based on the photoelectric effect allowing the characterization of the sample in a depth of up to 10 nm. Characteristic peaks at region of 398 and 248 eV on MCLEA XPS spectrum indicate the presence of nitrogen and carbon, respectively, suggesting the attachment of enzyme to support surface. With the exception of the lighter atoms (hydrogen and helium), all the elements in the sample can be identified by the XPS spectra. The sample is bombarded with a low-energy X-ray beam that causes a photoelectrons emission through the excitation of electrons, which are captured by a device capable of solving them in function of their kinetic energies characteristic of the atom of origin. The counting of the electrons as a function of the kinetic energy of these generates the spectrum of XPS that allows analyzing the surface of the sample, in a quantitative way being able to give information referring to the valence and the chemical bonds present in the sample [176].

### 1.2.6.3 X-ray diffraction (XRD)

The current trend of the use of nanomaterials as support for immobilized enzymes makes it necessary to characterize this support by different techniques among XRD is commonly used

to characterize the crystalline structure of the support. In general, as shown in Fig. 5b, recent researches have used XRD for the characterization of the support before and after immobilization of the enzymes [177-179]. It is a powerful technique to verify if there was any change in the crystalline structure of the support after modification with enzyme.

**Fig. 5.** a) XPS spectra of pure $Fe_3O_4$ and cellulase **MCLEA**; b) XRD patterns of, $Fe_3O_4$, $Fe_3O_4$-chitosan and cellulase MCLEA. Reprinted with permission from ref [153] and [155], respectively. Copyright Elsevier (2011) and American Chemical Society (2014).

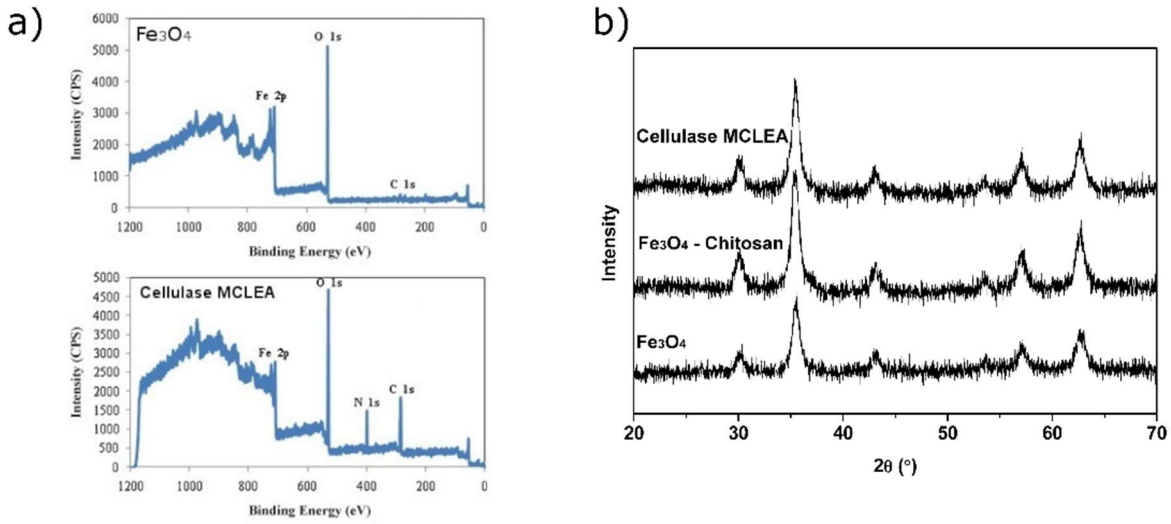


### 1.2.6.4 Circular dichroism spectroscopy (CDS)

The circular dichroism spectroscopy (CSD) technique is a powerful technique widely used in the characterization of proteins. The CSD is a spectroscopic method based on the differential absorption of light circularly polarized by optically active molecules and allows to determine its absolute configurations. As light passes through a stereogenic center present in the sample, there will be differential absorbance of the two circulating components to the right or to the left [180]. The technique is non-destructive, easy to operate, fast and requires low sample quantities and can be used in room temperature conditions [181]. As shown in Fig. 6a, effects of temperature in the conformational changes of the secondary structure can be studied using CDS measurements. The characteristic peak at 220 nm in CDS spectra is attributed to α-helix secondary structure of enzymes and normally has been used to investigate conformational changes. It allows quantification of the secondary structure of proteins in terms of the α-helical, β-strand and unordered structure using the distant UV range of the electromagnetic spectrum

(260-170 nm). The range between (260-300 nm) is used to record the aromatic residues of the proteins. Absorption of the radiation occurs with the promotion of the ground state electrons to an excited state, in protein molecules, the peptide bond exhibits two transitions in the far UV n-π* at ~ 220 nm and a π-π* transition at ~ 190 nm. Being the characteristic signal influenced secondary structure of the protein, in the signal spectra, are results of the sum of all the signals present throughout the structure of the sample. In general the technique presents great potential in the characterization of immobilized enzymes allowing the investigation of structural changes occurred during the immobilization of the samples on the support, however, their use in these cases must be interpreted with caution due to the appearance of artifacts since the enzymes after immobilization have a high scattering factor and lower colloidal stability that may interfere during the measurement [182].

#### 1.2.6.5 Fourier-transform infrared spectroscopy (FTIR)

FTIR is a very powerful tool for the detection and characterization of the enzymatic composites, allowing the investigation of the molecules because it allows identifying the vibration mode of chemical bonds presents in the sample [183-187]. The technique is based on the absorption or transmission of infrared radiation by the investigated sample. As shown in Fig. 6b, many bands near at 1540 and 1620 $cm^{-1}$ are characteristic of amide groups of enzymes and have been used to confirm its immobilization. FTIR is also important to identify if the functional group is on the surface of support before modification with enzyme.

#### 1.2.6.6 Thermal analysis

Thermogravimetric studies are used to evaluate the immobilization and to study the thermal stability of conjugate. It can also be used to calculate the amount of enzyme immobilized in the support [187,189-190]. In this type of analysis, a mass of the sample is submitted to a temperature cycle while its properties are recorded. In a thermogravimetric analysis (TGA) the heat is used to promote reactions, decomposition and structural physical processes while the mass of the sample is monitored as a function of temperature or time as it is subjected to a controlled atmosphere-temperature program. Based on this, thermogravimetric curves allow the characterization of different physicochemical properties of the analyzed samples, such as sample decomposition, thermal stability and kinetic parameters for chemical

reactions in the sample. Zang et al. [155] used TGA measurement to estimate the weight percentage of cellulase in a **MCLEA** based in $Fe_3O_4$ coated with chitosan. The amount of enzyme immobilized in the support was 10.26% (114.8 mg cellulase/g support), value consistent with the results determined by colorimetric Bradford assay (Fig. 6c), which show the importance and utility of thermal analyses.

**Fig. 6.** a) CDS spectra of amine dehydrogenases enzyme heated at different temperatures; b) FTIR spectra of cellulase **MCLEA** (bottom gray line) and free cellulase (top black line); c) TGA curves of $Fe_3O_4$ (a), $Fe_3O_4$-chitosan (b), $Fe_3O_4$-chitosan-glutaradehyde (c), cellulase MCLEA (d) and chitosan (e) . Reprinted with permission from ref [181], [148] and [155], respectively. Copyright Elsevier (2017), Springer Nature (2016) and American Chemical Society (2014).

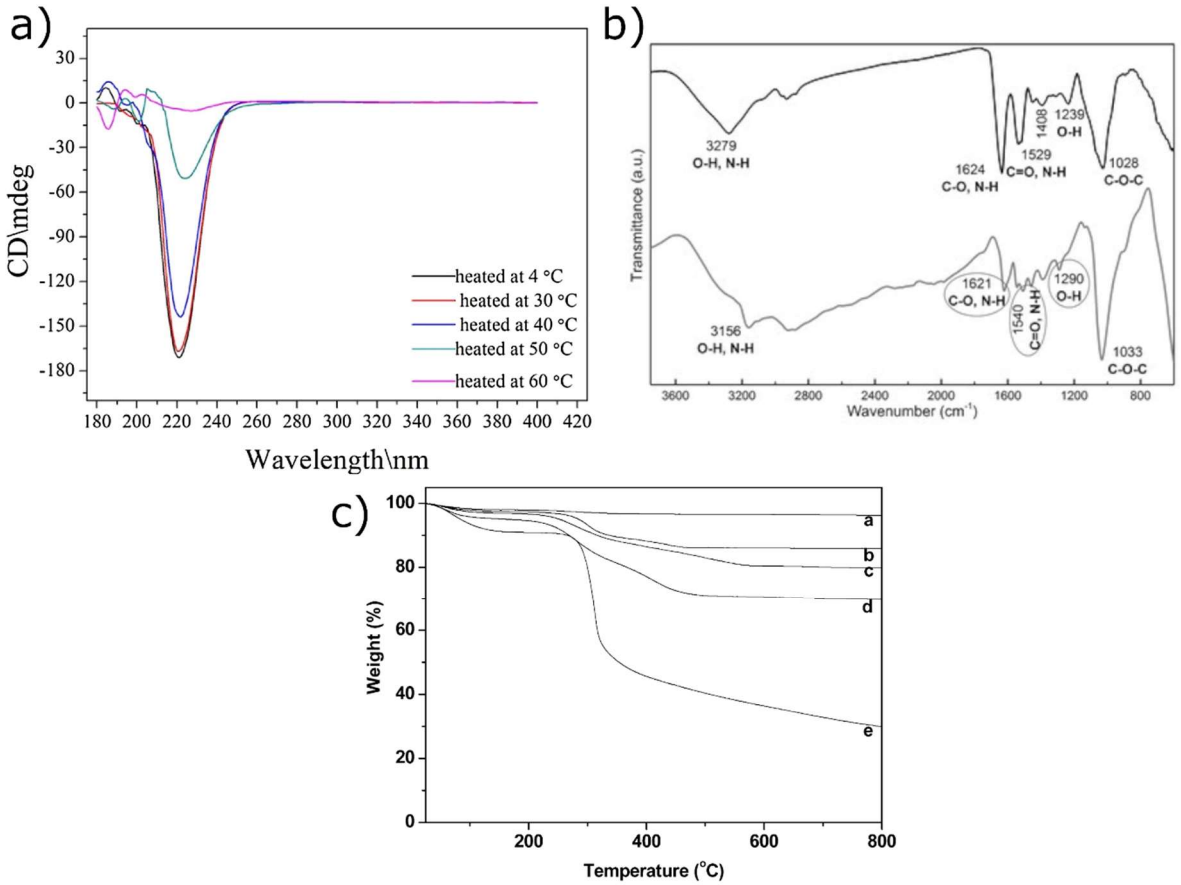


## 1.3 MCLEAs applied to biomass conversion

Biomass can be converted to a wide range of products and raw materials and currently the studies about new technologies, such as **MCLEAs** applied to biomass conversion, is growing. Here it is summarized some recent results of the **MCLEAs** applications to cellulose

and hemicellulose hydrolysis and, in the next section, applications in conversions to important chemicals from $C_6$ and $C_5$ sugars, as well as others biomass derived.

### 1.3.1 Cellulose conversion

The utilization of cellulosic biomass resources to produces value-added chemical by enzymatic processes is a beneficial green alternative facing fossil fuels. In this context, the use of **MCLEA** applied to hydrolysis of different cellulosic materials is growing [191-195]. Thus, aiming the bamboo biomass hydrolysis, Jia et al. [196] obtained a **MCLEA** based on cellulase glutaraldehyde cross-linked to amino-coated $Fe_3O_4$. As shown in Fig. 7a, after three and six cycles, this cellulase **MCLEA** retained 87 and 74% of its initial activity when carboxylmethyl cellulose was used as model substrate. A decrease in the recycle efficiency was observed when the authors applied the **MCLEA** in the bamboo biomass conversion (Fig. 7b). The hydrolysis activity of immobilized cellulase for two and four cycles was determined to be 63 and 38%, respectively. Besides that, while yield hydrolysis of bamboo biomass for free cellulase reached 44%, the **MCLEA** reached 21%. These decreases in the activity and recycle efficiency may be related to compact super-molecular feature of **MCLEAs**, which could lead to increasing diffusion limitations when the substrate were macromolecules [197]. Better results, however, were obtained by Sánchez-Ramírez et al. [148] using a cellulase **MCLEA** based on $Fe_3O_4$ coated with chitosan in the hydrolysis of *Agave atrovirens* leaves pre-treated. In this case, the yield of biomass conversion was showed to be 60.64 and 56.34 % for free enzyme and cellulase **MCLEA**, respectively. Already Abraham et al. [198] improve a hydrolysis yield of the hemp hurd biomass from 89% to 93% with a cellulase **MCLEA** based on zinc ferrite magnetic nanoparticles.

**Fig. 7.** a) Reuse assay of cellulase **MCLEA** using carboxylmethyl cellulose as model substrate; b) Reuse assay of cellulase **MCLEA** using bamboo biomass as substrate. Reprinted with permission from ref [196]. MDPI License CC BY 4.0. Open access.

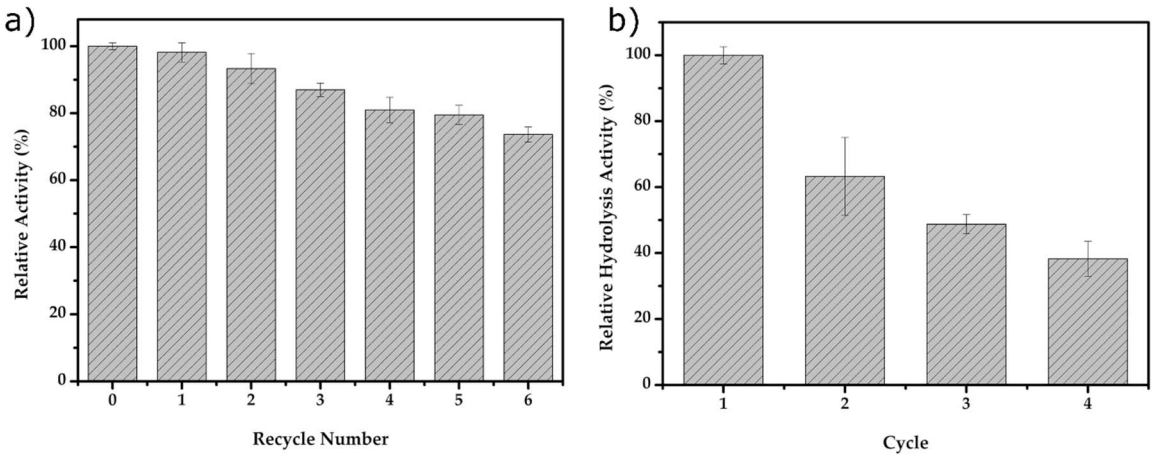


The catalysis of rice straw was studied with a **MCLEA** obtained by the combination of cellulase and β-cyclodextrin-$Fe_3O_4$ nanoparticles via 3-aminopropyltriethoxysilane and glutaraldehyde [199]. Although after immobilization, the cellulase activity was decreased by 10% compared to free cellulase, with the maintenance of 80% of the initial activity after 16 reaction cycles, these **MCLEA** showed to be able to produce 208.92 g $L^{-1}$ of sugar against only 10.5 g $L^{-1}$ of the free cellulase. This satisfactory result may be related to the improvement of bond between enzyme and support. Many factors can influence the activity losses after consecutives cycles reaction, among which are: enzyme activity losses associated to bond nanoparticles; enzyme deactivation during the reaction and release of enzyme from support. For example, Jordan & Theegala [200], measuring the enzyme mass in medium reaction for the each recycle, observed that after six cycle, only 35.24% of enzyme remaining attached to magnetite support and 64.76% of enzyme was released from support, attributing to this detachment, the loss in activity. This shows the importance of effective attachment of enzyme to support during **MCLEA** synthesis. Another excellent result was showed by Zhang et al. [159] in the hydrolysis of pretreated corncob. A cellulase **MCLEA** was successfully prepared through the cellulase immobilization onto amino-coated $Fe_3O_4$ nanoparticles via glutaraldehyde cross-linker. The immobilization method allowed to a 99.1% recovery of initial activity of the free enzyme and, as showed in Fig. 8a, at an initial corncob concentration of 2.0 mg $mL^{-1}$, 61.94% of corncob hydrolysis yield was obtained. Due to increasing in diffusion limitations, it is observed a corncob decomposition rate decreases when the corncob concentration was

gradually increased. A satisfactory reuse capacity with recovery of 91.1% of initial activity after 16 cycles was found using corncob at 2 mg $mL^{-1}$ with a time reaction of the 5 hours (Fig. 8b).

**Fig. 8.** a) Variation in decomposition rate of corncob as a function of initial corncob concentration and reaction time; b) Recovery and recycling stability using corncob at 2 mg $mL^{-1}$ and time reaction of 5 h. Both experiments were carried out at pH 6 and 40 °C. Reprinted with permission from ref [159]. Copyright Elsevier (2016).

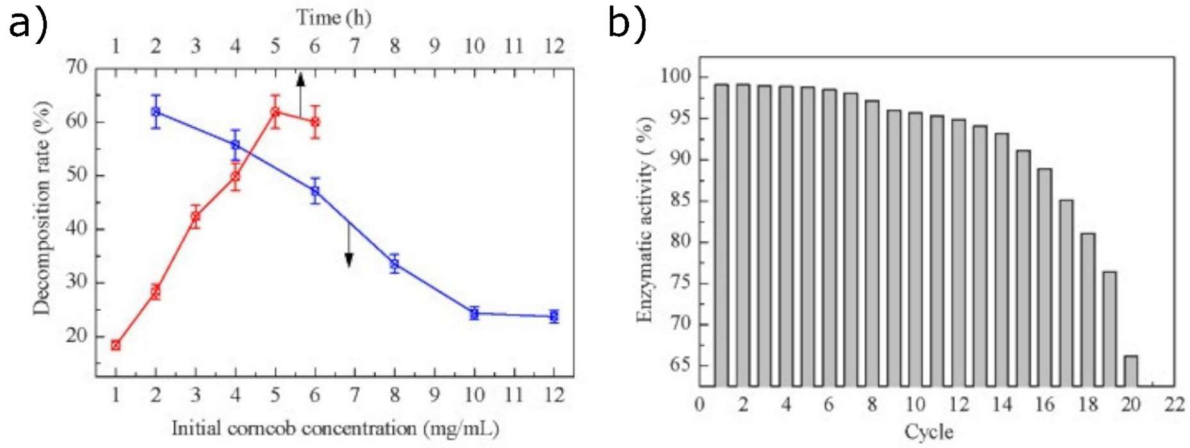


A new strategy that has been employed is a co-immobilization of two, or more, enzymes at the same magnetic support. In this context, Chen et al. [201] synthesized a **MCLEA** by co-immobilization of cellulase and lysozyme on amino-coated $Fe_3O_4$ nanoparticles, using glutaraldehyde as cross-linker, for extraction of lipids from microalgae, which have been recognized as excellent biomass resource for the third generation biodiesels [202]. Although competition during immobilization, a satisfactory activity recovery was showed, 78.9% and 69.6% for cellulase and lysozyme, respectively. For this **MCLEA**, 60% initial activity was retained after six cycles with 54.07% of yield of the lipids recovery from microalgae *Nannochloropsis sp.*

Driven by actual depletion of fossil fuels, the more prominent application of the biomass conversion is, certainly, the biofuels production. The first and second generation ethanol has mainly been produced from food crops and lignocellulosic materials due to its availability and low cost [203]. Thus, a comparative evaluation between of free and cellulase **MCLEA** for enzymatic hydrolysis of sugarcane bagasse was studied by Ingle et al. [204]. Free cellulase showed a bagasse hydrolysis yield of 78%, whereas in case of **MCLEA** a yield of 72% was found. However, with magnetic recovery, **MCLEA** can be reused in subsequent reactions, maintained 52% of yield in the third cycle. In the case ethanol production from glucose obtained by sugarcane bagasse hydrolysis, similar yields were obtained by free (93%) and cellulase immobilized (89%).

### 1.3.2 Hemicellulose conversion

In recent years, the biodegradation of hemicellulose to xylooligosaccharides has attracted attention in the industry of biofuels production and value-added chemicals, enhancing the efficiency of delignification and bleaching process in the pulp industry [205-206]. So, xylanases **MCLEAs** for hemicellulose hydrolysis have been obtaining and evaluated in different applications.

In this context, Purohit et al. [207] developed a xylanase **MCLEA** by cross-linking crude xylanase and $Fe_3O_4$ nanoparticles with glutaraldehyde for produce xylopentose and xylohexose from agro biomass. The xylanase **MCLEA** improved the xylooligosaccharides production and enzyme reusability. Free xylanase and xylanase **MCLEA** could convert respectively more than 45% and 60% of the powdered rice straw and corn cob into xylooligosaccharides. According to the authors, the process is environmentally friendly and the predominant xylopentose and xylohexose production could find unique applications in food industry and prebiotics. Liu et al. [208], supporting xylanase on $Fe_3O_4$-coated chitosan magnetic nanoparticles, also studied the production of xylooligosaccharides. The xylanase **MCLEA** synthesized by these authors can be recycled easily and exhibited improved stability, beyond released high concentration of xylooligosaccharides from birchwood xylan. Xylotriose (1.782 mg $mL^{-1}$) and xylobiose (2.023 mg $mL^{-1}$) were the main products released from birchwood xylan. The xylanase **MCLEA** recovery activity 56.5% for xylanase and the residual activity was 87.5%, even after seven recycling processes. Satisfactory results was also obtained by Shahrestani et al. [209] when they studied a hemicellulose hydrolysis aiming the clarification of fruit juices using a xylanase **MCLEA.** After 10 reaction cycles in the enrichment of the juice's clarification it still retain about 55% of the initial activity. Soozanipour et al al. [210] have studied a covalent attachment of xylanase on silica-coated magnetite nanoparticles using cyanuric chloride as cross-linker agent. This unusual strategy produced a xylanase **MCLEA** able to keep as high as 80% of activity of free xylanase. Notably, this **MCLEA** showed a quite impressive stability, even after 9 reaction cycles, maintaining almost 65% of the initial activity.

In addition to the mentioned examples, the multiple enzyme immobilizations have been tested recently also to xylanase. Perwez et al. [211] studied this new approach and prepared a reusable multipurpose magnetic nanobiocatalyst for industrial applications. The authors synthesized a **MCLEA** by conjugating Pectinex 3xL (a commercial enzyme complex containing xylanase, cellulase and pectinase) on 3-aminopropyltriethoxysilane coated $Fe_3O_4$ nanoparticles. This multipurpose **MCLEA** retained 69% of xylanase, 58% of cellulase and 87%

of pectinase activity after conjugation on coated nanoparticles as compared to their soluble counterparts, and was reused by 7 cycles maintaining more than 80% initial activity of all immobilized enzymes (Fig. 9a). The **MCLEA** was used for production of bioethanol from pretreated wheat straw. The Fig. 9b shows that the hydrolysis of pretreated wheat straw produced 1.39 g $L^{-1}$ and 1.59 g $L^{-1}$ after treatment with free Pectinex 3xL and **MCLEA**, respectively, and the bioethanol production also increases, from 0.37 to 0.5 g $L^{-1}$, with the use of **MCLEA** (Fig. 9c), showing that the approach is an ideal candidate for biotechnology industry applications.

**Fig. 9.** a) Reusability assay of Pectinex 3xL **MCLEA**; b) Reducing sugar produced from wheat straw using free and Pectinex 3xL **MCLEA**; c) Ethanol concentration produced by hydrolysate obtained from free and Pectinex 3xL **MCLEA**. Reprinted with permission from ref [211]. Copyright Elsevier (2017).

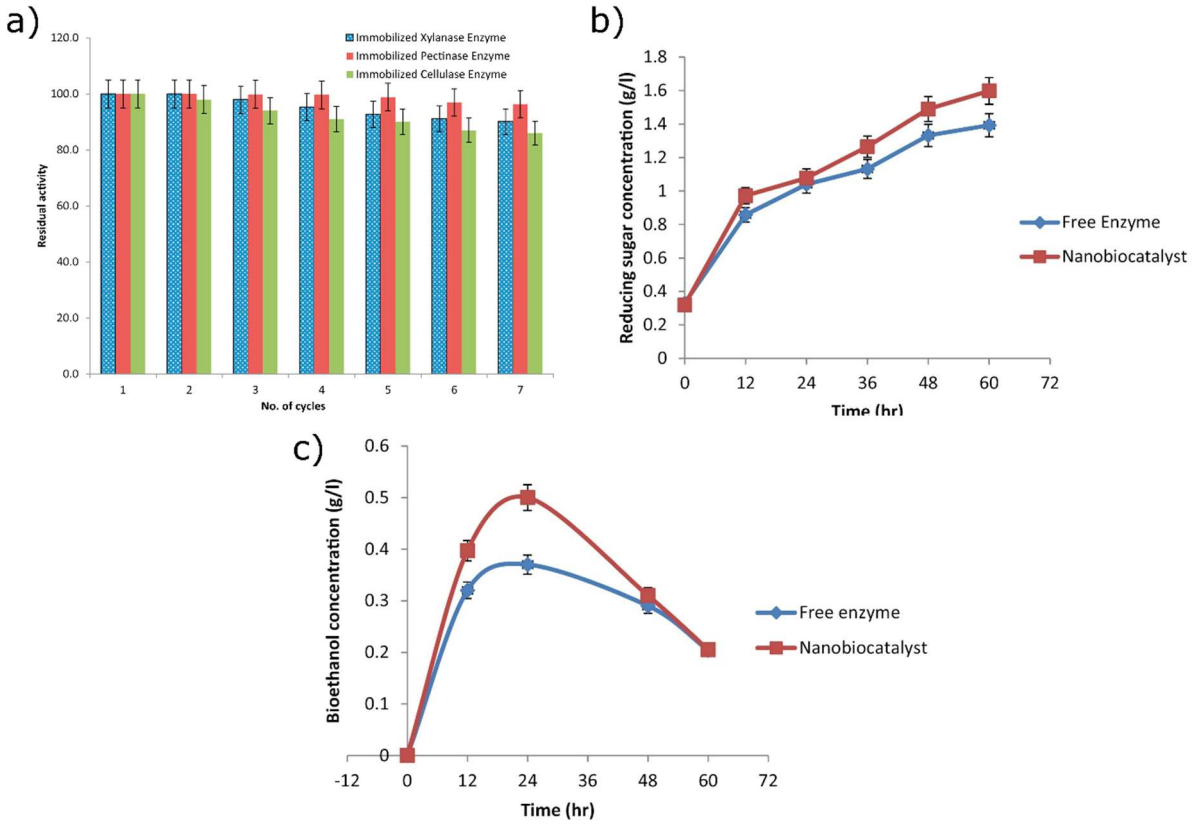


### 1.3.3 MCLEAs applied to another biomass-derived conversion

Indeed, the main applications of **MCLEAs** in biomass conversion have been targeted toward to hydrolysis of cellulosic and hemicellulosic biomass, aiming biofuels production.

However, it is known that many other conversions of the biomass-derived are activated by enzymatic reactions, which open several opportunities to **MCLEAs** application.

Sugar-based biomaterials have the advantage of being cheap, biocompatible, biodegradable and sustainable [212]. Among them, glucose is the best-known sugar and has a wide range of application in materials [213-215]. However, the most commonly found linkages between glucose residues are readily hydrolysable, making it necessary to modify the base structure to obtain materials with specific characteristics. One of the possible modifications in the glucose is to confer on it the lactone function glucaro-δ-lactone, enabling a new set of materials [216].

As shown in Fig. 10, the glucose molecule, when in the acyclic form, has an anomeric terminal carbon which makes up an aldehyde group. This group is oxidized and gives rise to a carboxylate group. The conversion occurs enzymatically allowing the specific oxidation of the aldehyde group while the remaining hydroxyls remain unchanged. The enzyme glucose oxidase (GOx) promotes the simultaneous conversion of glucose into gluconic acid [217] and molecular oxygen into hydrogen peroxide [218]. The obtained gluconic acid remains in equilibrium with the lactonic form in the reaction medium [219,220], and has been an important chemical used as chelating agent, food additive, cleanser and versatile intermediate in the pharmaceutical, polymer and cosmetics industries [221].

**Fig. 10.** Glucose to gluconic acid conversion

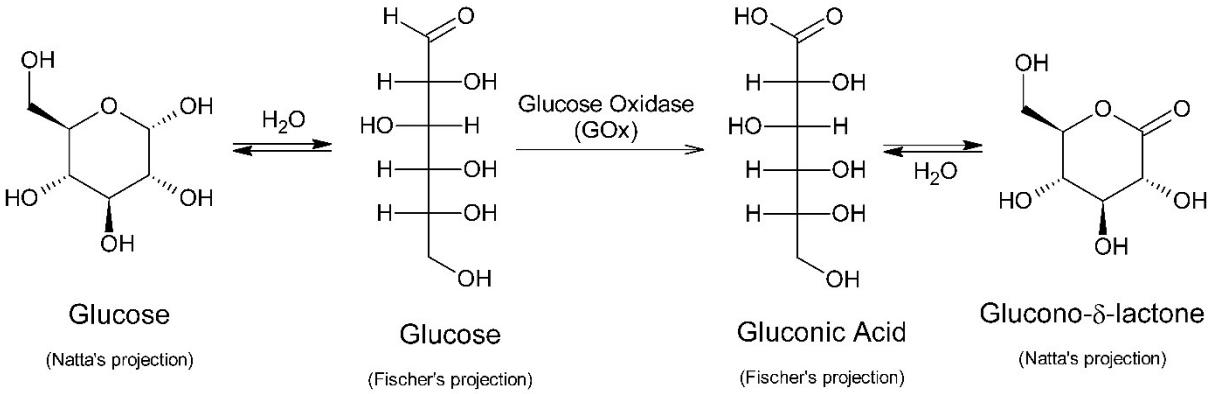


Abbasi et al. [222] immobilized glucose oxidade (GOx) on the silica-coated magnetic nanoparticles. The synthesized GOx **MCLEA** allow the enzyme to acquire the conformational and structural arrangement for a better activity and stability, and suggests that binding of enzyme onto magnetic nanoparticles was efficient for creating biomaterial composite that can

be used at wider range of pH (from 6 to 10) and temperature (from 25° to 60°C) for a variety of applications in health and food safety. As shown in Fig. 11a, in whole range of pH and temperature studied the GOx **MCLEA** showed better activity than the free enzyme. Besides that, Fig. 11b shows that the residual activity in assessing storage stability decreases for both free and immobilized GOx over time, but the loss of activity is more than 60% after 7 days for free enzyme while it is only 20% for immobilized enzyme.

**Fig. 11.** a) Enzyme pH dependence (square) and thermostability (circle) of GOx **MCLEA** (filled symbol) and free GOx (opened symbol); b) Storage stability of GOx **MCLEA** (filled circle) and free GOx (opened circle). Reprinted with permission from ref [222]. Copyright Elsevier (2016).

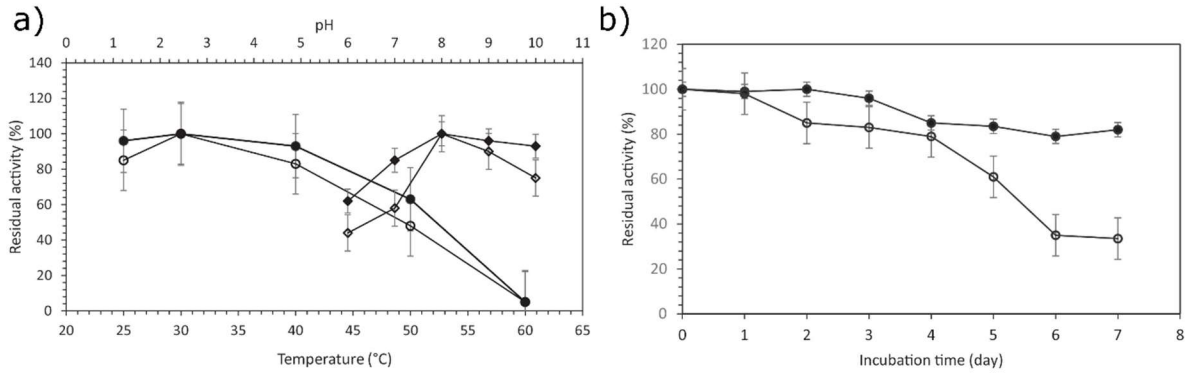


As showed in the item 1.2.3, glycerol can be also obtained from biomass hydrolysis. The conversion of glycerol into products of general interest, specifically biomaterials, has attracted significant effort from researchers community and industry [223]. The simple conversion of glycerol to dihydroxyacetone (DHA) is one of many solutions for the endeavor employed. DHA can be produced from the selective oxidation of glycerol through of the enzyme glycerol dehydrogenase (GlyDH). The enzyme acts on the secondary hydroxyl of the polyol, converting it into a ketone group [224]. The enzymatic conversion is presented as a sustainable, cheap option and allows industrial expansion.

Zheng and Zhang [225] immobilized GlyDH on magnetic silica nanoparticles containing free amine groups on the surface via glutaraldehyde cross-linker. The Fig. 12a shows that the immobilization did not significantly alter the optimum temperature and pH of the enzyme's maximum activity but made it less sensitive to changes in pH and temperature over the range studied. When pH or temperature deviated from the optimal conditions, better activity was retained for the GlyDH **MCLEA** compared to the free enzyme. The increase in tolerance to variations in pH and temperature was possible due to the chemical support-enzyme binding,

maintaining the original configuration of the enzyme. As shown in Fig. 12b, the enzyme activity recovery of 81.1% under the optimized immobilization condition and the immobilized GlyDH retained 91% of its original activity after 10 cycles.

**Fig. 12.** a) The optimal temperature and pH of enzymatic activity for free (square) and GlyDH **MCLEA** (circle); b) Activity loss over of 10 cycles of GLlyDH **MCLEA**. Reprinted with permission from ref [225]. Copyright Taylor & Francis (2011).

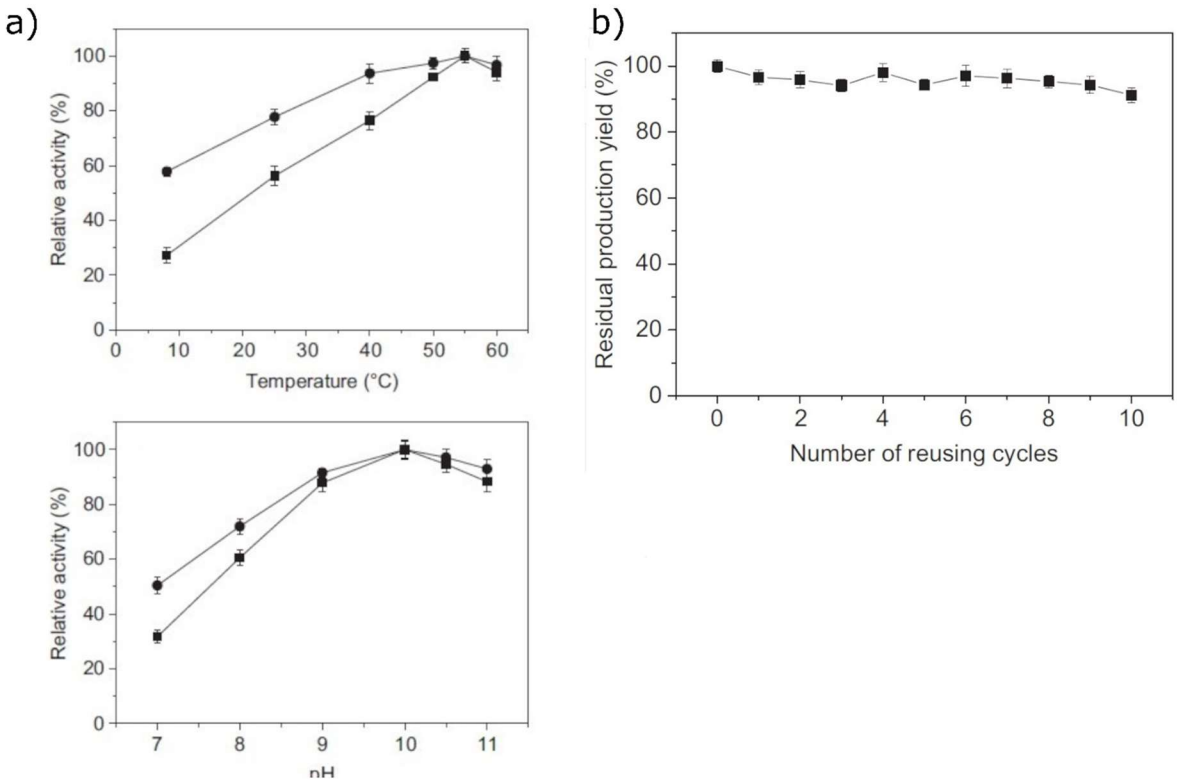


Regarding the possible applications for DHA, its use as a hydrophilic polymer has attracted interest from several researchers. Zelikin et al. [226] have used DHA as the monomer in the synthesis of a biomaterial whose surface can be easily functionalized in one-step-manner and has the strength compared to a human bone. Weiser et al. [227] has combined DHA with lactic acid, both biomass monomers, for the synthesis of a copolymer that can be applied to drug delivery, tissue engineering and surgeries. Similar to the previous example, Henderson et al. [228] have combined the qualities of DHA and polyethylene glycol in the synthesis of an effective and rapidly resorbable hemostatic agent which can find broad hemostatic application in a wide range of surgical procedures.

Lastly, **MCLEAs** have been also tested in the conversion of raw lignocellulosic biomassby lignin hydrolysis. As previously stated, lignin is a three-dimensional polymer of phenyl propane units and serves as a support for vascular plants [229,230]. Several phenolic compounds are used as cross-linking agents between the three-dimensional structure of lignin and the chains of hemicellulose [37]. Among these, is the ferulic acid (FA), which acts as a bridge between the arabinose residues of arabinoxylan belonging to hemicellulose and non-core lignin [231,232]. The enzyme ferulic acid esterase (FAE) can selectively hydrolysis the ester linkage of ferulic acid and xylan fragment, so, FA can be produced from different biomass substrates and used as precursor of several chemicals including the flavoring agent vanillin [233].

Thus, Gadalkar and Rathod [234] immobilized ferulic acid esterase on magnetic nanoparticles aiming to enhance of ferulic acid from defatted rice bran under ultrasound. This FAE **MCLEA** was obtained via attachment of FAE on amino-coated magnetite nanoparticles using glutaraldehyde as cross-linker agent. The optimization of the synthesis parameters (enzyme loading, solvent/solute ratio, temperature and sonication time) improved yield and reduced process time through a predictive model. An immobilization yield of about 77% was obtained after 1h, while by the conventional procedure the yield was close to 65% after 4h. After 5 reaction cycles, the FAE **MCLEA** allowed a retained activity up to 82%, showing that this strategy can be also applied in the value-added chemicals extraction from biomass.

## 1.4 Conclusions and outlooks

The current global demand for renewable raw materials as an alternative to fossil sources has driven the search by development of new green technologies. The lignocellulosic biomass shows promising due to its abundance and wide range of possible applications. Besides that, the enzyme immobilization and the use of magnetic cross-linked enzyme aggregate (**MCLEAs**) has spurred interest in the biomass conversion processes. Many studies described in this review showed increases in the activity and enzymatic stability after enzyme immobilization in magnetic supports, as well satisfactory recovery and improves in the reactions yield to obtaining a wide range of value-added chemicals of particular interest to fuels, materials, environment and food science. Moreover, because the enzymes can be applied in several chemical reactions, the **MCLEA** applications do not is limited to biomass conversions. These show that in future the **MCLEAs** can be used in important fields as medicines

production, biodiesel, textile industry, biosensors, cosmetics and bioremediation. Despite of recent advance in the production of these new nanohybrids materials, it is still desired more studies about optimization of synthesis and employ of new supports materials combined with magnetic nanoparticles to increase the efficiency of **MCLEAs** in lignocellulosic conversion and recovery. Certainly, when this objective is attained, a real step for the sustainable development will be given, once such improves can helpful to overcome some challenges as replace same applications of fossil sources as raw materials in a global scale.

## Acknowledgements

The authors are grateful for the financial support provided by the Brazilian funding agencies FAPESP, CNPq and Finep.

## References

[1] R.A. Sheldon, Green Chem. 18 (2016) 3180–3183.

[2] R.A. Sheldon, R. Soc. Chem. 1 (2016) 1–7.

[3] W. Kopp, T.P. Da Costa, S.C. Pereira, M. Jafelicci, R.C. Giordano, R.F.C. Marques, F.M. Araújo-Moreira, R.L.C. Giordano, Process Biochem. 49 (2014) 38–46.

[4] G. Schenk, I. Mateen, T.K. Ng, M.M. Pedroso, N. Mitić, M. Jafelicci, R.F.C. Marques, L.R. Gahan, D.L. Ollis, Coord. Chem. Rev. 317 (2016) 122–131.

[5] C.H. Zhou, X. Xia, C.X. Lin, D.S. Tong, J. Beltramini, Chem. Soc. Rev. 40 (2011) 5588–5617.

[6] F. Bilgili, I. Ozturk, Sustain. Energy Rev. 49 (2015) 132–138.

[7] J.M. Li, A.H. Li, P.S. Varbanov, Z.Y. Liu, J. Clean. Prod. 144 (2017) 426–436.

[8] A. Mirkouei, K.R. Haapala, J. Sessions, G.S. Murthy, Renew. Sustain. Energy Rev. 67 (2017) 15–35.

[9] D. Bourguignon, Briefing Biomass for electricity and heating Opportunities and challenges, European Parliament (2015) 2-8.

[10] U.S. Energy Information Administration, Monthly energy review - December 2014. https://www.eia.gov/totalenergy/data/monthly/archive/00351412.pdf, 2014 (accessed 13 March 2018).

[11] S. Azman, A.F. Khadem, J.B. Van Lier, G. Zeeman, C.M. Plugge, Crit. Rev. Environ. Sci. Technol. 45 (2015) 2523–2564.

[12] N. Mota, C. Alvarez-Galvan, R.M. Navarro, J.L.G. Fierro, Biofuels. 2 (2011) 325–343.

[13] F.A.F. Antunes, A.K. Chandel, L.P. Brumano, R. Terán Hilares, G.F.D. Peres, L.E.S. Ayabe, V.S. Sorato, J.R. Santos, J.C. Santos, S.S. Da Silva, Renew. Energy. 124 (2018) 189–196.

[14] P. Li, D. Cai, Z. Luo, P. Qin, C. Chen, Y. Wang, C. Zhang, Z. Wang, T. Tan, Bioresour. Technol. 206 (2016) 86–92.

[15] R.B. Nair, M. Kalif, J.A. Ferreira, M.J. Taherzadeh, P.R. Lennartsson, Bioresour. Technol. 245 (2017) 145–151.

[16] S.C. Nakanishi, L.B. Soares, L.E. Biazi, V.M. Nascimento, A.C. Costa, G.J.M. Rocha, J.L. Ienczak, Biotechnol. Bioeng. 114 (2017) 2211–2221.

[17] A.L.S. Reis, E.D. Damilano, R.S.C. Menezes, M.A. de Morais, Ind. Crops Prod. 92 (2016) 255–262.

[18] A.L. Scholl, D. Menegol, A.P. Pitarelo, R.C. Fontana, A.Z. Filho, L.P. Ramos, A.J.P. Dillon, M. Camassola, Bioresour. Technol. 192 (2015) 228–237.

[19] S. Chianese, J. Loipersböck, M. Malits, R. Rauch, H. Hofbauer, A. Molino, D. Musmarra, Fuel Process. Technol. 132 (2015) 39–48.

[20] B. Dawoud, E. Amer, D. Gross, Int. J. Energy Res. 31 (2007) 135–147.

[21] F. Jin, H. Sun, C. Wu, H. Ling, Y. Jiang, P.T. Williams, J. Huang, Catal. Today. 309 (2018) 2–10.

[22] W. Liu, Y. Cui, X. Du, Z. Zhang, Z. Chao, Y. Deng, Energy Environ. Sci. 9 (2016) 467–472.

[23] P. Parthasarathy, K.S. Narayanan, Renew. Energy. 66 (2014) 570–579.

[24] A. V. Puga, Coord. Chem. Rev. 315 (2016) 1–66.

[25] J.A. Rollin, J. Martin del Campo, S. Myung, F. Sun, C. You, A. Bakovic, R. Castro, S.K. Chandrayan, C.-H. Wu, M.W.W. Adams, R.S. Senger, Y.-H.P. Zhang, Proc. Natl. Acad. Sci. 112 (2015) 4964–4969.

[26] G. Choi, J. Kim, S. Lee, C. Lee, Bioresour. Technol. 257 (2018) 238–248.

[27] J. Martín Juárez, E. Riol Pastor, J.M. Fernández Sevilla, R. Muñoz Torre, P.A. García-Encina, S. Bolado Rodríguez, Bioresour. Technol. 257 (2018) 30–38.

[28] F. Passos, P.H.M. Cordeiro, B.E.L. Baeta, S.F. de Aquino, S.I. Perez-Elvira, Bioresour. Technol. 253 (2018) 49–54.

[29] C. Rodriguez, A. Alaswad, K.Y. Benyounis, A.G. Olabi, Renew. Sustain. Energy Rev. 68 (2017) 1193–1204.

[30] Y. Zheng, J. Zhao, F. Xu, Y. Li, Prog. Energy Combust. Sci. 42 (2014) 35–53.

[31] R. Kajaste, J. Clean. Prod. 75 (2014) 1–10.

[32] S. Montipó, I. Ballesteros, R.C. Fontana, S. Liu, A.F. Martins, M. Ballesteros, M. Camassola, Bioresour. Technol. 249 (2018) 1017–1024.

[33] D. Saygin, D.J. Gielen, M. Draeck, E. Worrell, M.K. Patel, Renew. Sustain. Energy Rev. 40 (2014) 1153–1167.

[34] B.H. Shanks, P.L. Keeling, Green Chem. 19 (2017) 3177–3185.

[35] R.A. Sheldon, Green Chem. 16 (2014) 950–963.

[36] G. Strappaveccia, L. Luciani, E. Bartollini, A. Marrocchi, F. Pizzo, L. Vaccaro, Green Chem. 17 (2015) 1071–1076.

[37] F.H. Isikgor, C.R. Becer, Polym. Chem. 6 (2015) 4497–4559.

[38] S.J. Birrell, D.L. Karlen, A. Wirt, Bioenergy Res. 7 (2014) 509–516.

[39] P. Andrić, A.S. Meyer, P.A. Jensen, K. Dam-Johansen, Appl. Biochem. Biotechnol. 160 (2010) 280–297.

[40] C. Mateo, J.M. Palomo, G. Fernandez-Lorente, J.M. Guisan, R. Fernandez-Lafuente, Enzyme Microb. Technol. 40 (2007) 1451–1463.

[41] T. Honda, T. Tanaka, T. Yoshino, Biomacromolecules. 16 (2015) 3863–3868.

[42] L.R. Lynd, M.S. Laser, D. Bransby, B.E. Dale, B. Davison, R. Hamilton, M. Himmel, M. Keller, J.D. McMillan, J. Sheehan, C.E. Wyman, Nat. Biotechnol. 26 (2008) 169–172.

[43] V. Singh, D. Singh, Ind. Eng. Chem. Res. 53 (2014) 3854–3860.

[44] Y. Wang, Z. Iqbal, S. V. Malhotra, Chem. Phys. Lett. 402 (2005) 96–101.

[45] L. Lei, Y. Bai, Y. Li, L. Yi, Y. Yang, C. Xia, J. Magn. Magn. Mater. 321 (2009) 252–258.

[46] H. Jia, G. Zhu, P. Wang, Bioresour. Technol. 83 (2002) 37–46.

[47] P. McKendry, Bioresour. Technol. 83 (2002) 37-46.

[48] S.D. Stefanidis, K.G. Kalogiannis, E.F. Iliopoulou, C.M. Michailof, P.A. Pilavachi, A.A. Lappas, J. Anal. Appl. Pyrolysis. 105 (2014) 143–150.

[49] H.M. Akil, M.F. Omar, A.A.M. Mazuki, S. Safiee, Z.A.M. Ishak, A.A. Bakar, Mater. Des. 32 (2011) 4107–4121.

[50] Y. Nishiyama, J. Sugiyama, H. Chanzy, P. Langan, J. Am. Chem. Soc. 125 (2003) 14300–14306.

[51] V.K. Thakur, M.K. Thakur, Carbohydr. Polym. 109 (2014) 102–117.

[52] S. Sun, S. Sun, X. Cao, R. Sun, Bioresour. Technol. 199 (2016) 49–58.

[53] H. Bamdad, K. Hawboldt, S. MacQuarrie, Renew. Sustain. Energy Rev. 81 (2018) 1705–1720.

[54] V. Juturu, J.C. Wu, Renew. Sustain. Energy Rev. 33 (2014) 188–203.

[55] C. Boisset, C. Pétrequin, H. Chanzy, B. Henrissat, M. Schlein, Biotechnol. Bioeng. 72 (2001) 339–345.

[56] P. Valjamae, V. Sild, G. Pettersson, G. Johansson, Eur J Biochem 1999; 266:327–34.

[57] L.R. Lynd, P.J. Weimer, W.H. Van Zyl, I.S. Pretorius, Bioresour. Technol. 66 (2002) 506–577.

[58] M. Qi, H.S. Jun, C.W. Forsberg, Appl. Environ. Microbiol. 73 (2007) 6098–6105.

[59] Y.H.P. Zhang, L.R. Lynd, Biotechnol. Bioeng. 88 (2004) 797–824.

[60] X.Z. Zhang, N. Sathitsuksanoh, Y.H.P. Zhang, Bioresour. Technol. 101 (2010) 5534–5538.

[61] S. Zhou, L.O. Ingram, J. Bacteriol. 182 (2000) 5676–5682.

[62] K.K. Wong, L.U. Tan, J.N. Saddler, Microbiol. Rev. 52 (1988) 305–317.

[63] T.W. Jeffries, Curr. Opin. Biotechnol. 7 (1996) 337–342.

[64] X.Z. Zhang, Y.H.P. Zhang, Cellulases: characteristics, sources, production and applications, in: S.T. Yang, H.A. El-Enshasy, N. Thongchul, (Eds.), Bioprocessing Technologies in Biorefinery for Sustainable Production of Fuels, Chemicals, and Polymers. John Wiley & Sons, New York, 2013, pp. 131–146.

[65] T. Collins, C. Gerday, G. Feller, FEMS Microbiol. Rev. 29 (2005) 3–23.

[66] B. Henrissat, F. Grenoble, J. Biochem. 280 (1991) 309–316.

[67] A. Corma-Canos, S. Iborra, A. Velty, Chem. Rev. 107 (2007) 2411–2502.

[68] J. Akhtar, A. Idris, R. Abd. Aziz, Appl. Microbiol. Biotechnol. 98 (2014) 987–1000.

[69] C. Delhomme, D. Weuster-Botz, F.E. Kühn, Green Chem. 11 (2009) 13–26.

[70] J.H. Sattler, M. Fuchs, K. Tauber, F.G. Mutti, K. Faber, J. Pfeffer, T. Haas, W. Kroutil, Angew. Chemie - Int. Ed. 51 (2012) 9156–9159.

[71] K.H. Kang, U.G. Hong, J.O. Jun, J.H. Song, Y. Bang, J.H. Choi, S.J. Han, I.K. Song, J. Mol. Catal. A Chem. 395 (2014) 234–242.

[72] Z. Shao, C. Li, X. Di, Z. Xiao, C. Liang, Ind. Eng. Chem. Res. 53 (2014) 9638–9645.

[73] A.R.C. Morais, M.D.D.J. Matuchaki, J. Andreaus, R. Bogel-Lukasik, Green Chem. 18 (2016) 2985–2994.

[74] S. Shi, H. Guo, G. Yin, Catal. Commun. 12 (2011) 731–733.

[75] N. Alonso-Fagúndez, M. Ojeda, R. Mariscal, J.L.G. Fierro, M. López Granados, J. Catal. 348 (2017) 265–275.

[76] T. Ishida, K. Kume, K. Kinjo, T. Honma, K. Nakada, H. Ohashi, T. Yokoyama, A. Hamasaki, H. Murayama, Y. Izawa, M. Utsunomiya, M. Tokunaga, Efficient, ChemSusChem. 9 (2016) 3441–3447.

[77] C.P. Jiménez-Gómez, J.A. Cecilia, D. Durán-Martín, R. Moreno-Tost, J. Santamaría-González, J. Mérida-Robles, R. Mariscal, P. Maireles-Torres, J. Catal. 336 (2016) 107–115.

[78] M.J. Gilkey, P. Panagiotopoulou, A. V. Mironenko, G.R. Jenness, D.G. Vlachos, B. Xu, ACS Catal. 5 (2015) 3988–3994.

[79] L. Yang, J. Su, S. Carl, J.G. Lynam, X. Yang, H. Lin, Appl. Catal. B Environ. 162 (2015) 149–157.

[80] J. Xiao, Z. Huo, D. Ren, S. Zhang, J. Luo, G. Yao, F. Jin, Process Biochem. 50 (2015) 793–798.

[81] L. Axelsson, M. Franzén, M. Ostwald, G. Berndes, G. Lakshmi, N.H. Ravindranath, Biofuels, Bioprod. Biorefining. 6 (2012) 246–256.

[82] C. Tang, J. Peng, X. Li, Z. Zhai, W. Bai, N. Jiang, H. Gao, Y. Liao, Green Chem. 17 (2015) 1159–1166.

[83] P. Mäki-Arvela, I.L. Simakova, T. Salmi, D.Y. Murzin, Chem. Rev. 114 (2014) 1909–1971.

[84] J. Peng, X. Li, C. Tang, W. Bai, Green Chem. 16 (2014) 108–111.

[85] H.M. Mirzaei, B. Karimi, Green Chem. 18 (2016) 2282–2286.

[86] P. V. Rathod, S.D. Nale, V.H. Jadhav, ACS Sustain. Chem. Eng. 5 (2017) 701–707.

[87] .J. Kumalaputri, G. Bottari, P.M. Erne, H.J. Heeres, K. Barta, ChemSusChem. 7 (2014) 2266–2275.

[88] H. Ait Rass, N. Essayem, M. Besson, ChemSusChem. 8 (2015) 1206–1217.

[89] J. Tuteja, H. Choudhary, S. Nishimura, K. Ebitani, ChemSusChem. 7 (2014) 96–100.

[90] D. Santhanaraj, M.R. Rover, D.E. Resasco, R.C. Brown, S. Crossley, ChemSusChem. 7 (2014) 3132–3137.

[91] J.J. Bozell, G.R. Petersen, Green Chem. 12 (2010) 539–554.

[92] X. Jin, M. Zhao, J. Shen, W. Yan, L. He, P.S. Thapa, S. Ren, B. Subramaniam, R. V. Chaudhari, J. Catal. 330 (2015) 323–329.

[93] T.C. Gehret, A.S. Frobese, J.S. Zerbe, H.K. Chenault, J. Org. Chem. 74 (2009) 8373–8376.

[94] Z.X. Wang, J. Zhuge, H. Fang, B.A. Prior, Biotechnol. Adv. 19 (2001) 201–223.

[95] M.R. Nanda, Z. Yuan, W. Qin, C. (Charles) Xu, Catal. Rev. 58 (2016) 309–336.

[96] Y. Zhou, F. Ouyang, Z. Song, Z. Yang, D. Tao, CATCOM. (2015).

[97] R. Estevez, D. Luna, F.M. Bautista, Chem. Eng. J. (2015).

[98] W. Tong, Y. Xu, M. Xian, W. Niu, J. Guo, Appl. Microbiol. Biotechnol. 100 (2016) 4901–4907.

[99] M. Zheng, S. Zhang, Biocatal. Biotransform. 29 (2011) 278–287.

[100] X. Jiang, X. Meng, M. Xian, Appl. Microbiol. Biotechnol. 82 (2009) 995–1003.

[101] A. Vidra, Á. Németh, Period. Polytech. Chem. Eng. 62 (2018) 156–166.

[102] T. Haas, M. Meier, C. Brossmer, D. Arntz, A. Freund, A. DE Patent 19629372, 1996.

[103] F. Cherubini, A.H. Stremman, Biofuels, Bioprod. Biorefining. 5 (2011) 548–561.

[104] R. Rajagopal, Sustainable value creation in the fine and speciality chemicals industry, John Wiley & Sons, New York, 2014.

[105] E.A. Manoel, C.S. José, D.M.G. Freire, N. Rueda, R. Fernandez-lafuente, Enzyme Microb. Technol. 71 (2015) 53–57.

[106] S.Z. Ljiljana, I.M. Karad, B.M. Joki, Biochem. Eng. J. 93 (2015) 73–83.

[107] G. Bayramoglu, M.Y. Arica, A. Genc, V.C. Ozalp, Bioprocess Biosyst. Eng. 39 (2016) 871–881.

[108] C. Tang, C.D. Saquing, S.W. Morton, B.N. Glatz, R.M. Kelly, S.A. Khan, ACS Appl. Mater. Interfaces 6 (2014) 11899-11906.

[109] V.R.R. Marthala, M. Friedrich, Z. Zhou, M. Distaso, S. Reuss, S.A. Al-thabaiti, W. Peukert, W. Schwieger, M. Hartmann, Adv. Funct. Mater. 25 (2015) 1832–1836.

[110] X. Wu, M. Hou, J. Ge, Catal. Sci. Technol. 5 (2015) 5077–5085.

[111] H. Shahrestani, A. Taheri-kafrani, A. Soozanipour, O. Tavakoli, Biochem. Eng. J. 109 (2016) 51–58.

[112] J. Xu, J. Sun, Y. Wang, J. Sheng, F. Wang, M. Sun, Molecules 19 (2014) 11465–11486.

[113] Y. Zhu, X. Ren, Y. Liu, Y. Wei, L. Qing, X. Liao, Mater. Sci. Eng. C. 38 (2014) 278–285.

[114] K. Atacan, C. Bekir, Int. J. Biol. Macromol. 97 (2017) 148–155.

[115] L. Chen, Z. Xu, H. Dai, S. Zhang, J. Alloys Compd. 497 (2010) 221–227.

[116] X. Xie, B. Li, Z. Wu, S. Dong, L. Li, Adv. Mat. Res, 550-553 (2012) 1566–1571.

[117] W. Zhang, J. Qiu, H. Feng, L. Zang, E. Sakai, J. Magn. Magn. Mater. 375 (2015) 117–123.

[118] E. Cheraghipour, A.M. Tamaddon, S. Javadpour, I.J. Bruce, J. Magn. Magn. Mater. 328 (2013) 91–95.

[119] L. Feng, M. Cao, X. Ma, Y. Zhu, C. Hu, J. Hazard. Mater. 217–218 (2012) 439–446.

[120] A.K. Gupta, M. Gupta, Biomaterials 26 (2005) 3995–4021.

[121] M.S. Kandelousi, Eur. Phys. J. Plus. 129 (2014) 1–12.

[122] V. V. Mody, A. Cox, S. Shah, A. Singh, W. Bevins, H. Parihar, Appl. Nanosci. 4 (2014) 385–392.

[123] M. Sheikholeslami, M. Mehdi, J. Taiwan Inst. Chem. Eng. 56 (2015) 6–15.

[124] T. Shin, Y. Choi, S. Kim, J. Cheon, Chem. Soc. Rev. 44 (2015) 4501–4516.

[125] H. Niu, Y. Zheng, S. Wang, L. Zhao, S. Yang, Y. Cai, J. Hazard. Mater. 346 (2018) 174–183.

[126] Y. Shao, T. Jing, J. Tian, Y. Zheng, RSC Adv. 5 (2015) 103943–103955.

[127] M. Sharafeldin, G.W. Bishop, S. Bhakta, A. El-Sawy, S.L. Suib, J.F. Rusling, Biosens. Bioelectron. 91 (2017) 359–366.

[128] X. Yang, X. You, B. Zhang, C. Guo, C. Yu, Water Science and Technology. 76 (2017) 1676–1686.

[129] G. del C. Pizarro, O.G. Marambio, M. Jeria-Orell, J. Sánchez, D.P. Oyarzún, Chem. Phys. Lett. 693 (2018) 183–187.

[130] F. Gambinossi, S.E. Mylon, J.K. Ferri, Adv. Colloid Interface Sci. 222 (2015) 332–349.

[131] M. Bilal, M. Asgher, R. Parra-Saldivar, H. Hu, W. Wang, X. Zhang, H.M.N. Iqbal, Sci. Total Environ. 576 (2017) 646–659.

[132] S.K. Smith, L.Z. Lugo-Morales, C. Tang, S.P. Gosrani, C.A. Lee, J.G. Roberts, S.W. Morton, G.S. Mccarty, S.A. Khan, L.A. Sombers, Chem. Phys. Chem. 19 (2018) 1–9.

[133] R.R. De Melo, R.C. Alnoch, A.F.L. Vilela, E.M. De Souza, N. Krieger, R. Ruller, H.H. Sato, C. Mateo, Molecules. 22 (2017) 1–18.

[134] A. Márquez, K. Kocsis, G. Zickler, G.R. Bourret, A. Feinle, N. Hüsing, M. Himly, A. Duschl, T. Berger, O. Diwald, J. Nanobiotechnology. 15 (2017) 55.

[135] K.J. Khorshidi, H. Lenjannezhadian, M. Zeinali, J. Chem. Technol .Biotechnol. 91 (2015) 539–546.

[136] R. Lakra, M.S. Kiran, K.P. Sai, Biomed. Mater. (Bristol, U. K.) 10 (2015) 1–9.

[137] L. Cao, Carrier-bound Immobilized Enzymes: Principles, Application and Design, John Wiley & Sons, New York, 2005.

[138] B.M. Brena, F. Batista-Viera, Immobilization of enzymes, in: J.M. Guisan (Ed.), Methods in Biotechnology: Immobilization of Enzymes and Cells, Humana Press Inc, New York, 2006, pp. 15-30.

[139] N.R. Mohamad, N.H.C. Marzuki, N.A. Buang, F. Huyop, R.A. Wahab, Biotechnol. Biotechnol. Equip. 29 (2015) 205–220.

[140] Y. Chen, C.P. Xiao, X.Y. Chen, L.W. Yang, X. Qi, J.F. Zheng, M.C. Li, J. Zhang, J. Mol. Catal. B Enzym. 100 (2014) 84–90.

[141] F. Kartal, M.H.A. Janssen, F. Hollmann, R.A. Sheldon, A. Kilinc, J. Mol. Catal. B Enzym. 71 (2011) 85–89.

[142] C. Roberge, D. Amos, D. Pollard, P. Devine, J. Mol. Catal. B Enzym. 56 (2009) 41–45.

[143] R. Taboada-Puig, C. Junghanns, P. Demarche, M.T. Moreira, G. Feijoo, J.M. Lema, S.N. Agathos, Bioresour. Technol. 102 (2011) 6593–6599.

[144] S. Talekar, V. Ghodake, T. Ghotage, P. Rathod, P. Deshmukh, S. Nadar, M. Mulla, M. Ladole, Bioresour. Technol. 123 (2012) 542–547.

[145] K. Jafari Khorshidi, H. Lenjannezhadian, M. Jamalan, M. Zeinali, J. Chem. Technol. Biotechnol. 91 (2016) 539–546.

[146] M.Q. Liu, X.J. Dai, R.F. Guan, X. Xu, Catal. Commun. 55 (2014) 6–10.

[147] D. Zhang, H.E. Hegab, Y. Lvov, L. Dale Snow, J. Palmer, SpringerPlus. 5 (2016) 1-20.

[148] J. Sánchez-Ramírez, J.L. Martínez-Hernández, P. Segura-Ceniceros, G. López, H. Saade, M.A. Medina-Morales, R. Ramos-González, C.N. Aguilar, A. Ilyina, Bioprocess Biosyst. Eng. 40 (2017) 9–22.

[149] A. Landarani-Isfahani, A. Taheri-Kafrani, M. Amini, V. Mirkhani, M. Moghadam, A. Soozanipour, A. Razmjou, Langmuir 31 (2015) 9219–9227.

[150] V. Singh, S. Kaul, P. Singla, V. Kumar, R. Sandhir, J.H. Chung, P. Garg, N.K. Singhal, Int. J. Biol. Macromol. 115 (2018) 590–599

[151] M. Royvaran, A. Taheri-Kafrani, A. Landarani Isfahani, S. Mohammadi, Chem. Eng. J 288 (2016) 414–422.

[152] R. Velmurugan, A. Incharoensakdi, Biochem. Eng. J. 122 (2017) 22–30.

[153] J. Jordan, C.S.S.R. Kumar, C. Theegala, J. Mol. Catal. B: Enzym. 68 (2011) 139–146.

[154] K. Selvam, M. Govarthanan, D. Senbagam, S. Kamala-Kannan, B. Senthilkumar, T. Selvankumar, Chin. J. Catal. 37 (2016) 1891–1898.

[155] L. Zang, J. Qiu, X. Wu, W. Zhang, E. Sakai, Y. Wei, Ind. Eng. Chem. Res. 53 (2014) 3448–3454

[156] Y.C. Lee, C.T. Chen, Y.T. Chiu, K.C.W. Wu, ChemCatChem. 5 (2013) 2153–2157.

[157] M.R. Ladole, J.S. Mevada, A.B. Pandit, Bioresour. Technol. 239 (2017) 117–126.

[158] Y. Li, X.-Y. Wang, R.-Z. Zhang, X.-Y. Zhang, W. Liu, X.-M. Xu, Y.-W. J. Nanosci. Nanotechnol. 14 (2014) 2931–2936.

[159] Q. Zhang, J. Kang, B. Yang, L. Zhao, Z. Hou, B. Tang, Chin. J. Catal. 37 (2016) 389–397.

[160] R.A. Bohara, N.D. Thorat, S.H. Pawar, Korean J. Chem. Eng. 33 (2016) 216–222.

[161] W. Zhang, J. Qiu, L. Zang, E. Sakai, H. Feng, Nano 10 (2015) 1550013.

[162] P.J. Huang, K.L. Chang, J.F. Hsieh, S.T. Chen, BioMed Res. Int. 2015 (2015) 1–9.

[163] R.E. Abraham, M.L. Verma, C.J. Barrow, M. Puri, Biotechnol. Biofuels 7 (2014) 1–12.

[164] S.H. Hosseini, S.A. Hosseini, N. Zohreh, M. Yaghoubi, A. Pourjavadi, J. Agric. Food Chem. 66 (2018) 789–798.

[165] M.L. Verma, R. Chaudhary, T. Tsuzuki, C.J. Barrow, M. Puri, Bioresour. Technol. 135 (2013) 2–6.

[166] T. Chen, W. Yang, Y. Guo, R. Yuan, L. Xu, Y. Yan, Enzyme Microb. Technol. 63 (2014) 50–57.

[167] Y. Zhou, S. Yu, Q. Liu, D. Yan, Y. Wang, L. Gao, J. Han, Sci. Rep. 7 (2017) 41741.

[168] E. Su, M. Yang, C. Ning, X. Ma, S. Deng, J. Biotechnol. 271 (2018) 1–7.

[169] M.N. Gupta, V.S. Bisaria, J. Biosci. Bioeng. 126 (2018) 445-450.

[170] K. Periyasamy, L. Santhalembi, G. Mortha, M. Aurousseau, A. Boyer, S. Subramanian, Langmuir 34 (2018) 6546–6555.

[171] J. Cui, S. Jia, L. Liang, Y. Zhao, Y. Feng, Sci. Rep. 5 (2015) 14203.

[172] L. Zhou, Y. He, L. Ma, Y. Jiang, Z. Huang, L. Yin, J. Gao, Bioresour. Technol. 247 (2018) 568–575.

[173] I.A. Pavel, S.F. Prazeres, G. Montalvo, C. García Ruiz, V. Nicolas, A. Celzard, F. Dehez, L. Canabady-Rochelle, N. Canilho, A. Pasc, Langmuir. 33 (2017) 3333–3340.

[174] D.M. Liu, J. Chen, Y.P. Shi, Int. J. Biol. Macromol. 105 (2017) 308–316.

[175] W.J. Goh, V.S. Makam, J. Hu, L. Kang, M. Zheng, S.L. Yoong, C.N.B. Udalagama, G. Pastorin, Langmuir 28 (2012) 16864–16873.

[176] P.S. Bagus, E.S. Ilton, C.J. Nelin, Surf. Sci. Rep. 68 (2013) 273–304.

[177] M. Eltarahony, S. Zaki, Z. Kheiralla, D. Abd-El-haleem, Biotechnol. Rep. (Amsterdam) 18 (2018) e00257.

[178] M. Yu, D. Liu, L. Sun, J. Li, Q. Chen, L. Pan, J. Shang, S. Zhang, W. Li, Int. J. Biol. Macromol. 103 (2017) 424–434.

[179] J. Epp, X-ray diffraction (XRD) techniques for materials characterization, Elsevier, New York, 2016.

[180] A.J. Miles, B.A. Wallace, Biophys. Charact. Proteins Dev. Biopharm. (2014) 109–137.

[181] H. Ren, Y. Zhang, J. Su, P. Lin, B. Wang, B. Fang, S. Wang. J. Biotechnol. 241 (2017) 33–41.

[182] I. Correia, S. Aksu, P. Adão, J.C. Pessoa, R.A. Sheldon, I.W.C.E. Arends, J. Inorg. Biochem. 102 (2008) 318–329.

[183] A.B. Muley, S.A. Chaudhari, K.H. Mulchandani, R.S. Singhal, Int. J. Biol. Macromol. 111 (2018) 1047–1050.

[184] A. Gricajeva, S. Kazlauskas, L. Kalėdienė, V. Bendikienė, Int. J. Biol. Macromol. 108 (2017) 1165-1175.

[185] A. Gong, C.T. Zhu, Y. Xu, F.Q. Wang, D.K. Tsabing, F.A. Wu, J. Wang, Sci. Rep. 7 (2017) 1–15.

[186] S.A. Chaudhari, R.S. Singhal, Int. J. Biol. Macromol. 98 (2017) 610–621.

[187] F. Secundo, Chem. Soc. Rev. 42 (2013) 6250-6261.

[188] J. Cui, Y. Zhao, Z. Tan, C. Zhong, P. Han, S. Jia, Int. J. Biol. Macromol. 98 (2017) 887–896.

[189] Z. Chen, Y. Wang, W. Liu, J. Wang, H. Chen, Int. J. Biol. Macromol. 95 (2017) 650–657.

[190] M. Khoobi, S.F. Motevalizadeh, Z. Asadgol, H. Forootanfar, A. Shafiee, M.A. Faramarzi, Mater. Chem. Phys. 149 (2015) 77–86.

[191] J. Grewal, R. Ahmad, S.K. Khare, Bioresour. Technol. 242 (2017) 236–243.

[192] J. Han, L. Wang, Y. Wang, J. Dong, X. Tang, L. Ni, L. Wang, Biochem. Eng. J. 130 (2018) 90–98.

[193] K. Jafari Khorshidi, H. Lenjannezhadian, M. Jamalan, M. Zeinali, J. Chem. Technol. Biotechnol. 91 (2016) 539–546.

[194] A. Kumar, S. Singh, L. Nain, Int. J. Curr. Microbiol. Appl. Sci. 7 (2018) 881–893.

[195] M.R. Ladole, J.S. Mevada, A.B. Pandit, Bioresour. Technol. 239 (2017) 117–126.

[196] J. Jia, W. Zhang, Z. Yang, X. Yang, N. Wang, X. Yu, Molecules. 22 (2017) 269-282.

[197] Q. Zhen, M. Wang, W. Qi, R. Su, Z. He, Catal. Sci. Technol. 3 (2013) 1937–1941.

[198] R.E. Abraham, M.L. Verma, C.J. Barrow, M. Puri, Biotechnol. Biofuels. 7 (2014) 1–12.

[199] P.J. Huang, K.L. Chang, J.F. Hsieh, S.T. Chen, Biomed Res. Int. 2015 (2015) 1–9.

[200] J. Jordan, C. Theegala, Biomass Conv. Bioref. 4 (2014) 25–33.

[201] Q. Chen, D. Liu, C. Wu, K. Yao, Z. Li, N. Shi, F. Wen, I.D. Gates, Bioresour. Technol. 263 (2018) 317–324.

[202] Y. Xu, P. Hellier, S. Purton, F. Baganz, N. Ladommatos, Appl. Energy. 172 (2016) 80–95.

[203] M. Balat, Energy Convers. Manag. 52 (2011) 858–875.

[204] A.P. Ingle, J. Rathod, R. Pandit, S. Silverio, Cellulose. 24 (2017) 5529–5540.

[205] B.C. Saha, J Ind Microbiol Biotechnol. 30 (2003) 279–291.

[206] L. Jia, G.A.L.G. Budinova, Y. Takasugi, S. Noda, T. Tanaka, H. Ichinose, M. Goto, N. Kamiya, Biochem. Eng. J. 114 (2016) 268–275.

[207] A. Purohit, S.K. Rai, M. Chownk, R.S. Sangwan, M. Clea, Bioresour. Technol. 244 (2017) 793–799.

[208] M.Q. Liu, X.J. Dai, R.F. Guan, X. Xu, Catal. Commun. 55 (2014) 6–10.

[209] H. Shahrestani, A. Taheri-kafrani, A. Soozanipour, O. Tavakoli, Biochem. Eng. J. 109 (2016) 51–58.

[210] A. Soozanipour, A. Taheri-kafrani, A. Landarani, Chem. Eng. J. 270 (2015) 235–243.

[211] M. Perwez, R. Ahmad, M. Sardar, Int. J. Biol. Macromol. 103 (2017) 16–24.

[212] Y. Zhang, J.W. Chan, A. Moretti, K.E. Uhrich, J Control Release. 10 (2016) 355–368.

[213] E. Zakharova, S. León, A. Martínez, D. Ilarduya, Eur. Polym. J. 92 (2017) 1–12.

[214] H. Shin, J.W. Nichol, A. Khademhosseini, Acta Biomater. 7 (2011) 106–114.

[215] R.K. Tekade, X. Sun, Drug Discov. Today. 22 (2017) 1637–1653.

[216] N.M. Xavier, A.P. Rauter, Y. Queneau, Top Curr. Chem. 295 (2010) 19–62.

[217] S. Ramachandran, P. Fontanille, A. Pandey, C. Larroche, Food Technol. Biotechnol. 44 (2006) 185–195.

[218] C.M. Wong, K.H. Wong, X.D. Chen, Appl Microbiol Biotechnol. 78 (2008) 927–938.

[219] J.C. Barbe, G. De Revel, A. Bertrand, J. Agric. Food Chem. 50 (2002) 6408–6412.

[220] Y. Pocker, E. Green, J. Am. Chem. Soc. 95 (1973) 113–119.

[221] K. Morawa Eblagon, M.F.R. Pereira, J.L. Figueiredo, Appl. Catal. B Environ. 184 (2016) 381–396.

[222] M. Abbasi, R. Amiri, A.K. Bordbar, E. Ranjbakhsh, A.R. Khosropour, Appl. Surf. Sci. 364 (2016) 752–757.

[223] N. Pachauri, B. He, Am. Soc. Agric. Biol. Eng. 300 (2006) 1–16.

[224] S.N. Ruzheinikov, J. Burke, S. Sedelnikova, P.J. Baker, R. Taylor, P. a. Bullough, N.M. Muir, M.G. Gore, D.W. Rice, Structure 9 (2001) 789–802.

[225] M. Zheng, S. Zhang, Biocatal. Biotransformation. 29 (2011) 278–287.

[226] A.N. Zelikin, P.N. Zawaneh, D. Putnam, Biomacromolecules. 7 (2006) 3239–3244.

[227] J.R. Weiser, P.N. Zawaneh, D. Putnam, Biomacromolecules. 12 (2011) 977–986.

[228] P.W. Henderson, D.J.M. Kadouch, S.P. Singh, P.N. Zawaneh, J. Weiser, S. Yazdi, A. Weinstein, U. Krotscheck, B. Wechsler, D. Putnam, J.A. Spector, J. Biomed. Mater. Res. - Part A. 93 (2010) 776–782.

[229] K. Iiyama, T. Lam, B.A. Stone, Covalent Cross-Links in the Cell Wall, Plant Physiol. 104 (1994) 315–320.

[230] P.T. Martone, J.M. Estevez, F. Lu, K. Ruel, M.W. Denny, C. Somerville, J. Ralph, Curr. Biol. 19 (2009) 169–175.

[231] G. de Gonzalo, D.I. Colpa, M.H.M. Habib, M.W. Fraaije, J. Biotechnol. 236 (2016) 110–119.

[232] G. Janusz, A. Pawlik, J. Sulej, U. Świderska-Burek, A. Jarosz-Wilkolazka, A. Paszczyński, FEMS Microbiol. Rev. 41 (2017) 941–962.

[233] E.N. Zwane, P.J. van Zyl, K.G. Duodu, S.H. Rose, K. Rumbold, W.H. van Zyl, M. Viljoen-Bloom, J. Food Sci. Technol. 54 (2017) 778–785.

[234] S.M. Gadalkar, V.K. Rathod, Biocatal. Agric. Biotechnol. 10 (2017) 342–351.

# *Chapter 2*

## *Synthesis and characterization of magnetic cross-linked enzyme aggregates of cellulases for the potential application in producing cello-oligosaccharides*

**ABSTRACT**

Formation of magnetic cross-linked enzyme aggregates (MCLEAs) is an interesting enzyme immobilization approach. In this study, different MCLEAs of cellulases were prepared and evaluated for the potential application in producing cello-oligosaccharides. Firstly, the MCLEAs were prepared in the presence of magnetic nanoparticles with three different precipitation agents (ammonium sulfate, ethanol and PEG 600). After cellulases immobilization, highest values of enzymatic activity (193.42 U $g^{-1}$) and activity recovery (43.53 %) were observed with the use of ethanol as precipitation agent, while that PEG leaded to MCLEAs with the highest reusability capacity (80% of initial relative activity after five reaction cycles). For the first time, the colloidal properties of MCLEAs were characterized by dynamic light scattering (DLS) and zeta potential analyses, which were correlated with the activity of MCLEAs. The results showed that the increased enzyme activity and thermostability of the MCLEAs were attributed to improvement in colloidal stability compared to free cellulase. Finally, the MCLEAs were assessed for the hydrolysis of cellulose-derived from sugarcane bagasse and straw. Despite the low hydrolysis efficiency, the use of MCLEAs led to the production of cello-oligosaccharides (COS) with degrees of polymerization (DP) of 3, 6 and 12 compared to the DP of 3 and 6 with free cellulase. The increase in DP may lead to the production of high-value COS prebiotics from lignocellulosic biomass compared to low DP COS.

**Keywords:** magnetic nanoparticles, enzyme immobilization, glucose polymers, biomass waste, enzymatic catalyst

## 2.1 Introduction

Cellulases are a complex of enzymes consisting of endoglucanases, exoglucanases and β-glucosidase [1]. These three enzymes act synergistically to produce glucose from cellulose, the most abundant low-cost carbohydrate polymer in nature [2]. Briefly, endoglucanases hydrolyze 1,4-glycosidic bonds at amorphous regions of the cellulose fiber and produce long-chain oligomers while exoglucanases act on the ends of cellulose oligomers with the production of cello-oligosaccharides (COS) [3]. Furthermore, COS are broken to glucose by β-glucosidases [4]. Enzymatic hydrolysis of cellulose to produce glucose has been extensively studied for second generation ethanol production [5], [6], [7]. However, the high enzyme cost is one of the significant cost barriers towards commercialization of cellulosic ethanol production [8]. In order to reduce the enzyme cost, recovery and recycling of cellulases have been extensively studied [9], [10], [11], [12]. Among various recovery and recycling methods, cellulase immobilization is often investigated [13], [14], [15], [16].

Cross-linked enzyme aggregates (CLEAs) is a robust immobilization technology because maintenance of pre-organized superstructures in the formation of CLEAs leads to good mechanical stability and retaining high enzyme activity [17]. CLEAs consist in physical aggregates of enzyme molecules obtained by use of precipitation agents (e.g., solvents, salts or polymers), which maintain their native tertiary structure, interlinked with each other through of cross-linked agents as glutaraldehyde [17]. When precipitation is carried out on solid support surface, CLEAs can be covalent bonded to support by cross-linked agent, allowing to ally vantages from CLEAs to inherent properties of the support, strategy which can produces unique catalysts. Among many supports, magnetic nanoparticles (MNP), such as magnetite ($Fe_3O_4$) has gained attention due to its high surface area, loading capacity, low toxicity and mainly, magnetic properties, which allow selective recovering from the reaction medium by applying an external magnetic [18], [19], [20].

MNPs can be functionalized through several approaches, including chitosan-based surface, silica-based surface, graphene-based surface, amino-based surface, which have been summarized in review papers [21], [22]. In one recent study MCLEAs of cellulases on amino-functionalized MNPs showed a better activity at a wider temperature range and pH values than that of the free cellulase and achieved an activity recovery of 74% on carboxymethylcellulose after six reaction cycles [23]. However, hydrolysis yield on bamboo biomass by MCLEAs was only 21% compared to 44% achieved with free cellulases at a biomass concentration of 0.075%. In the other study, cellulase MCLEAs on aminosilane-coated MNPs retained about 45% of its

maximum activity at pH above 4.89 while free cellulase lost its activity sharply [24]. In addition, MCLEAs retained about 65% of its maximum activity at 80 °C and had improved thermal stability at 65 °C. Lastly, MCLEAs retained 30% of its initial activity through 6 cycles of reuse.

Despite the interest in cellulase immobilization, the studies on MCLEAs of cellulases are still very limited. In addition, the mechanisms of the improved stability and enzyme activity of cellulase MCLEAs have not been fully understood. Furthermore, previous studies on cellulase immobilized were mainly focused on the hydrolysis of biomass to fermentable sugars for producing biofuels (e.g., ethanol), which will not be economically feasible in the near future due to the relatively high enzyme and immobilization cost and low value of biofuels. In this study, cellulase MCLEAs were further studied. MCLEAs were firstly prepared on chitosan-modified MNPs with the use of different precipitation agents. MNPs and MCLEAs were characterized, including dynamic light scattering (DLS) and zeta potential analyses to understand colloidal properties of MCLEAs, which were correlated with the activity of MCLEAs for the first time. Furthermore, the MCLEAs was used to hydrolyze cellulose from sugarcane bagasse and straw and assessed to cello-oligosaccharides (COS) production, an important class of biologically active carbohydrates with prebiotic properties [25], [26], [27]. In addition to monitoring the hydrolysis yield, the degree of polymerization (DP) of the COS obtained were also determined. Since higher molecular weight COS are currently produced in small amounts and with a 500 times more expensive cost than those with lower DP [28], [29], the results indicated that the MCLEAs may be used to produce COS with higher DP for higher value application compared to the use of free cellulases.

## 2.2 Experimental section

### 2.2.1 Materials

Iron(II) chloride tetrahydrate (≥99 %), iron(III) chloride hexahydrate (97%), chitosan with low molecular weight and 70% deacetylation degree, glutaraldehyde (25%), cellulase from *Trichoderma longibrachiatum* (~0.5 U $mg^{-1}$ enzyme activity and 175 mg $g^{-1}$ protein content), PEG 600, citric acid (≥99.5) and Bradford reagent were purchased from Sigma-Aldrich (USA). Ammonium sulfate (≥99.5%), ethanol (96%), carboxymethylcellulose sodium salt (CMC), 3,5-dinitrosalicylic acid (98%) (DNS) and sodium phosphate dibasic (>99%) were acquired from

Neon (Brazil) and ammonium hydroxide (28%) was obtained from Merck (USA). All the starting materials and solvents were used without further purification. Sugarcane bagasse and straw were obtained from the São Martinho Mill (Américo Brasiliense, São Paulo, Brazil).

### 2.2.2 Characterization

Magnetic nanoparticles and MCLAs were characterized by powder X-ray diffraction (PXRD), Fourier transform infrared (FT-IR) spectroscopy, thermogravimetric analyses (TGA) and dynamic light scattering (DLS). PXRD patterns were obtained using a Rigaku model RINT 2000 diffractometer, in the 2θ range 5-70°, with Cu Kα radiation (λ = 1.5418 Å), a scanning speed of 1 s/step, and a step size interval of 0.02°. For magnetite, PXRD diffractogram was simulated using Mercury 3.0 software and Cu Kα radiation (λ= 1.5418 Å) and CIF file AMCSD-2400, crystal system cubic and space group Fd3m. FTIR spectra were acquired in the range 4000-400 $cm^{-1}$, with resolution of 4 $cm^{-1}$ and 32 scanning, using KBr pellets and a PerkinElmer FT-IR Frontier spectrophotometer. TGA measurements were performed using a PerkinElmer TGA 4000 thermogravimetric analyzer, with heating from room temperature to 800 °C at a rate of 10 °C $min^{-1}$, under a $N_2$ atmosphere (20 mL $min^{-1}$). DLS measures were carried out in a Malvern Instruments Zetasizer Nano Series System in quartz cuvettes and performed in triplicates at 25 °C.

In order to better understanding the effect of pH and temperature in the activity of MCLEAs and free cellulase, DLS measurements were carried out at the same net conditions studied in the enzymatic activity assay. At the same Malvern Instruments Zetasizer Nano Series System, zeta-potential (ζ-potential ) measures were obtained to evaluate the influence of pH at colloidal stability of MCLEAs.

Molecular weights (Mn and Mw), polydispersity index (PDI) and degree of polymerization (DP) of COS obtained after hydrolysis of cellulose from sugarcane bagasse and straw mixture were characterized by a Malvern Instrument GPC analysis system, using three conjoined chromatography columns (SHODEX – Ohpak SB-806M HQ) at 45 °C, where aqueous $NaNO_3$ 0.1 mol $L^{-1}$ with flow rate of 1 mL $mim^{-1}$ was used as eluent and polystyrene (Malvern instrument) as the calibration standard. The retention volume was determined by a refraction index detector. DP values were calculated as the ratio between molecular weight (Mn) and the molecular mass of glucose (180.16 g $mol^{-1}$).

### 2.2.3 One-step synthesis of chitosan-coated magnetic nanoparticles (NP-CH)

NP-CH was synthesized in an one-step processing by conventional co-precipitation method using iron(II) and iron(III) in alkaline medium [30]. In a three-neck round-bottom flask equipped with a reflux condenser and argon atmosphere were added 100 mL of $Fe^{2+}$:$Fe^{3+}$ (1:2) solution and 125 mg of chitosan. The mixture was kept under a stirring speed of 400 rpm at 50 °C until complete dispersion of chitosan. The precipitation of NP-CH was carried out with a dropwise addition of 30 mL of ammonium hydroxide, followed by keeping the stirring at 400 rpm at 50 °C for 30 min. NP-CH were recovered by using a permanent magnetic, washed several times and stored in ultrapure water until characterization and MCLEAs synthesis.

### 2.2.4 Synthesis of cellulases MCLEAs

MCLEAs were obtained using glutaraldehyde as a cross-linker and three different precipitation agents: ammonium sulfate (MCLEA-AS), PEG 600 (MCLEA-PEG) and ethanol (MCELA-ET). For MCLEAs synthesis, 100 mg of NP-CH and 120 µL of glutaraldehyde were dispersed in 10 mL of phosphate-buffered saline (pH 7) and kept under stirring at 120 rpm and room temperature. After 1 h, 10 mL of 5 mg $mL^{-1}$ cellulase solution in acetate buffer were added and the mixture was stirred at 120 rpm and room temperature for 1 h. After that, 10 mL of precipitation agent were added to the above mixture, and the new mixture was stirred at 120 rpm and 4 °C for 12 h to form cellulase aggregates. After enzyme immobilization, MCLEAs were recovered by magnetic adsorption, washed 3 times with distillated water and stored in acetate buffer until characterization, enzyme activity assay and COS production.

### 2.2.5 Determination of enzyme loading efficiency

Enzyme loading efficiency was determined by two methods. The first method was based on protein loss in the solution before and after immobilization using Bradford assay [31]. Enzyme loading efficiency was calculated based on the following equation:

$$Enzyme\ loading\ efficiency\ (\%) = \frac{C_0V_0 - C_sV_s}{C_0V_0}\ x\ 100 \qquad Eq.1$$

where $C_0$ is the initial protein concentration (mg $mL^{-1}$), $V_0$ the initial volume of protein (mL), $C_s$ the protein concentration in the total supernatant (mg $mL^{-1}$) and $V_s$ is the total volume of supernatant (mL).

The second method was based on TGA of MCLEAs and the calculation method was presented in Eq. 2. For this purpose, enzyme loading efficiency (%) was obtained from the ratio between final protein mass calculated by mass loss attributed to cellulase in the TGA curves of the MCLEAs and the initial protein mass used in the immobilization processes.

$$Enzyme\ loading\ efficiency\ (\%) = \frac{Final\ protein\ mass}{Initial\ protein\ mass}\ x\ 100 \qquad Eq.2$$

### 2.2.6 Enzyme activity assay (optimal pH and temperature condition)

The activities of MCLEAs and free cellulase were determined by measuring of reducing sugar production after reaction of each sample with CMC, based on DNS method and using glucose as a standard [32]. The reaction mixture contained 0.9 mL of 0.44% CMC solution in citrate-phosphate buffer (pH 5) and 0.1 mL of enzyme solution. The CMC hydrolysis reaction was carried out for 1 h at 30, 37, 45, 50, 55, 63 and 70 °C, after which 1.5 mL of DNS reagent was added to stop the reaction, followed by heating the mixture in boiling water for 5 min to allow color formation. After cooling the reaction solutions to room temperature, the optical density (OD) of the solution was measured at 540 nm using a UV-Vis spectrophotometer. Reducing sugar concentration was calculated based on OD values with the use of glucose as the standard. In the respective optimal temperature condition for each sample, was determined the optimal pH (3, 4, 5, 6 and 7) for enzymatic activity as described above. The amount of enzyme needed to catalyze the release of 1 μmol of reducing sugar equivalent per min was defined as one unit (1 U) of enzymatic activity.

For free cellulase and all MCLEAs, the enzymatic activity was expressed as the relative activity, i.e., the ratio between the activity on each set of values of pH and temperature and the activity in the optimal condition. Lastly, for each MCLEA was calculated the activity recovery value, the ratio between the MCLEA and the free cellulase activity.

### 2.2.7 MCLEAs reusability assay

Reusability assay was carried out in the optimal conditions of pH and temperature using 0.44% CMC solution in citrate-phosphate buffer as substrate. In an Erlenmeyer flask was added 9 mL of CMC solution and 1 mL of respective MCLEA. After 1 h of reaction under stirring of 120 rpm, MCLEAs were magnetically recovered, washed with citrate-phosphate buffer and submitted to new reaction, whereas the obtained hydrolysates were evaluated to UV-Vis measure to determine the reducing sugar production in each cycle as well total production after all cycles.

### 2.2.8 Cellulose obtained from sugarcane bagasse and straw mixture

Cellulose was obtained from sugarcane bagasse and straw mixture (1:1 w/w) after thermic and alkali pre-treatment. Delignification was carried out in autoclave using a 1000 mL Erlenmeyer flask with 2.5% (w/v) NaOH solution and 1:20 solid-liquid fraction, at temperature of 110 °C. After 20 min of delignification process, the solid fraction obtained was recovery and washed several times until pH 7 and lignin removal. After this, the cellulosic fraction was dried at room temperature and characterized regarding cellulose, lignin, hemicellulose and ash content. Dried cellulose showed 59.68 ± 1.42 % of cellulose, 11.06 ± 1.59 % of lignin, 26.68 ± 0.44 % of hemicellulose and 1.48 ± 0.62 % of ash.

### 2.2.9 Hydrolysis of cellulose from sugarcane bagasse and straw

Cellulose hydrolysis assay was carried out in water-bath with stirring of 120 rpm, at same optimal conditions determined in enzymatic activity assay for free cellulase enzyme and each MCLEAs. In a 125 mL Erlenmeyer flask, 25 mL of acetate buffer, 2.5 mL of enzymatic solution and 1.25 g of cellulose from sugarcane bagasse and straw mixture were added and the mixture was kept under heating and stirring by 24 h. After reaction, the supernatant was recovered by filtration and submitted to UV-Vis analysis based on DNS method to reducing sugar quantification and GPC analysis for qualitative characterization of COS produced. Hydrolysis efficiency was defined as ratio between reducing sugar produced by units of enzymatic activity employed in the hydrolysis reaction.

## 2.3 Results and discussion

### 2.3.1 Synthesis and characterization of NP-CH and MCLEAs

The one-step synthesis by coprecipitation method leaded to a satisfactory obtention of chitosan-coated magnetic nanoparticles. As shown in Fig. 1, matching curves were obtained between the PXRD patterns of NP-CH and simulated profile of magnetite ($Fe_3O_4$), indicating formation of this crystalline phase. In respect to cellulase enzymes immobilization, independent of precipitation agent used, no changes in crystalline structure of NP-CH was observed, which is an important aspect to maintaining of magnetic properties of nanoparticles and, consequently, of reusability capacity of biocatalyst.

**Fig. 1.** PRXD patterns simulated of magnetite ($Fe_3O_4$), and as-synthesized NP-CH and of all MCLEAs obtained with different precipitation agents.

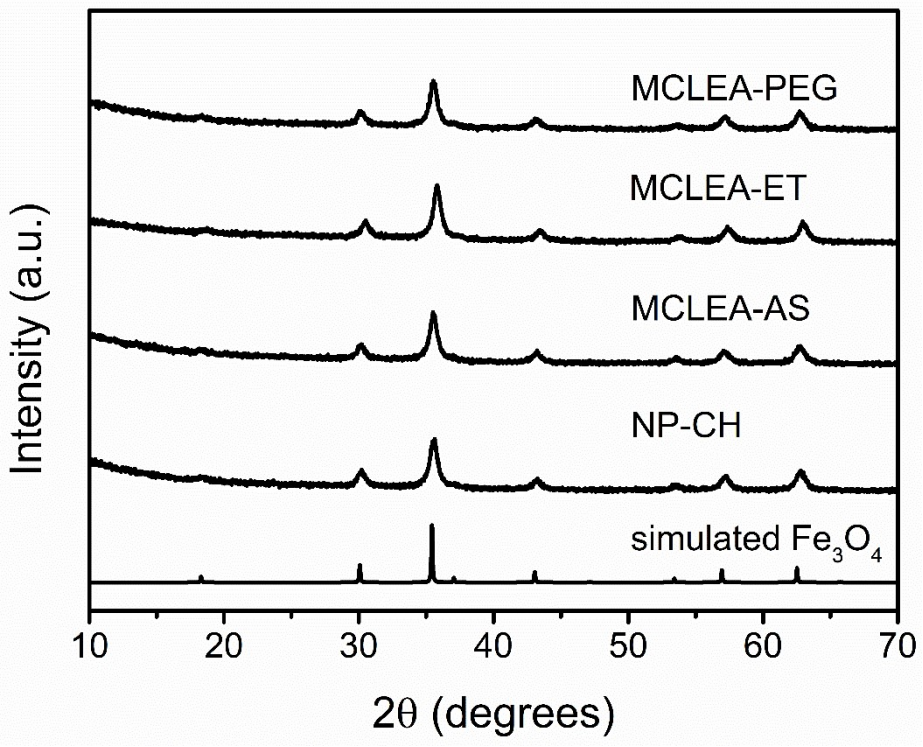


The peaks broadening viewed in the diffractograms of Fig. 1 can be used as an evidence of the nanometric scale of NP-CH and MCLEAs and [33], indeed, as shown in Tab. 1, measures of hydrodynamic diameter (Dh) performed by DLS confirm this evidence. NP-CH showed a Dh of almost 65 nm and after enzyme immobilization was observed an increase in the Dh of

nanoparticles attributed to aggregation and cross-linker of cellulase enzyme on the magnetic nanoparticle surface. Besides that, this increase in the Dh of NP-CH is an indicative of enzyme immobilization. The highest Dh (121.93 nm) was observed using ethanol as precipitation agent. Both NP-CH and all MCLEAs showed a small polydispersity index (PDI), always lower than 0.20, indicating a satisfactory homogeneity of particle-size distribution.

**Tab. 1.** Hydrodynamic diameter (Dh, mean ± standard deviation) and polydispersity index (PDI, mean ± standard deviation) for NP-CH and MCLEAs obtained with different precipitation agents.

| Sample | Dh (nm) + sd | PDI + sd |
|---|---|---|
| **NP-CH** | 65.23 ± 2.23 | 0.20 ± 0.04 |
| **MCLEA-AS** | 118.45 ± 1.00 | 0.16 ± 0.01 |
| **MCLEA-ET** | 121.93 ± 0.71 | 0.10 ± 0.01 |
| **MCLEA-PEG** | 103.35 ± 0.23 | 0.11 ± 0.01 |

The surface modification of magnetic nanoparticles and cellulase immobilization can also be observed by the FTIR spectra showed in Fig. 2. In accordance with that reported in the literature, the FTIR spectrum of NP-CH (Fig 2a), the presence of chitosan was confirmed with the bands assigned to stretching (ν) of the O–H and N–H bonds at 3334 $cm^{-1}$; C–H at 2896 $cm^{-1}$; C–N at 1382 $cm^{-1}$ and C–O–C at 1079; as well to bending mode (δ) of N–H bond at 1654 $cm^{-1}$ [30]. The band centered at 580 $cm^{-1}$ in the FTIR spectrum of NP-CH was attributed to characteristic νFe-O of the magnetite structure [34]. Regarding the cellulase immobilization, the presence of the enzyme in all MCLEAs synthesized was confirmed by characteristic bands of protein structure of cellulase (Fig 2b) at 1609 $cm^{-1}$ assigned to stretching of the C–O bond and at 1384 attributed to bending mode of N–H bond. The band centered at 1245 $cm^{-1}$ can be assigned to interaction of the carbonyl group of cellulases enzymes with a hydroxyl group of NP-CH nanoparticles [35].

**Fig. 2.** (a) FTIR spectra of chitosan and NP-CH; (b) FTIR spectra of free cellulase enzyme, NP-CH and all MCLEAs obtained with different precipitation agents.

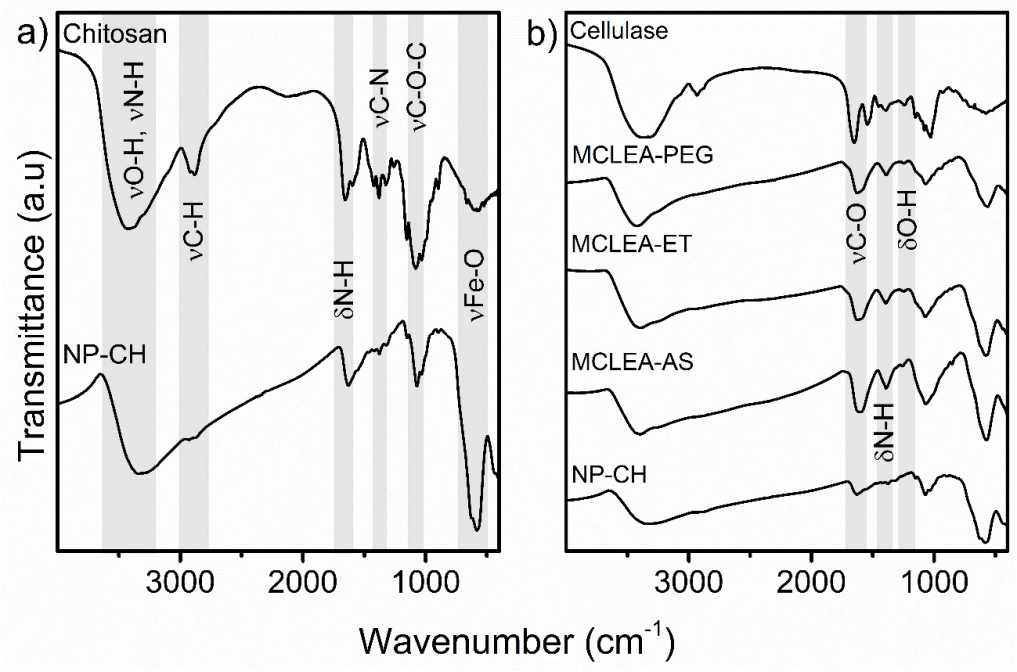


Quantitative analysis of immobilization is showed by TGA and Bradford protein assay. The Fig. 3 shows the TGA curves for NP-CH, chitosan, free cellulase enzymes and all MCLEAs synthesized. The TGA curve of NP-CH (black solid line) showed a mass loss of ~8% from room temperature until ~400 °C, attributed to the thermal decomposition of chitosan molecules (black dashed line). When compared to NP-CH TGA curve, an increase in the mass loss from room temperature until ~400 °C of 13.77% for MCLEA-AS, 14.66 % for MCLEA-PEG and 15.75% for MCLEA-ET were observed and assigned to thermal decomposition of cellulase enzymes cross-linked to NP-CH surface.

**Fig. 3.** TGA curves for NP-CH, free cellulase enzyme, chitosan and all MCLEAs synthesized with different precipitation agents.

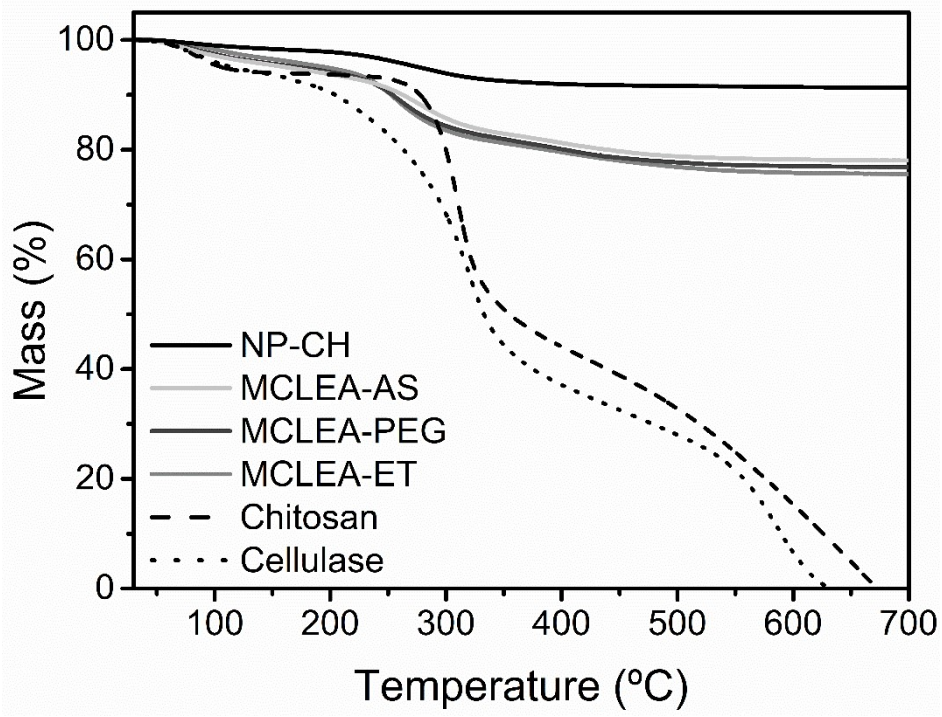


These mass losses were used to determine the enzyme loading efficiency, which is shown in Tab. 2. In all cases, independent of precipitation agent used in the MCLEAs syntheses, an enzyme loading efficiency higher than 40% was obtained, especially when ethanol was used as precipitation agent (47.25% of loading efficiency). Bradford protein assay also was carried out in order to assess the enzyme loading efficiency. In all cases, an immobilization efficiency upper to 50% and higher than those calculated by TGA was observed, mainly when PEG was used as precipitation (59.68% of efficiency). In general, a difference near at 10% was observed between the enzyme loading efficiency obtained by TGA and by Bradford protein assay. In the Bradford method, the protein loading onto the support surface is calculated indirectly measuring the initial and final protein concentration in supernatant immobilization media, using bovine serum albumin (BSA) as standard. Aspects as significant differences in the molecular weights, amino acid sequence and exposed structure to aqueous solutions between BSA and many enzymes have been found as some limitations of Bradford method [36], [37]. Meanwhile, TGA measures the amount of protein onto support surface directly. Despite that TGA have shown a smaller loading efficiency than the Bradford method, in summary the results illustrated in this work are satisfactory when compared to many reported works [35], [38], [39]. In addition, highest cellulase loading efficiency have been observed to chitosan-coated magnetic NP, such

as the 66% observed by Sánchez-Ramírez and co-workers [35], when compared to the almost 15% for aminosilane-coated magnetic nanoparticles [38], both obtained at similar conditions of initial enzyme concentration used in this work and by Bradford protein assay. In order to enhance the stability parameters, chitosan, a biodegradable polymer, have been extensively used as a coating agent in enzyme immobilization on magnetic nanoparticles surface, mainly because can provide a positively charged surface, while acts as an adhesive enhancer for simple immobilization processes [21].

**Tab. 2.** Cellulase loading efficiency obtained by TGA and Bradford protein assay.

| Sample | Enzyme loading efficiency (%) | |
|---|---|---|
| | **TGA** | **Bradford protein assay** |
| **MCLEA-AS** | 41.31 | 51.74 |
| **MCLEA-ET** | 47.25 | 57.08 |
| **MCLEA-PEG** | 43.98 | 59.68 |

Indeed, the enzyme loading efficiency is an important aspect when considering the synthesis of satisfactory MCLEAs, but not the only one involved. In many cases, the immobilization can be attached to enzyme denaturation and, consequently, to significant losses in the enzymatic activity [40]. Thus, aspects as enzymatic activity and their stability in function of pH and temperature, recovery activity percentage and reuse capacity also are fundamental in practice applications.

### 2.3.2 Enzymatic activity assay

Aiming determination of optimal operational conditions of cellulose hydrolysis were observed the effect of pH and temperature in the MCLEAs activity. Fig. 4 shows the effect of temperature in the relative enzymatic activity of the free cellulase enzyme and MCLEAs. Changes in the temperature of CMC hydrolysis reaction provided significant changes in the relative activity of all samples. As already established in the literature, free cellulase enzymes shows a higher activity at 50 °C [41] [42]. An increase in the optimal temperate to 55 °C was observed when ethanol and ammonium sulfate were used as precipitation and to 63 °C with PEG.

**Fig. 4.** Effect of temperature at pH 5 in the relative enzymatic activity of free cellulase enzyme and MCLEAs obtained with different precipitation agents.

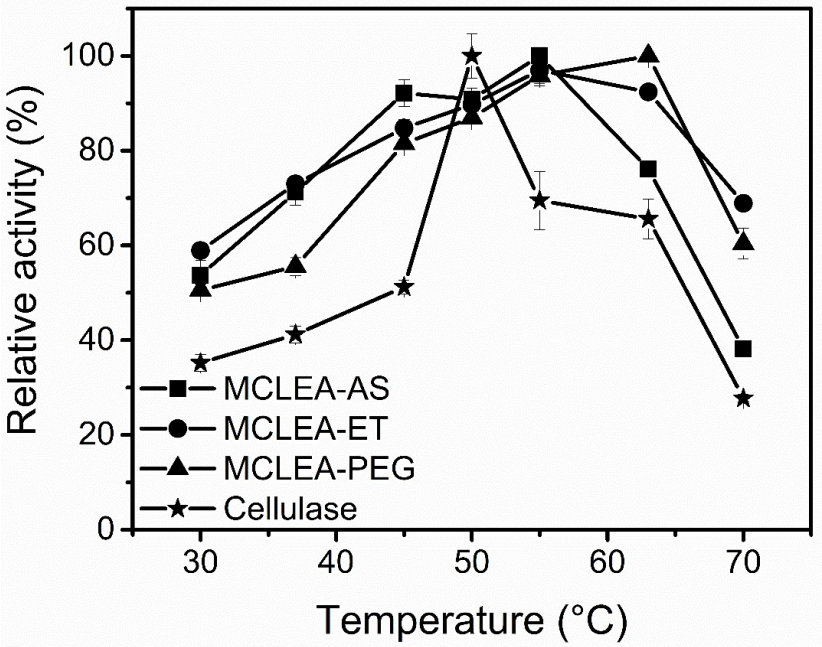


In all evaluated sample was observed the same effect of the temperature in the activity of enzymes, i.e., increase in the relative activity from low temperatures until the respective optimal temperature with subsequent activity losses. For each kind of enzyme there is an optimal temperature which the largest number of molecular collisions as possible is observed, allowing thus, the maximum reaction rate without an enzymatic denaturation [43]. However, high temperatures lead to rupture of native enzyme structure and, consequently, to significant loss in the enzymatic activity, as well observed in Fig. 4. Besides that, free enzymes tend to be more sensitive to temperature than when are in immobilized form as MCLEAs. For free cellulase, the relative activity can vary as much as 50% from optimal temperature until 45 °C and 30% until 63 °C. Meanwhile, in MCLEAs cases, changes around optimal temperature provide variation in the relative activity as little as 3% for MCLEA-PEG and MCLEA-ET, and 7% for MCLEA-AS. Thus, MCLEAs demonstrated significantly improved in preserving enzymatic activity after changes in optimal temperature compared with free cellulase. Besides that, the aggregates obtained here shows a higher thermal stability in the enzyme activity than those previously reported, e.g., when compared to variation of approximately 20% around optimal temperature observed to cellulase immobilized on silica-coated [44] or chitosan-coated [42] magnetic nanoparticles, synthesized by physical adsorption and covalent bond, respectively. The cross-linked method have produced biocatalysts by inexpensive and effective

synthesis, while precipitation agent produces physical aggregates of enzyme molecules without perturbation of their tertiary structure, cross-linker agent glutaraldehyde held it covalent bonded to nanoparticle surface, leading to obtention of highly stable and reusable biocatalysts [45]. Faced it, the cross-linking reaction employed in this work show as an important strategy to enhance thermal stability of the immobilized enzyme when compared to other immobilization method.

Particle-size distribution (PSD) measures performed by DLS were used to reach a better understanding of the temperature effect in the activity of free cellulase enzymes and MCLEAs. As shown in Fig. 5a, increasing in the temperature affects the PSD profile of cellulase enzyme. In the optimal temperature of 50 °C and below it, the native structure of cellulase appears partially aggregated near at 7 nm and 54 nm. However, above the 50 °C, PSD profile is severely affected by temperature increasing which leaded to formation of large aggregates near at 100 and 500 nm, especially in high temperature as 63 and 70 °C. This change in the PSD profile of free cellulase enzyme suggests that denaturation mechanism of cellulase enzyme by temperature effect is tied to protein aggregation, which can be causing changes in the cellulase structure as steric block of the active site. For MCLEAs, independently of the type of precipitation agent used, variations in the optimal temperature did not induce changes in the PSD profile (Fig. 5a-c), suggesting an excellent colloidal stability of these materials, which can be used to justify the most significant stability of their enzymatic activity if compared to free cellulase. The aggregation of nanoparticles has been shown to significantly reduce the activity of nanomaterials, resulting in inferior performance [46] and, therefore, one of the essential advantages of the enzyme immobilization have been to enhance the enzymatic catalytic stability [47], as shown in this work. Furthermore, nanoparticles colloidal stability, or lack thereof, will determine the dispersity and diffusion of nanomaterials as MCLAs, important aspect when goal the employment of heterogenous catalysts.

**Fig. 5.** Effect of temperature in the particle-size distribution of cellulase and MCLEAs obtained with different precipitation agents.

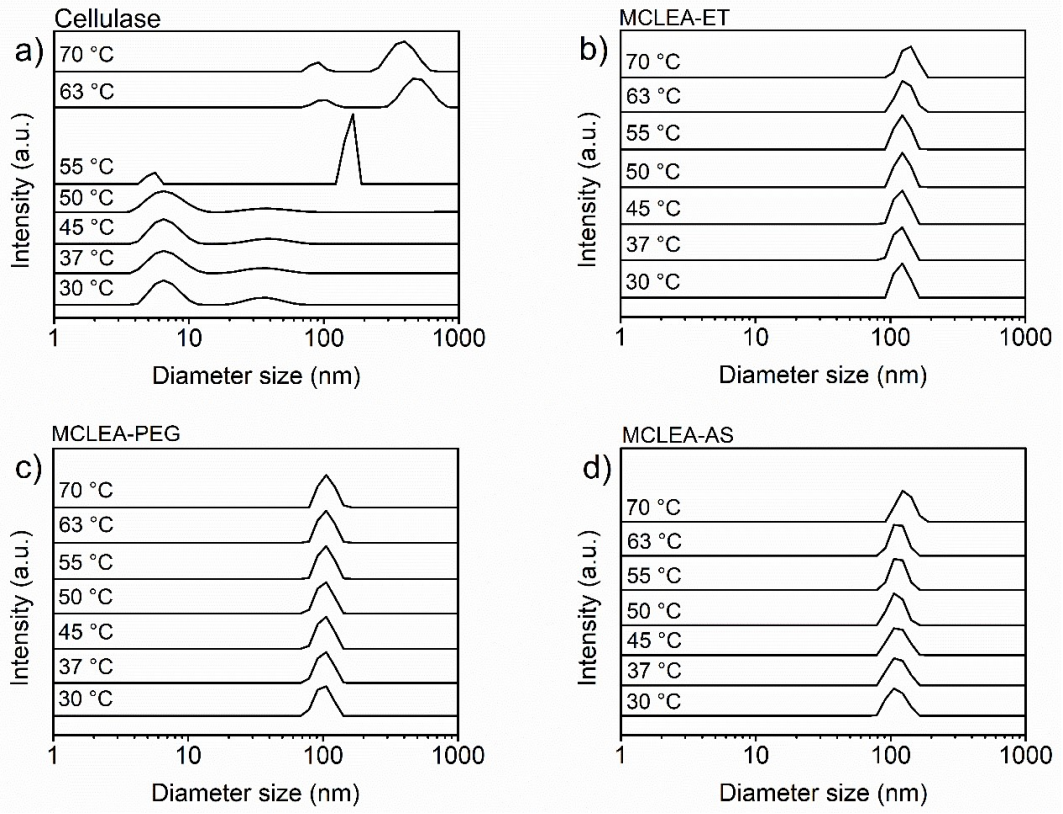


Also was observed the pH effect on the enzymatic activity of free cellulase and MCLEAs in their respective optimal temperature and these results are shown in Fig 6. The free cellulase shows the highest relative activity at pH 5, while all MCLEAs at pH 4. The presence of charges in support surface makes the concentration of charged species been different in the enzyme microenvironment in relationship to bulk solution [45] and, changes in the optimal pH of enzymes after immobilization process can be ascribed to this charge gradient [39].

**Fig. 6.** Effect of pH at optimal temperature in the relative enzymatic activity of free cellulase enzyme and MCLEAs obtained with different precipitation agents.

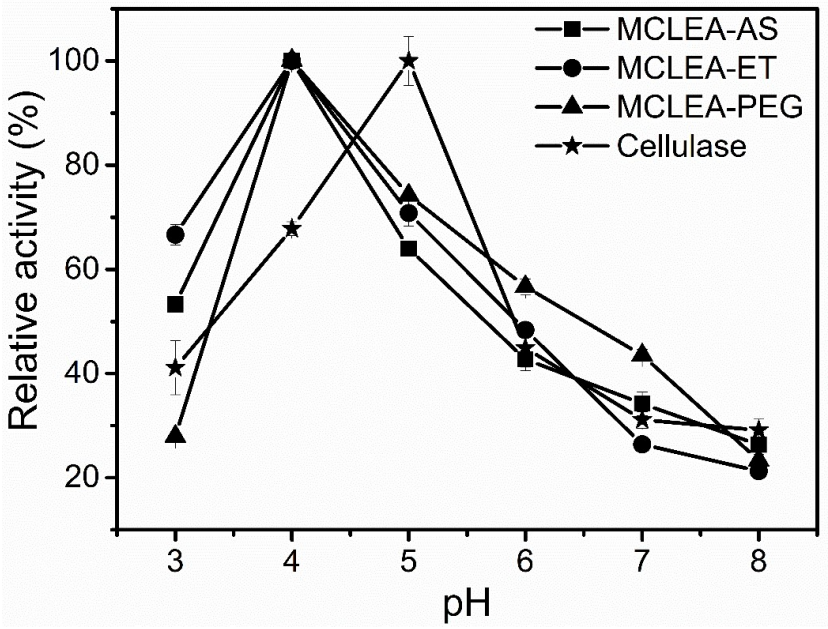


However, the obtention of MCLEAs did not increase the stability of enzymatic activity due to changes in the pH of CMC hydrolysis reaction. However, colloidal behavior of these samples can be helpfully to understand it. The pH plays an essential role in the colloidal stability of free and immobilized enzyme since dissociation reactions affect the surface charge of molecules and particles, which determines the surface potential and aggregation state [48]. As shown in Fig. 7, for free cellulase enzyme, both above and below of the optimal pH 5, was observed severe changes in its PSD profile. In more acid medium there was a formation of aggregates with almost 800 nm and more alkaline medium nearly to 200 nm.

All MCLEAs showed in pH 4 its highest relative activity and, in general, the same effect of pH in PSD profile. For MCLEA-ET, increases in pH leaded to decreases in mean particle-size from 177 nm to almost 140 nm, while decreases in pH leaded to an aggregation with a mean particle-size nearly to 230 nm. In MCLEA-AS case, was observed decreases in mean particle-size from 270 nm at pH 4 until around 140 nm with increases in pH, and pH decreases leaded to increases in mean particle-size nearly to 320 nm. Lastly, for MCLEA-PEG increases in pH leaded to decreases in mean particle-size from 188 nm to almost 120 nm, while decreases in pH leaded to an aggregation with a mean particle-size nearly to 260 nm.

**Fig. 7.** Effect of pH in the particle-size distribution of cellulase and MCLEAs obtained with different precipitation agents.

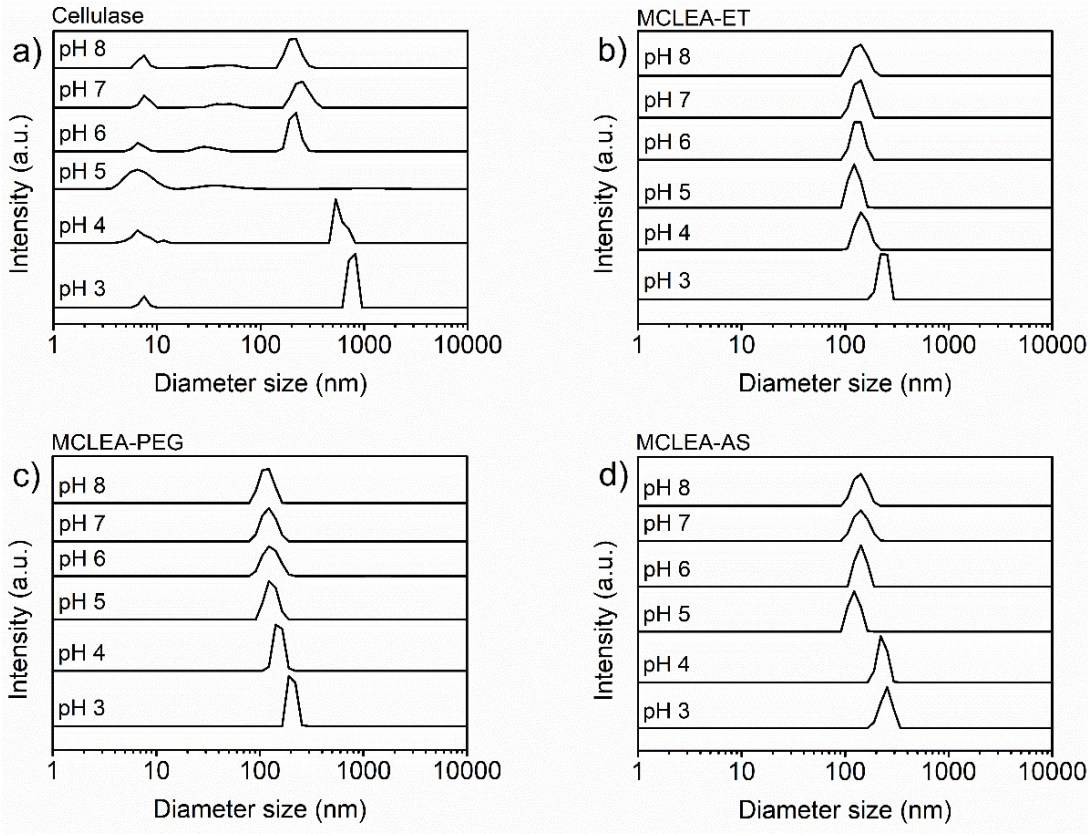


It is well established at colloidal science that changes in pH produce changes in charge of particle surface and, consequently, its aggregation state. The Fig. 8 shows the ζ-potential curve in the function of pH for each MCLEA. At pH 3, especially the MCLEA-AS and MCLEA-PEG, show a smaller ζ-potential, and its proximity with isoelectric point justify the observed increase in mean particle-size for these samples. On the other hand, in higher pH, increases in the ζ-potential leaded to an increase in the colloidal stability of particles and, due it, to a smaller increasing in the mean particle-size of MCLEAs was observed.

**Fig. 8.** ζ-potential curve in function of pH for the MCLEAs obtained with different precipitation agents.

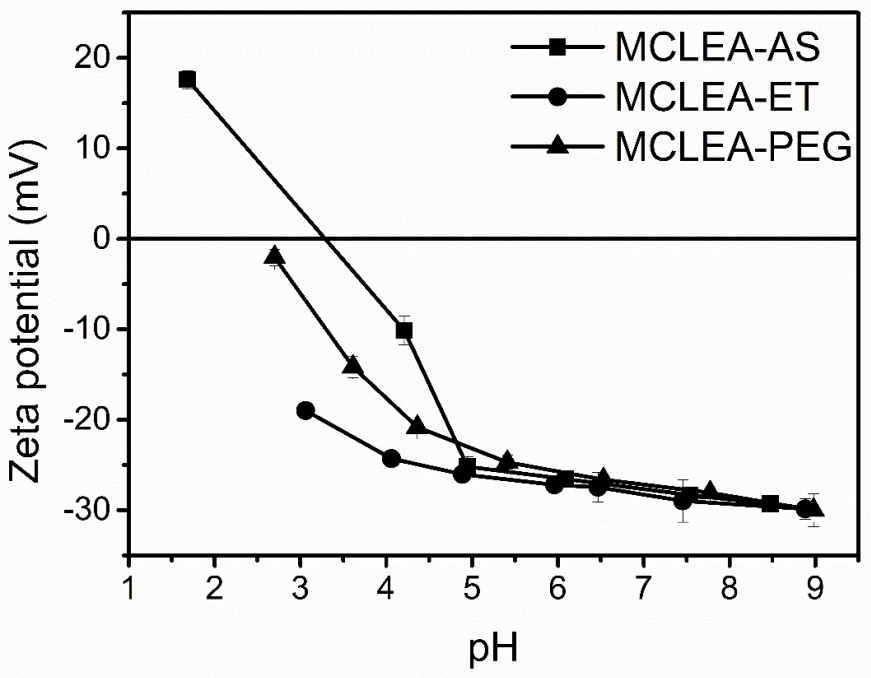


Quantitatively, different precipitation agents showed different effect in the cross-linking and enzyme aggregation, consequently, in the enzymatic activity and activity recovery of the MCLEAs. Tab. 3 shows the enzymatic activity value for the MCLEAs and free cellulase enzyme and recovery activity value for all MCLEAs. Activity recovery is a number that gives an idea of the success of immobilization process, whereof the activity of the immobilized is divided by total starting activity of the free enzyme [49].

For MCLEAs, the highest activity enzymatic was observed using ethanol as precipitation agent (193.42 U $g^{-1}$ for MCLEA-ET), while was obtained an activity of 123.40 and 130.90 U $g^{-1}$ when ammonium sulfate and PEG were used as precipitation agent, respectively. Besides having the higher enzymatic activity, ethanol also has proportioned the higher activity recovery (43.53%) when compared to 29.46 and 27.77 % of MCLEA-PEG and MCLEA-AS, respectively. Other than reducing the dielectric constant of medium leading to enzyme precipitation on support surface, organic solvents as ethanol interact with hydrophobic portion of enzymes, providing their aggregation due to electrostatic interactions between groups with opposite charge in the hydrophilic portion of enzyme, without prejudice the native protein structure and consequent denaturation [50]. When compared to free cellulase enzyme, decreases in the activity recovery values and activity losses after immobilization processes for MCLEAs can be attributed to factors as the presence of multipoint attachment to support which can result

in changes enzyme conformation, block up of active site of cellulase and losses of enzyme flexibility [21], [22]. Although have been observed losses in activity after immobilization process, the obtained values to activity recovery shows comparatively close and, in some cases, higher to some works reported in literature, e.g., to 30% showed for cellulase immobilized on silica-coated nanoparticles [51]; to 37% observed in cellulase on chitosan-coated nanoparticles [35]; and to 40% seen for cellulase immobilized on polyvinyl alcohol/$F_2O_3$ magnetic nanoparticles [52].

**Tab. 3.** Enzymatic activity and activity recovery for free cellulase enzyme and MCLEAs (mean ± sd) and their respective condition of pH and temperature.

| Sample | Enzymatic activity (U $g^{-1}$) | Activity recovery (%) | Optimal condition | |
|---|---|---|---|---|
| | | | pH | T (°C) |
| **Cellulase** | 444.24 ± 5.34 | - | 5 | 50 |
| **MCLEA-ET** | 193.42 ± 2.22 | 43.53 ± 6.78 | 4 | 55 |
| **MCLEA-AS** | 123.40 ± 1.70 | 27.77 ± 5.24 | 4 | 55 |
| **MCLEA-PEG** | 130.90 ± 2.35 | 29.46 ± 3.11 | 4 | 63 |

Frequently, the reduced enzymatic activity, low stability faced to changes in operational conditions and losses in efficiency enzymatic, characterized by low values in activity recovery, difficult the use of immobilized enzymes in industrial process [53]. However, the synthesis of cross-linked enzyme aggregates and their immobilization on magnetic support, as the MCLEAs obtained in this work, can be useful in to overcome these challenges, due principally to their satisfactory values of enzymatic activity, activity recovery and colloidal stability. Furthermore, the magnetic properties of MCLEAs can improve their reusability capacity, favoring the employment in many reaction cycles, which can significantly increase yield in process and decrease industrial cost.

### 2.3.3 Reusability assay

Fig. 9 shows the relative activity of MCLEAs after successive cycles of CMC hydrolysis. Different precipitation agents have changed the reuse capacity of MCLEAs. Samples obtained with ammonium sulfate and ethanol, MCLEA-AS and MCLEA-ET, respectively, retained almost 90% of relative activity after 3 cycles, losing their hydrolytic capacity only in the seventh cycle. Better results were observed with PEG as precipitation agent. Like the other samples, MCLEA-PEG retained 90% of relative activity after 3 cycles, however,

in the fifth cycle yet retained 80% of relative activity, losing its hydrolytic capacity only in the ninth cycle.

**Fig. 9.** Activity loss over after successive cycles of CMC hydrolysis using different MCLEAs.

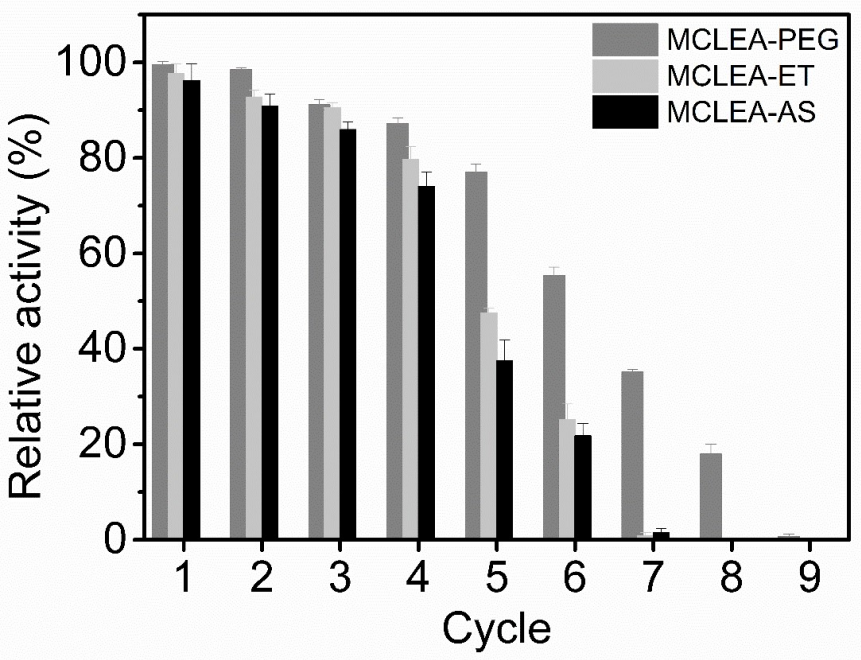


The Tab. 4 shows some results reported in the literature about recovery capacity of cellulase immobilized on magnetic nanoparticle surface.

**Tab. 4.** Summary of retained activity of cellulase immobilized on MNPs with CMC as substrate.

| Sample | Experimental condition | Cycles | Retained activity (%) | ref |
|---|---|---|---|---|
| MCLEA-AS | pH 4 and 55 °C | 3 | 90 | This work |
| MCLEA-ET | pH 4 and 55 °C | 3 | 90 | This work |
| MCLEA-PEG | pH 4 and 63 °C | 5 | 80 | This work |
| $Fe_3O_4$-chitosan | pH 5 and 50 °C | 5 | 75 | [54] |
| Zn-Ferrite-glutaraldehyde | pH 4 and 60 °C | 6 | 40 | [55] |
| $Fe_3O_4$-silica | pH 3.8 and 50 °C | 6 | 30 | [24] |
| $Fe_3O_4$-silica | pH 4and 50 °C | 7 | 77 | [44] |

The activity loss after successive hydrolysis reaction can be attributed to factors as enzyme inhibition by products or denaturation by long time heating [39]. However, these effects showed less expressive in the MCLEA-PEG. Nonionic polymers as PEG have been extensively

used as precipitation agents for different enzymes and proteins, due its neutrality, wide range of molecular mass e water solubility, which make it highly versatilely for enzyme precipitation [56]. Even not showing the higher values for enzymatic activity and activity recovery, the best reusability capacity allows it the highest reducing sugar production after successive cycles, once it were produced 30.74, 14.53 and 9.53 mg $mL^{-1}$ of sugar by MCLEA-PEG, MCLEA-ET and MCLEA-AS, respectively.

From the viewpoint of industrial applications, the reusability capacity of MCLEAs is a variable of great importance and represent a challenge and a high cost in biomass conversion processes due to the high amount of cellulase needed to cellulose hydrolysis [57]. Thus, there is a need to improve application of MCLEAs in different biomass conversion process, as shown in this work.

### 2.3.4 Cellulose hydrolysis and cello-oligosaccharides (COS) production

COS are carbohydrates biologically active with physiological properties that can benefit the health and growth of animals and humans due to their metabolic functions and ability to stimulate the growth of probiotic bacteria [25], [26], [27]. In this context, several methods have been employed to produce COS, either by polymerization from glucose or cellobiose monomers or by partial hydrolysis of the cellulose. Polymerization by both chemical [58] and enzymatic [59] approaches are challenging due to the technical and cost barriers (e.g., regioselectivity and stereoselectivity by catalytic synthesis and high enzyme cost). COS can also be produced by acid hydrolysis of cellulose, however, this method is nonselective and accompanied by co-product formation and low COS yields [60]. Lastly, enzymatic hydrolysis carried out by cellulases complex lead to mainly glucose production, as result of the synergism between endoglucanases, exoglucanases and β-glucosidases [3], [4].

In face of importance of this class of compound and technical difficulties in its obtention is that arise the needs for an alternative approach of COS production. Thus, MCLEAs and free cellulases were used in the production of COS from hydrolysis of cellulose obtained from alkali pretreated sugarcane bagasse and straw. The data of hydrolysis efficiency are shown in Tab. 5. The highest hydrolysis efficiency (38.14 mg $U^{-1}$) was observed for free enzyme. Even MCLEAs not showing the best results, if one considers the numbers of possible cycles due to magnetic nanoparticles support it allows the highest yields of sugar production. As discussed for enzymatic activity, cellulose hydrolysis efficiency loss can be attributed to alteration of active

site structure after cellulase immobilization on NP-CH. Moreover, considering that cellulose is a biopolymer with high molecular weight, diffusion process to the active site of the immobilized cellulase and steric impediments for enzyme-substrate interactions also need to be taken into account when evaluating its efficiency loss [61], [62].

Among MCLEAs prepared in this work, the highest hydrolysis efficiency were observed for MCLEA-PEG (9.98 mg $U^{-1}$) and MCLEA-ET (7.65 mg $U^{-1}$). Interestingly, MCLEA-AS e MCLEA-PEG presented similar enzymatic activity (Tab. 3), but MCLEA-PEG showed highest efficient compared to MCLEA-AS in cellulose hydrolysis.

**Tab. 5.** Hydrolysis efficiency obtained by free cellulase and MCLEAs in cellulose hydrolysis.

| Sample | Hydrolysis efficiency (mg $U^{-1}$) |
|---|---|
| **Cellulase** | 38.14 |
| **MCLEA-AS** | 1.36 |
| **MCLEA-ET** | 7.65 |
| **MCLEA-PEG** | 9.98 |

The hydrolyzed produced by both free and immobilized cellulase were investigated by GPC (Fig. 10), which allowed molecular mass determination and confirm cello-oligosaccharides production from cellulose hydrolysis.

**Fig. 10.** Chromatogram of hydrolysates obtained from cellulose hydrolysis carried out by free cellulase enzymes and MCLEAs. The peaks a to k are analyzed in Tab. 6.

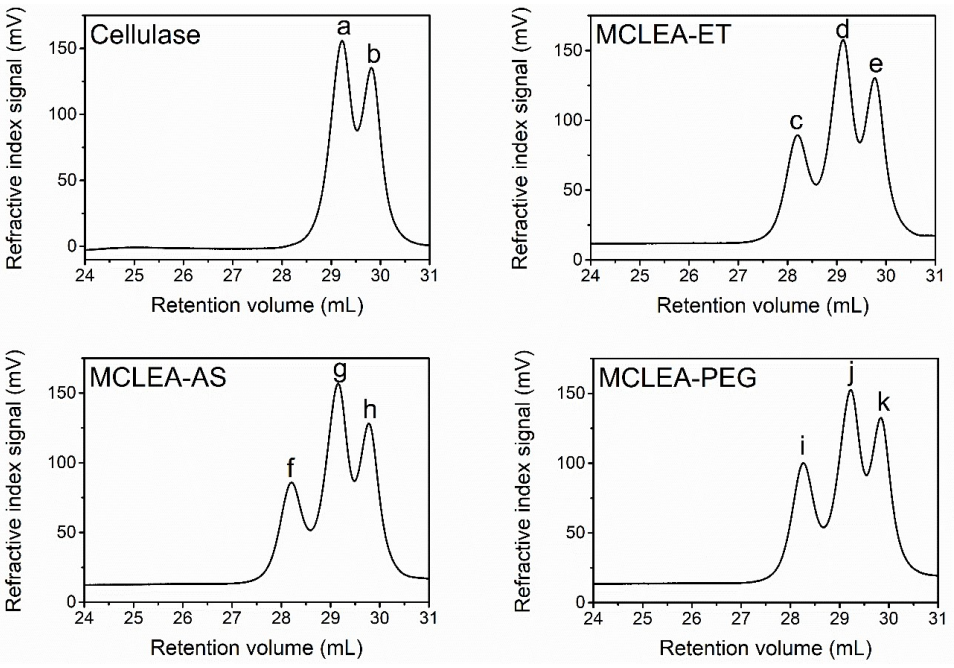

Although they have not been more efficient than free cellulase, MCLEAs leaded to a wide variety of products in hydrolysis of cellulose from sugarcane bagasse. COS with DP 3 and 6 were obtained in the hydrolysis of cellulose carried out by both free cellulase and all MCLEAs. However, MCLEAs also can produced COS with DP 12. Currently, higher molecular weight cello-oligosaccharides are produced in small amounts and with a 500 times more expensive cost than those with lower DP [28], [29]. Thus, a low cost-effective process for COS with DP 12 production as developed in our work will enable sustainable industrial applications.

The peaks analysis for chromatograms from Fig. 10 with their respective weight-average molecular weight (Mw), number-average molecular weight (Mn), PDI (Mw/Mn) and DP are shown in Tab. 5.

**Tab. 6.** Molar mass determination for each peak of Fig. 10. Software used to peak analysis: Omini SEC v. (5.1).

| Sample | Peak | Mn (Da) | Mw (Da) | PDI (Mw/Mn) | DP |
|---|---|---|---|---|---|
| **Cellulase** | a | 1,061 | 1,104 | 1.04 | 6 |
| | b | 584 | 609 | 1.04 | 3 |
| **MCLEA-ET** | c | 2,244 | 2,350 | 1.05 | 12 |
| | d | 1,104 | 1,136 | 1.03 | 6 |
| | e | 599 | 627 | 1.04 | 3 |
| **MCLEA-AS** | f | 2,203 | 2,312 | 1.05 | 12 |
| | g | 1,081 | 1,112 | 1.03 | 6 |
| | h | 597 | 623 | 1.04 | 3 |
| **MCLEA-PEG** | i | 2,122 | 2,217 | 1.04 | 12 |
| | j | 1,029 | 1,054 | 1.02 | 6 |
| | k | 568 | 592 | 1.04 | 3 |

Currently, industrial applications of COS have been found in food and pharmaceutical industries, however, biorefineries based on the hydrolysis of lignocellulosic biomass will certainly encounter in these compounds an important raw material for their processes [63], [64]. In this context, the diversity of COS produced by MCLEAs make these materials an important tool in the obtention of value-added chemical from lignocellulosic biomass.

## 2.4 Conclusions

Magnetic cross-linked enzymes aggregates were synthesized based on immobilization of cellulases in chitosan-coated magnetic nanoparticles using different precipitation agents (ethanol, ammonium sulfate and PEG 600). In quantitative terms, ethanol and PEG 600 show more effective as precipitation agent than the ammonium sulfate. After cellulase immobilization, highest values of enzymatic activity (193.42 U $g^{-1}$) and activity recovery (43.53 %) were observed with the use of ethanol as precipitation agent. While the use of PEG leaded to MCLEAs with the highest reusability capacity, which retained 80% of initial relative activity after five cycles of reaction. As consequence, the use of PEG resulted in better performing MCLEA, since that allowed, in general, a sugar production two times higher than the observed for other precipitation agents in the CMC hydrolysis.

Dynamic light scattering (DLS) analyses showed that the colloidal stability can be applied to reach a better understanding of thermal stability of cellulases in their both free and MCLEA form. Free cellulase show a low thermal stability and alterations in its particle-size distribution faced to changes in temperature suggests that such low thermal stability can be associated to a denaturation mechanism based on molecular aggregation, which can lead to steric block of active site. Differently, its immobilized form, i.e., the MCLEAs, showed a higher thermal stability, which can be assigned to high colloidal stability obtained independently of precipitation agent used. In addition, DLS measurements reported here for the first time to assess the thermal stability of MCLEAs, show as an interesting approach to better understand the operational behavior of other enzymes and proteins, faced to several denaturation conditions.

Lastly, while free cellulase can produce only COS with low DP (3 and 6), a variety of COS with different DP (3, 6 and 12) were obtained by MCLEAs applied in hydrolysis of cellulose from sugarcane bagasse and straw. Thus, due to higher value-added of COS obtained by MCLEAs, in addition to their important prebiotic properties, the cellulases immobilization method employed in this work can enable a sustainable production of value-added chemical from lignocellulosic biomass.

**Acknowledgments**

The authors are grateful for the financial support provided by the Brazilian funding agencies: National Council for Scientific and Technological Development (CNPq, grant number 142288/2016-0) and Financier of Studies and Projects (FINEP, grant number 01.14.0151.00).

**References**

[1] R. Tiwari, L. Nain, N.E. Labrou, P. Shukla, Bioprospecting of functional cellulases from metagenome for second generation biofuel production: a review, Crit. Rev. Microbiol. 44 (2018) 244–257. https://doi.org/10.1080/1040841X.2017.1337713.

[2] C. Qiao, G. Chen, J. Zhang, J. Yao, Structure and rheological properties of cellulose nanocrystals suspension, Food Hydrocoll. 55 (2016) 19–25. https://doi.org/10.1016/j.foodhyd.2015.11.005.

[3] V. Juturu, J.C. Wu, Microbial cellulases: engineering, production and applications, Renew. Sustain. Energy Rev. 33 (2014) 188–203. https://doi.org/10.1016/j.rser.2014.01.077.

[4] Y. Kuba, Y. Kashiwagi, G. Okada, T. Sasaki, Production of cello-oligosaccharides by enzymatic hydrolysis in the presence of activated carbon, Enzyme Microb. Technol. 12 (1990) 72–75.

[5] C. Manochio, B.R. Andrade, R.P. Rodriguez, B.S. Moraes, Ethanol from biomass: A comparative overview, Renew. Sustain. Energy Rev. 80 (2017) 743–755. https://doi.org/10.1016/j.rser.2017.05.063.

[6] M. Perwez, R. Ahmad, M. Sardar, A reusable multipurpose magnetic nanobiocatalyst for industrial applications, Int. J. Biol. Macromol. 103 (2017) 16–24. https://doi.org/10.1016/j.ijbiomac.2017.05.029.

[7] P. Li, D. Cai, Z. Luo, P. Qin, C. Chen, Y. Wang, C. Zhang, Z. Wang, T. Tan, Effect of acid pretreatment on different parts of corn stalk for second generation ethanol production, Bioresour. Technol. 206 (2016) 86–92. https://doi.org/10.1016/j.biortech.2016.01.077.

[8] G. Liu, J. Zhang, J. Bao, Cost evaluation of cellulase enzyme for industrial-scale cellulosic ethanol production based on rigorous Aspen Plus modeling, Bioprocess Biosyst. Eng. 39 (2016) 133–140. https://doi.org/10.1007/s00449-015-1497-1.

[9] J. Alftre, T.J. Hobley, Immobilization of cellulase mixtures on magnetic particles for hydrolysis of lignocellulose and ease of recycling, Biomass and Bioenergy. 65 (2014) 72–78. https://doi.org/10.1016/j.biombioe.2014.03.009.

[10] P.J. Huang, K.L. Chang, J.F. Hsieh, S.T. Chen, Catalysis of rice straw hydrolysis by the combination of immobilized cellulase from aspergillus niger on β -Cyclodextrin-Fe nanoparticles and ionic liquid, Biomed Res. Int. 2015 (2015) 1–9. https://doi.org/10.1155/2015/409103.

[11] L. Lei, Y. Bai, Y. Li, L. Yi, Y. Yang, C. Xia, Study on immobilization of lipase onto magnetic microspheres with epoxy groups, J. Magn. Magn. Mater. 321 (2009) 252–258. https://doi.org/10.1016/j.jmmm.2008.08.047.

[12] H. Jørgensen, M. Pinelo, Enzyme recycling in lignocellulosic biorefineries, Biofuels, Bioprod. Biorefining. 11 (2016) 150–167. https://doi.org/10.1002/bbb.

[13] C. Mateo, J.M. Palomo, G. Fernandez-lorente, J.M. Guisan, R. Fernandez-lafuente, Improvement of enzyme activity , stability and selectivity via immobilization techniques, Enzyme Microb. Technol. 40 (2007) 1451–1463. https://doi.org/10.1016/j.enzmictec.2007.01.018.

[14] H.H. Nguyen, M. Kima, An overview of techniques in enzyme immobilization, Appl. Sci. Converg. Technol. 26 (2017) 157–163. https://doi.org/10.5757/ASCT.2017.26.6.157.

[15] S.H. Hosseini, S.A. Hosseini, N. Zohreh, M. Yaghoubi, A. Pourjavadi, Covalent immobilization of cellulase using magnetic poly (ionic liquid) support; improvement of the enzyme activity and stability, J. Agric. Food Chem. 66 (2018) 789–798. https://doi.org/10.1021/acs.jafc.7b03922.

[16] H. Roth, S.P. Schwaminger, F. Peng, S. Berensmeier, Immobilization of cellulase on magnetic nanocarriers, Chem. Open. 5 (2016) 183–187. https://doi.org/10.1002/open.201600028.

[17] R.A. Sheldon, Cross-linked enzyme aggregates (CLEAs): stable and recyclable

biocatalysts, Biochem. Soc. Trans. 35 (2007) 1583–1587.

[18] G.N. Lucena, C.C. Santos, G.C. Pinto, C.O. Rocha, J. V. Brandt, A. Veloso, A. V. Paula, M. Jafelicci Jr, R.F.C. Marques, Magnetic cross-linked enzyme aggregates (MCLEAs) applied to biomass conversion, J. Solid State Chem. 270 (2019) 58–70. https://doi.org/10.1016/j.jssc.2018.11.003.

[19] H. Vaghari, H.J. Mojgan, Application of magnetic nanoparticles in smart enzyme immobilization, Biotechnol. Lett. 38 (2016) 223–233. https://doi.org/10.1007/s10529-015-1977-z.

[20] W. Kopp, T.P. Da Costa, S.C. Pereira, M. Jafelicci, R.C. Giordano, R.F.C. Marques, F.M. Araújo-Moreira, R.L.C. Giordano, Easily handling penicillin G acylase magnetic cross-linked enzymes aggregates: catalytic and morphological studies, Process Biochem. 49 (2014) 38–46. https://doi.org/10.1016/j.procbio.2013.09.024.

[21] K. Khoshnevisan, E. Poorakbar, H. Baharifar, Recent advances of cellulase immobilization onto magnetic nanoparticles: an update review, Magnetochemistry. 5 (2019) 1–22. https://doi.org/10.3390/magnetochemistry5020036.

[22] K. Khoshnevisan, F. Vakhshiteh, M. Barkhi, H. Baharifar, Immobilization of cellulase enzyme onto magnetic nanoparticles: Applications and recent advances, Mol. Catal. 442 (2017) 66–73. https://doi.org/10.1016/j.mcat.2017.09.006.

[23] J. Jia, W. Zhang, Z. Yang, X. Yang, N. Wang, X. Yu, Novel magnetic cross-linked cellulase aggregates, Molecules. 22 (2017) 2–14. https://doi.org/10.3390/molecules22020269.

[24] K. Jafari Khorshidi, H. Lenjannezhadian, M. Jamalan, M. Zeinali, Preparation and characterization of nanomagnetic cross-linked cellulase aggregates for cellulose bioconversion, J. Chem. Technol. Biotechnol. 91 (2016) 539–546. https://doi.org/10.1002/jctb.4615.

[25] X. Liu, W. Wei, S. Wu, M. Lei, Y. Liu, A promptly approach from monosaccharides of biomass to oligosaccharides via sharp-quenching thermo conversion (SQTC), Carbohydr. Polym. 189 (2018) 204–209. https://doi.org/10.1016/j.carbpol.2018.01.107.

[26] L. Bhatia, A. Sharma, R.K. Bachheti, A.K. Chandel, Lignocellulose derived functional oligosaccharides: production, properties, and health benefits, Prep. Biochem.

Biotechnol. 49 (2019) 744–758. https://doi.org/10.1080/10826068.2019.1608446.

[27] L.K. Tolonen, M. Juvonen, K. Niemelä, A. Mikkelson, M. Tenkanen, H. Sixta, Supercritical water treatment for cello-oligosaccharide production from microcrystalline cellulose, Carbohydr. Res. 401 (2015) 16–23. https://doi.org/10.1016/j.carres.2014.10.012.

[28] P. Chen, A. Shrotri, A. Fukuoka, Soluble cello-oligosaccharides produced by carbon-catalyzed hydrolysis of cellulose, ChemSusChem. 8628 (2019) 2576–2580. https://doi.org/10.1002/cssc.201900800.

[29] E. Billès, V. Coma, F. Peruch, S. Grelier, Water-soluble cellulose oligomers production by chemical and enzymatic synthesis: a mini-review, Polym. Int. 66 (2017) 1227–1236. https://doi.org/10.1002/pi.5398

[30] Y. Osuna, K.M. Gregorio-jauregui, J.G. Gaona-lozano, I.M. De Garza-rodr, A. Ilyna, D. Enrique, H. Saade, Chitosan-coated magnetic nanoparticles with low chitosan content prepared in one-step, J. Nanomater. 2012 (2012) 1–7. https://doi.org/10.1155/2012/327562.

[31] M.M. Bradford, A rapid and sensitive method for the quantitation microgram quantities of protein utilizing the principle of protein-dye binding, Anal. Biochem. 254 (1976) 248–254.

[32] M. Tanaka, M. Taniguchi, R. Matsuno, T. Kamikubo, Purification and properties of cellulases from Eupenicillium javanicum, J. Ferment. Technol. 59 (1981) 177–183.

[33] A. Stukowski, J. Markmann, J. Weissmu, Atomistic origin of microstrain broadening in diffraction data of nanocrystalline solids, Acta Mater. 57 (2009) 1648–1654. https://doi.org/10.1016/j.actamat.2008.12.011.

[34] R.D. Waldron, Infrared spectra of ferrites, Phys. Rev. 99 (1955) 1727–1735.

[35] S J. Sánchez-Ramírez, J.I. Martıínez-Hernández, P. Segura-Ceniceros, G. López, H. Saade, M.A. Medina-Morales, R. Ramos-González, A. Ilyina, Cellulases immobilization on chitosan-coated magnetic nanoparticles: application for Agave Atrovirens lignocellulosic biomass hydrolysis, Bioprocess Biosyst Eng. 40 (2017) 9–22. https://doi.org/10.1007/s00449-016-1670-1.

[36] P. Nicolás, V.L. Lassalle, M.L. Ferreira, Quantification of immobilized Candida

antarctica lipase B (CALB) using ICP-AES combined with Bradford method, Enzyme Microb. Technol. 97 (2017) 97–103. http://dx.doi.org/10.1016/j.enzmictec.2016.11.009

[37] V.L. Lassalle, S. Pirillo, E. Rueda, M.L. Ferreira, An accurate UV/visible method to quantify proteins and enzymes: Impact of aggregation, buffer concentration and the nature of the standard, Curr. Top. Anal. Chem. 8 (2011) 83–93.

[38] W. Zhang, J. Qiu, H. Feng, L. Zang, E. Sakai, Increase in stability of cellulase immobilized on functionalized magnetic nanospheres, J. Magn. Magn. Mater. 375 (2015) 117–123. https://doi.org/10.1016/j.jmmm.2014.09.067.

[39] W. Zhang, J. Qiu, H. Feng, L. Zang, E. Sakai, Increase in stability of cellulase immobilized on functionalized magnetic nanospheres, J. Magn. Magn. Mater. 375 (2015) 117–123. https://doi.org/10.1016/j.molcatb.2010.09.010.

[40] A.A. Homaei, R. Sariri, F. Vianello, R. Stevanato, Enzyme immobilization: an update, J. Chem. Biol. 6 (2013) 185–205. https://doi.org/10.1007/s12154-013-0102-9.

[41] R. Saini, J.K. Saini, M. Adsul, A.K. Patel, A. Mathur, D. Tuli, R.R. Singhania, Enhanced cellulase production by Penicillium oxalicum for bio-ethanol application, Bioresour. Technol. 188 (2015) 240–246. https://doi.org/10.1016/j.biortech.2015.01.048.

[42] L. Zang, J. Qiu, X. Wu, W. Zhang, E. Sakai, Y. Wei, Preparation of magnetic chitosan nanoparticles as support for cellulase immobilization, Ind. Eng. Chem. Res. 53 (2014) 3448−3454. https://doi.org/10.1021/ie404072s

[43] M. Elias, G. Wieczorek, S. Rosenne, D.S. Tawfik, The universality of enzymatic rate-temperature dependency, Trends Biochem. Sci. 39 (2014) 1–7. https://doi.org/10.1016/j.tibs.2013.11.001.

[44] Q. Tao, Y. Li, Y. Shi, R. Liu, Y. Zhang, J. Guo, Application of molecular imprinted magnetic $Fe_3O_4$@$SiO_2$ nanoparticles for selective immobilization of cellulase, J. Nanosci. Nanotechnol. 16 (2016) 6055–6060. https://doi.org/10.1166/jnn.2016.10853.

[45] R. Ahmad, M. Sardar, Enzyme immobilization: an overview on nanoparticles as immobilization matrix, Biochem. Anal. Biochem. 4 (2015) 2–8 https://doi.org/10.4172/2161-1009.1000178.

[46] Z. Shi, J. Tang, L. Chen, C. Yan, S. Tanvir, W.A. Anderson, R.M. Berry, K.C. Tam,

Enhanced colloidal stability and antibacterial performance of silver nanoparticles/cellulose nanocrystal hybrids, J. Mater. Chem. B. 3 (2015) 603–611.. https://doi.org/10.1039/b000000x.

[47] H. Peng, F. Jakob, U. Schwaneberg, A. Pich, Tunable enzymatic activity and enhanced stability of cellulase immobilized in biohybrid nanogels, Biomacromolecules. 17 (2016) 3619−3631. https://doi.org/10.1021/acs.biomac.6b01119.

[48] M. Baalousha, Aggregation and disaggregation of iron oxide nanoparticles: influence of particle concentration, pH and natural organic matter, Sci. Total Environ. 407 (2008) 2093–2101. https://doi.org/10.1016/j.scitotenv.2008.11.022.

[49] R.A. Sheldon, S. van Pelt, Enzyme immobilisation in biocatalysis: why, what and how, Chem. Soc. Rev. 42 (2013) 6223–6235. https://doi.org/10.1039/c3cs60075k.

[50] P.A.G. Soares, A.F.M. Vaz, M.T.S. Correia, A. Pessoa, M.G. Carneiro-da-cunha, Purification of bromelain from pineapple wastes by ethanol precipitation, Sep. Purif. Technol. 98 (2012) 389–395. https://doi.org/10.1016/j.seppur.2012.06.042.

[51] Y. Li, X.-Y. Wang, R.-Z. Zhang, X.-Y. Zhang, W. Liu, X.-M. Xu, Y.-W. Zhang, Molecular imprinting and immobilization of cellulase onto magnetic $Fe_3O_4$@$SiO_2$ nanoparticles, J. Nanosci. Nanotechnol. 14 (2014) 2931–2936. https://doi.org/10.1166/jnn.2014.8625.

[52] H. Liao, D. Chen, L. Yuan, M. Zheng, Y. Zhu, X. Liu, Immobilized cellulase by polyvinyl alcohol/$Fe_2O_3$ magnetic nanoparticle to degrade microcrystalline cellulose, Carbohydr. Polym. 82 (2010) 600–604. https://doi.org/10.1016/j.carbpol.2010.05.021.

[53] S. Velasco-lozano, E. Favela-torres, Cross-linked enzyme aggregates (CLEA) in enzyme improvement-a review, Biocatalysis. 1 (2015) 166–177. https://doi.org/10.1515/boca-2015-0012.

[54] Y. Lin, X. Liu, Z. Xing, Y. Geng, J. Wilson, Preparation and characterization of magnetic Fe3O4–chitosan nanoparticles for cellulase immobilization, Cellulose. (2017). *Cellulose* **2017**. https://doi.org/10.1007/s10570-017-1520-6.

[55] R.E. Abraham, M.L. Verma, C.J. Barrow, M. Puri, Suitability of magnetic nanoparticle immobilised cellulases in enhancing enzymatic saccharification of pretreated hemp biomass, Biotechnol. Biofuels. 7 (2014) 1–12. https://doi.org/10.1186/1754-6834-7-90.

[56] S. Sim, T. He, A. Tscheliessnig, M. Mueller, R.B.H. Tan, Protein precipitation by polyethylene glycol: A generalized model based on hydrodynamic radius, J. Biotechnol. 157 (2012) 315–319. https://doi.org/10.1016/j.jbiotec.2011.09.028.

[57] C. Tsai, A.S. Meyer, Enzymatic cellulose hydrolysis: enzyme reusability and visualization of β-glucosidase immobilized in calcium alginate, Molecules. 19 (2014) 19390–19406. https://doi.org/10.3390/molecules191219390.

[58] F. Nakatsubo, H. Kamitakahara, M. Hori, K.U. V, Cationic ring-opening polymerization of 3,6-Di-O-benzyl-a-D-glucose 1,2,4-orthopivalate and the first chemical synthesis of cellulose, J. Am. Chem. Soc. 118 (1996) 1677–1681. https://doi.org/10.1021/ja953286u.

[59] E. Samain, C. Lancelon-pin, V. Moreau, H. Chanzy, A. Heyraud, H. Driguez, Phosphorolytic synthesis of cellodextrins, Carbohydr. Res. 271 (1995) 217–226.

[60] D. Knappert, H. Grethlein, Partial acid hydrolysis of cellulosic materials as a pretreatment for enzymatic hydrolysis, Biotechnol. Bioeng. 22 (1980) 1449–1463.

[61] J. Hu, S. Li, B. Liu, Properties of immobilized pepsin on modified PMMA microspheres, Biotechnol. J. 1 (2006) 75–79. https://doi.org/10.1002/biot.200500022.

[62] M. Arroyo, Inmobilized enzymes: theory, methods of study and applications, Ars Pharm. 39 (1998) 23–39.

[63] S. Sophonputtanaphoca, C. Pridam, J. Chinnak, M. Nathong, Production of non-digestible oligosaccharides as value-added by-products from rice straw, Agric. Nat. Resour. 52 (2018) 169–175. https://doi.org/10.1016/j.anres.2018.06.013.

[64] S. Kobayashi, S. Shoda, Chemical synthesis of cellulose and cello-oligomers using a hydrolysis enzyme as a catalyst, Int. J. Biol. Macromol. 17 (1995) 373–379.

# *Chapter 3*

## *Synthesis, characterization and evaluation of the alternating magnetic field effects in the catalytic activity of a magnetic cross-linked enzyme aggregate*

**ABSTRACT**

Magnetic supports have emerged as an interesting tool for enzyme immobilization. In this study, a magnetic cross-linked enzyme aggregate (MCLEA) of cellulases and a non-magnetic analogue (CLEA) were synthesized and further studied. The obtained MCLEA and CLEA showed a high enzyme loading efficiency of 90 and 88%, respectively. However, the MCLEA presented an activity of 1.33 times higher than the its non-magnetic counter-part, suggesting a catalytic enhancement effect as a result of presence of the magnetic nanoparticle in cellulase cross-linked aggregate structure. In addition, MCLEA shows an unusual behavior with highest enzymatic activity at low temperatures. Lastly, a factorial design (2x2) with two variables at two levels (-1 and +1), frequency (203-420 kHz) and amplitude (3-6 kA $m^{-1}$), was used in order to better investigate the effects of an alternating magnetic field (AMF) on MCLEA activity. As result, was observed that AMF application decrease MCLEA activity when compared to field free condition. In addition, frequency implied in more significant effects on MCLEA activity when compared to AMF amplitude and that further studies should carried out in conditions of lower AMF frequency.

**Keywords:** magnetic nanoparticles, enzyme immobilization, magnetic supports, enzymatic catalyst, cellulases

## 3.1 Introduction

Enzymes are biocatalyst that speed up biochemical reactions used in the wide range of biotechnological interest areas such as energy production, food, biomedical, pharmaceutical, environment and so on [1], [2], [3], [4]. Applications as diverse as these occur due to inherent characteristic of enzymes as high substrate specificity, low waste generation and mild operational conditions, which together, lead to processes more efficient and sustainable [5], [6]. Although the use of enzyme has brought to more sustainable industrial processes, the high production and purification cost, structural instability caused by changes in pH, temperature and ionic strength, inhibition, activity loss and separation difficult, have become problem in many applications [7]. In order to overcome these challenges, the obtention of cross-linked enzyme aggregate (CLEA) has emerged as essential tool. CLEAs consist of physical aggregates of the enzyme, obtained as a result of the action of precipitation agents (e.g., salts, solvents or polymers), and cross-linked among themselves by reticulation agents (e.g., glutaraldehyde) [8]. The main characteristic of CLEAs are maintenance the native enzyme structure, increase structural stability, easy preparation, decrease in activity loss and improvement in recovery capacity [9], [10]. In addition, when precipitation is carried out on solid support surface and the CLEAs are covalently bonded to it by cross-linked agent, it is possible to produce new biocatalysts that gather advantages from CLEA to intrinsic properties of the support.

With the development of nanotechnology many nanomaterials have been studied as support for enzyme immobilization, among which, highlight the magnetic nanoparticles (MNP) as magnetite ($Fe_3O_4$). Magnetite consists of $Fe^{2+}$ and $Fe^{3+}$ (1:2) iron oxide with reverse spinel structure, and when to be in nanometric scale, it shows properties as high surface area, adsorption capacity, diffusivity and biocompatibility, making it an ideal support enzyme immobilization [11], [12]. In addition, the easy surface modification can increase its enzyme loading capacity, and the intrinsic magnetic properties, allows it to be magnetically recovered from different medium by an external magnetic field, leading to decreasing in process cost [13], [14], [15]. In this context, many works have used MNP as support for CLEAs immobilization of different enzymes. In summary, these magnetic cross-linked enzyme aggregates (MCLEAs) have shown increases in enzyme stability faced to changes pH and temperature, decreases in inhibition, high activity and, mainly, an exceptional recovery capacity, making it an essential strategy in the improvement of enzymatic processes [16], [17], [18].

Lastly, even though positive results have been observed, advances are still necessary when thought in the use of MNP as enzyme support, mainly in concern to better understood of

the magnetic properties effect on enzymatic activity. It is worth mentioning that the use of magnetic properties of MNP is not restricted to magnetic recovery. Under an alternating magnetic field (AMF), as a result of the both Néel and Brown relaxation, MNP rotate and collide among themselves producing heat, a phenomenon known as magnetic hyperthermia [19]. An AMF can perturb enzymatic kinetic by increase in the collision rate between biocatalyst and substrate, change MCLEA aggregation state, trigger conformational changes on enzymatic or increase diffusion rate, leading to improvements of MCLEA activity [20], [21]. And, although has been extensively used in biomedical application as cancer treatment and drug delivery, magnetic hyperthermia remains almost unexplored in enzymatic catalysis, especially those based on MCLEAs. Specifically, Liu and co-works have reported the improvement in the activity of lipase MCLEA under AMF when compared to the free enzyme in the resolution of (*R,S*)-2-octanol, where, according to authors, frequency played a more dominant role than the field intensity [22]. However, advances regarding to different enzymes and AMF with different amplitudes and frequencies need to be carefully investigated.

Faced it, here is reported the synthesis of a cellulases MCLEA with an unusual behavior of highest enzymatic activity at low temperatures, as well as a further investigation in regard to effects of an AMF in its catalytic activity. As enzyme model was chosen cellulases, an important enzymatic complex extensively studied in lignocellulosic biomass conversion process [23], [24]. In order to AMF effects evaluation, two levels of frequency (203-420 kHz) and amplitude (3-6 kA $m^{-1}$) of field was used in a factorial design (2x2) and, in such conditions, was observed that frequency implies in more significant effects on MCLEA activity when compared to AMF amplitude and that further studies should carried out in conditions of lower AMF frequency.

## 3.2 Experimental section

### 3.2.1 Materials and measurements

For syntheses, cellulase from *Aspergillus niger*, iron(II) chloride tetrahydrate (≥99 %), iron(III) chloride hexahydrate (97%), 3-aminopropyl-triethoxisilane (APTS, 99%), phosphate buffer saline (PBS) and glutaraldehyde, were purchased from Sigma-Aldrich; ammonium sulfate (>99.6%) and sodium hydroxide were obtained from Neon. In activity and loading efficiency assays, were used 3,5-Dinitrosalicylic acid (DNS, 98%) and sodium phosphate

dibasic purchased form Neon, while citric acid and Bradford reagent were obtained from Sigma-Aldrich. All the starting chemicals and solvents were used without further purification. Powder x-ray diffraction (PXRD) patterns were obtained using a Rigaku model RINT 2000 diffractometer, in the 2θ range 5-70°, with Cu Kα radiation (λ = 1.5418 Å), scan speed of 1 s/step, and step size of 0.02°. For magnetite, the PXRD diffractogram was simulated using Mercury 3.0 software and Cu Kα radiation (λ= 1.5418 Å) and magnetite CIF file AMCSD-2400, crystal system cubic and space group Fd3m. Fourier transform infrared (FTIR) spectra were acquired in the range 4000-400 $cm^{-1}$, with resolution of 4 $cm^{-1}$ and 32 scanning, using KBr pellets and a PerkinElmer FT-IR Frontier spectrophotometer. Scanning electron microscopy (SEM) images were acquired with a Topcon SM-300 field emission gun (FEG) instrument, using carbon as a sample support. For spectrophotometric measurements, a Perkin Elmer Lambda 465 spectrophotometer equipped with a UV-Vis photodiode array detector was used. The magnetic hyperthermia measurements were performed on the DM100 Series of the brand Nanoscale Biomagnetics.

### 3.2.2 Synthesis of APTS coated magnetite nanoparticles (NP-APTS)

Magnetite nanoparticles (NP) were prepared by the conventional coprecipitation method [25] and coated with APTS in a one-step. In a three-neck round-bottom flask equipped with a reflux condenser and argon atmosphere, were added 3.3 mL of $Fe^{2+}$:$Fe^{3+}$ (1:2) solution in a 3 mol $L^{-1}$ of sodium hydroxide aqueous solution, being the mixture kept under stirring of 360 rpm at 75 °C for 30 min. So, 5 mL of APTS were added and the suspension maintained at the same conditions for more 40 min. Lastly, NP-APTS were recovered by using a permanent magnetic, washed several times with water and stored in ultrapure water until characterization and MCLEA synthesis.

### 3.2.3 Syntheses of magnetic cross-linked cellulase aggregate (MCLEA)

In a falcon tube containing 10 mL of 0.01 mol $L^{-1}$ of PBS buffer pH 7, 100 mg of cellulase enzyme and a suspension of functionalized magnetic nanoparticles with 200 mg of NP-APTS were incubated at room temperature, under shaking of 125 rpm, for 2 h. Then, 9 mL of chilled precipitant agent ammonium sulfate were added to the tube for depositing the cellulase on NP-APTS surface for 30 minutes under repose, after which, 1 mL of 3%

glutaraldehyde aqueous solution was added to cross-linked reaction. The system was incubated for 7 h at room temperature under shaking of 125 rpm. The MCLEA obtained was washed 3 times with 0.05 mol $L^{-1}$ of acetate buffer pH 5 and kept in acetate buffer at 5 °C until activity assay and characterization. Parallelly, it was carried out a synthesis without NP-APTS aiming obtention of no-magnetic cross-linked cellulase aggregate (CLEA).

The immobilization efficiency was determined measuring the amount of protein in the supernatant before and after immobilization by the Bradford protein assay [26] and using the Eq. 1 below:

$$Enzyme\ loading\ efficiency\ (\%) = \frac{C_0V_0 - C_sV_s}{C_0V_0}\ x\ 100 \qquad \textbf{Eq. 1}$$

where $C_0$ is the initial protein concentration (mg $mL^{-1}$), $V_0$ the initial volume of protein (mL), $C_s$ the protein concentration in the total supernatant (mg $mL^{-1}$) and $V_s$ is the total volume of supernatant (mL).

### 3.2.4 Cellulase activity assay: central composite design

Enzymatic activity assay was determined by measuring reducing sugar production after the reaction of immobilized cellulase with carboxymethylcellulose sodium salt (CMC) [27]. The reaction mixture contained 0.9 mL of 0.44% CMC solution in citrate-phosphate buffer and 0.1 mL of MCLEA or CLEA. The CMC hydrolysis reaction was carried out for 1 h under heating, after which 1.5 mL of DNS reagent was added to stop the reaction. The samples were heated in boiling water for 5 min to allow suitable color formation. After cooled to room temperature, the reducing sugar concentration was measured at 540 nm on a UV-Vis spectrophotometer. The amount of enzyme needed to catalyze the release of 1 μmol of reducing sugar equivalent per min was defined as one unit (1 U) of enzymatic activity. For calculus purposes, enzymatic activity was expressed as relative activity, i.e., the ratio between the activity on each set of values of pH and temperature and the activity in the optimal condition.

A central composite design (CCD) was employed for enzymatic activity optimization of the MCLEA and CLEA under different pH and temperature conditions. Both independent variables were studied in five levels, pH (3.6, 4.0, 5.0, 6.0 and 6.4) and temperature (25.7, 29.0, 37.0, 45.0 and 48.3 °C). A total of 11 experiments were employed in this work, including 4 cube points, 3 replications at the central point and 4 axial points. For statistical analysis, the

independent variables (*X*) pH and temperature were coded as $x_i$ according to the following Eq. 2:

$$x_i = \frac{X_i - X_0}{\delta X} \qquad \textbf{Eq. 2}$$

where, *Xi* is the real valor of *X* to be codified, $X_0$ is the real value of *X* at the central point, and $\delta X$ presents the step-change [28]. The experimental ranges and levels of the independent variables $X_i$ are given in Table 1.

**Tab. 1.** Experimental range and levels (coded and real) of the independent variables used in CCD for enzymatic activity optimization of the CLEA and MCLEA.

| **Independent variables** | **Ranges and levels** | | | | |
|---|---|---|---|---|---|
| | -1.41 | -1 | 0 | +1 | +1.41 |
| **pH** | 3.6 | 4 | 5 | 6 | 6.4 |
| **Temperature** | 25.7 | 29 | 37 | 45 | 48.3 |

The Tab.2 shows the set conditions of pH and temperature for the 11 experiments carried out in the CCD.

**Tab. 2.** Experimental conditions carried out in the CCD for enzymatic activity optimization of the CLEA and MCLEA.

| **Experiment** | **pH** | **T** |
|---|---|---|
| 1 | 4 | 29 |
| 2 | 4 | 45 |
| 3 | 6 | 29 |
| 4 | 6 | 45 |
| 5 | 3.6 | 37 |
| 6 | 6.4 | 37 |
| 7 | 5 | 25.7 |
| 8 | 5 | 48.3 |
| 9 | 5 | 37 |
| 10 | 5 | 37 |
| 11 | 5 | 37 |

The statistical significance of the full quadratic models predicted was evaluated by the analysis of variance (ANOVA) and least squares techniques using Statistica v.8 software.

### 3.2.5 Hyperthermia assay of the MCLEA

Evaluation of the effect of the alternating magnetic field (AMF) on MCLEA activity was carried out in the frequency (f) and amplitude (B) range of 203-420 kHz and 3-6 kA $m^{-1}$, respectively. For this purpose, a factorial design (2x2) was performed with 2 levels for both variables and its respective levels are shown in Tab. 3. Enzymatic activity was measured as stated in section 2.4, however, with experimental vial immersed in an AMF. Analysis of the significance of the effects of AMF frequency and amplitude on MCLEA activity was carried out via variance analysis (ANOVA) using Statistica v.8 software.

**Tab. 3.** Experimental ranges and levels (coded and real) of the independent variables in the factorial design for optimization of magnetic hyperthermia assay of MCLEA.

| **Independent variables** | **Ranges and levels** | |
|---|---|---|
| | -1 | +1 |
| **f / kHz** | 203 | 420 |
| **B / kA $m^{-1}$** | 3 | 6 |

## 3.3 Results and discussion

### 3.3.1 Synthesis and characterization of MCLEA

As shown in PXRD patterns from Fig.1, the one-step synthesis employed in this work leaded to a satisfactory obtention of nanoparticles based on magnetite phase ($Fe_3O_4$) of the magnetic iron oxide and that further the modification of MNP surface with cellulase enzyme maintained its crystalline structure. In addition to inherent magnetic properties of the nanoparticles of magnetite, which can increase significantly the reusability of immobilized enzymes on its surface, this iron oxide phase have been one the materials most studied as enzyme support due low toxicity, high surface area, diffusivity, easy surface modification and high protein affinity [11], [12].

**Fig. 1.** PXRD patterns simulated of magnetite ($Fe_3O_4$) and as synthesized NP-APTS and MCLEA.

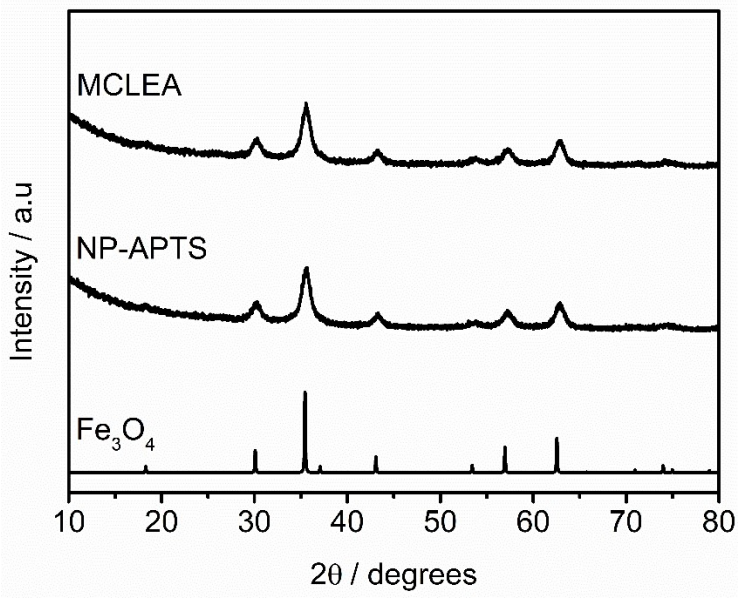


The nanometric scale of NP-APTS and MCLEA synthesized was confirmed by representative SEM images as well as their corresponding particle-size distributions shown in Fig 2. In the SEM imagens are observed spherical nanoparticles with an average diameter of 15 and 26 nm for NPTS and MCLEA samples, respectively.

**Fig. 2.** FEG-SEM images of NP-APTS (a) and MCLEA (b).

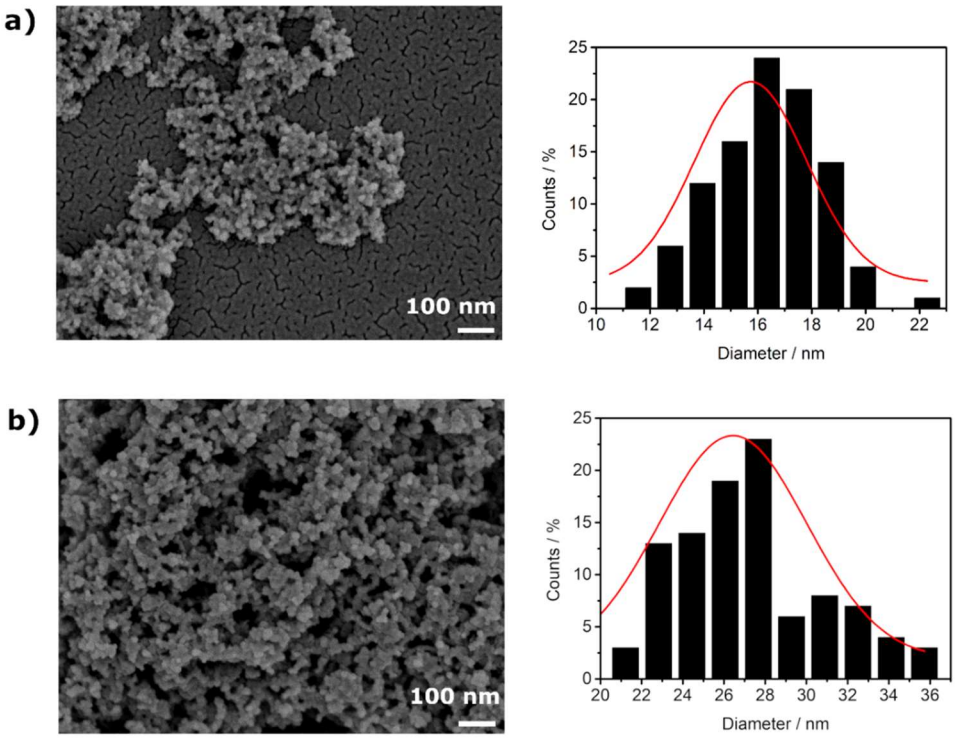

The Fig. 3 shows the FTIR spectra of the samples NP-APTS, MCLEA and free cellulase enzyme. In the NP-APTS and MCLEA FTIR spectra, the bands attributed to the υFe–O stretching mode appear at 600 and 443 $cm^{-1}$. Due to finite size of nanoparticles there is a split of the energy levels of the quantized nanoparticles and the band near to 600 $cm^{-1}$ shows split into two peaks at 635 and 582 $cm^{-1}$ [29]. The APTS coating on magnetic NP surface was confirmed in the NP-APTS FTIR spectrum with the band centered at 1010 $cm^{-1}$ assigned to υSi–O bond stretching mode [30]. In addition, the band in the region of 1630-1590 $cm^{-1}$ can be attributed to bending modes from δC–$NH_2$ bond [31]. Lastly, immobilization of cellulase on NP-APTS surface was observed with bands centered at 1570 $cm^{-1}$ and 1408 $cm^{-1}$, assigned to νC–O bond stretching mode and δN–H bending mode, respectively [32].

**Fig. 3.** FTIR spectra of the NP-APTS, MCLEA and free cellulase enzyme.

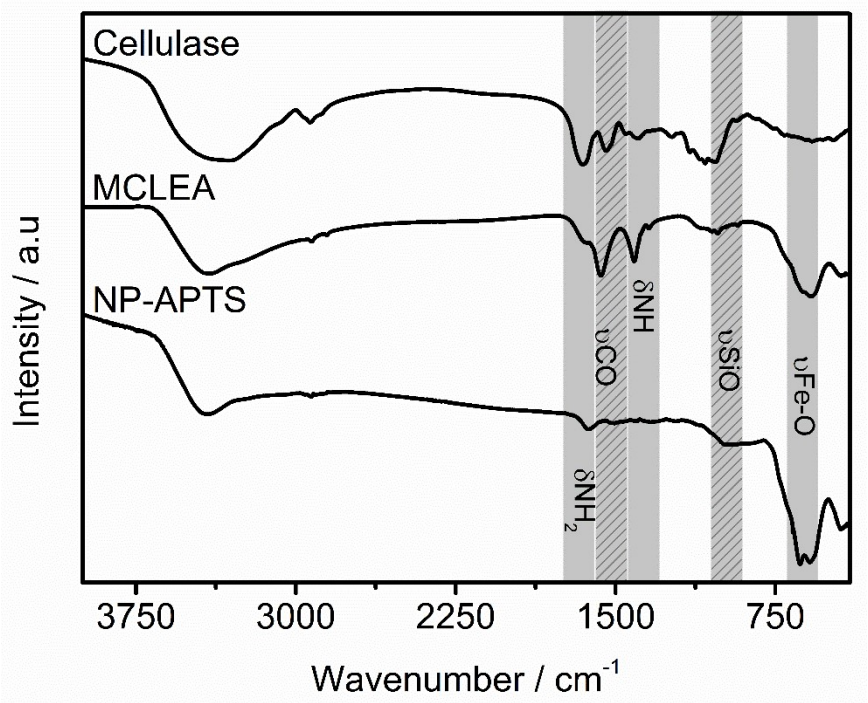


### 3.3.2 Cellulase immobilization and activity assay optimized by CCD

Quantitative analysis of cellulase immobilization in the CLEA and MCLEA was performed by assaying the amount of cellulase (measured as protein) in the supernatant both before and after immobilization using Bradford protein assay. A high enzyme loading efficiency of the 88.9% and 90.7% was observed for CLEA and MCLEA, respectively. The

formation of cross-linked enzyme aggregates has been successful recognized as a highly efficient and eco-friendly immobilization method mainly due to its high stability combined with high loading capacity [9], [10], which, in this work, did not suffered changes due to MNP as support.

In order to investigate the stability of the CLEA and MCLEA faced to changes in pH and temperature, a CCD was used. The statistical significance of each regression model was evaluated via ANOVA using the *F*-test shown in Tab. 4. The model predicts for MCLEA relative activity shows statistically significant at 95% of significance level, i.e., presents *F*-value of the model (8.5611) higher than *F*-critical (5.0503). Besides, the *F*-value of lack of fit (8.8099) was lower than the *F*-critical value (19.1642). On the other hand, the model predicts for CLEA relative activity did not show statistically meaning at 95% of significance, because *F*-value of the model is lower than *F*-critical (2.1356 < 5.0503). Moreover, the model shows a high lack of fit, i.e., *F*-value of the lack of fit higher than *F*-critical (248.3161 > 19.16442).

**Tab. 4.** ANOVA for the quadratic models predicted for the relative activity of the CLEA and MCLEA.

| Source | Sample | Degrees of freedom | Sum of squares | Mean of squares | *F*-value | *F*-critical | *p*-value |
|---|---|---|---|---|---|---|---|
| **Model** | CLEA | 5 | 1188.3989 | 237.6798 | 2.1356 | 5.0503 | 0.2123 |
| | MCLEA | 5 | 5725.7825 | 1145.1565 | 8.5611 | 5.0503 | 0.0171 |
| **Residual** | CLEA | | | | | | |
| | MCLEA | 5 | 668.8070 | 133.7614 | | | |
| **Pure error** | CLEA | 2 | 1.490 | 0.7450 | | | |
| | MCLEA | 2 | 47.04944 | 23.5247 | | | |
| **Lack of fit** | CLEA | 3 | 554.969 | 184.9897 | 248.3161 | 19.16442 | 0.0040 |
| | MCLEA | 3 | 621.7576 | 207.2525 | 8.8099 | 19.1642 | 0.1036 |

Faced it, a regression analysis was carried out in order to determine the coefficients of the significant effects on MCLEA relative activity and the results are presented in Tab. 5.

**Tab. 5.** Significance of coefficients of the quadratic regression of MCLEA relative activity.

| Coefficient | Value | Degrees of freedom | Sum of squares | Mean of squares | *F*-value | *F*-critical | *p*-value |
|---|---|---|---|---|---|---|---|
| **pH** | 1.9544 | 1 | 30.469 | 30.4685 | 1.2951 | 18.5128 | 0.3730 |
| **$pH^2$** | -19.5150 | 1 | 2133.360 | 2133,36 | 90.6858 | 18.5128 | 0.01084 |
| **T** | -1.6515 | 1 | 21.757 | 21.7566 | 0.92484 | 18.5128 | 0.4376 |
| **$T^2$** | -28,8441 | 1 | 4660.588 | 4660.588 | 198.114 | 18.5128 | 00050 |
| **pH x T** | 8.0201 | 1 | 257.288 | 257.2883 | 10.9369 | 18.5128 | 0.0805 |

For MCLEA, only quadratic terms of pH and temperature show statistically significative at 95% of significance, i.e., show *F*-value (90.6858 and 198.114, respectively) higher than *F*-

critical (18.5128). The quadratic model obtained for MCLEA relative activity as a response to pH and temperature changes can be represented by both responses and contour quadratic surface plotted in Fig. 4, which is described by the inserted equation (in coded values).

**Fig. 4.** Quadratic response surface (a) and contour surface (b) for MCLEA relative activity as a response to pH and temperature changes.

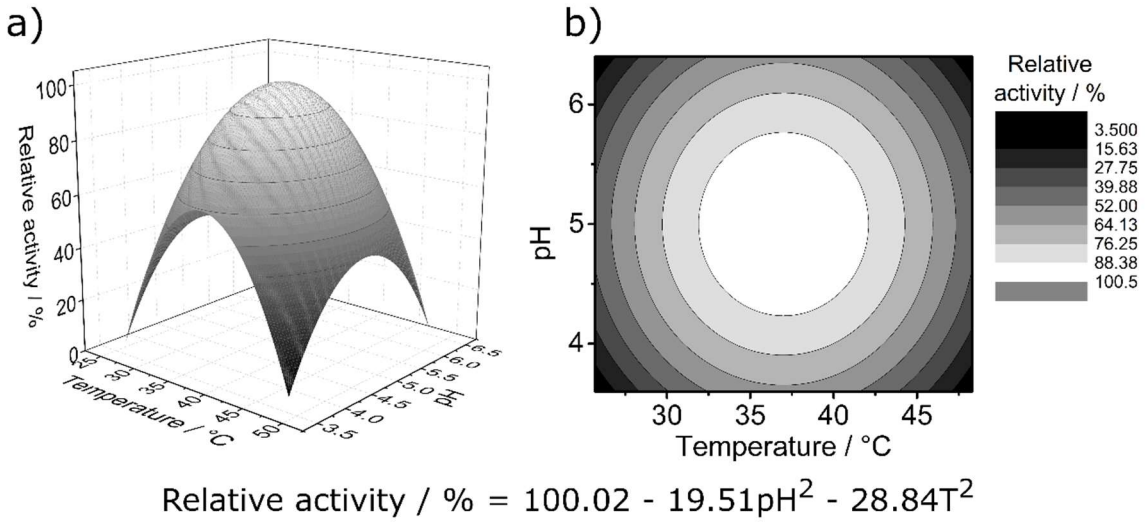


$$\text{Relative activity / \%} = 100.02 - 19.51pH^2 - 28.84T^2$$

From analysis of Fig. 4b can be observed the high stability of MCLEA activity around central point. In relationship to pH, MCLEA shows an expressive stability in the region from pH 4 until 6. It is common knowledge in the literature [33], [34] that free cellulases enzymes show its highest catalyst activity at pH 5 and, usually, after immobilization procedures have been observed either acid-shift [35] or alkaline-shift [36] in its optimal pH. However, unusual behavior was observed regarding temperature effects. While free cellulases enzymes act mainly at 50 °C and after its immobilization have been reported changes to highest temperature values [37], the MCLEA synthesized in this work show a stable and atypical ideal catalytic behavior at temperatures below 45 °C. Although nearly all cellulase applications have been carried out at 50 °C or higher, this MCLEA emerges as an interesting tool for modern approaches of second-generation ethanol (2GE) production from lignocellulosic biomass, e.g., simultaneous saccharification and fermentation (SSF) process. Briefly, in SSF process the fermentation step is simultaneously carried out to saccharification (hydrolysis) of cellulose, whose main aim consists in decrease the cost of 2GE production and to avoid cellulase inhibition by cellulose hydrolysis products [38]. However, this strategy meets obstacles in the fact that saccharification and hydrolysis to be performed at very different temperatures, 37 °C and 50 °C, respectively

[39]. Thus, the possibility of to conduct cellulose hydrolysis in temperatures near at 37 °C shows as promising in the development of new sustainable processes for the obtention of value-added products from lignocellulosic biomass.

The highest value of relative activity for MCLEA observed in the region along to central point in CCD assay, i.e., 100% at pH 5 and 37 °C, has a real value corresponding to 79.37 U $g^{-1}$. Although the proposed model for CLEA relative activity has shown high lack of fit, during CCD assay, its highest enzymatic activity was observed at pH 4 and 45 °C, whose real valor corresponding to only 59.25 U $g^{-1}$.

Although similar results were observed in enzyme loading efficiency, CLEA and MCLEA showed different enzymatic activity measured using CMC as substrate. Similar result was also observed by Kopp and co-workers immobilizing penicillin G acylase in amino-coated superparamagnetic nanoparticles using different precipitation agents (e.g., dimethoxyethane; tert-butanol and polyethylene glycol 600) [40]. In the synthesis, several factors as protein concentration, precipitant agent, ionic strength, cross-linked agent, pH and so on can affect the catalyst properties of aggregates [41], [42]. The higher activity observed for MCLEA in comparison with CLEA suggests a significative effect of MNP in the cellulase cross-linked aggregate structure. In enzyme immobilization procedures, the support determines features as enzyme stability and orientation end, consequently, the catalytic activity [43]. Since that the same conditions were employed for CLEA and MCLEA synthesis, the higher enzymatic activity observed for MCLEA can be assigned, e.g., to improvements in chemical structure stability and proper spatial orientation of enzyme established by MNP presence of MCLEA structure, as well as, and unblock of its respective active site.

Many positive effects have been attributed to the use of MNP as support for enzymes immobilization [44], among which highlight some observed in this work, such as high loading efficiency, activity and stability faced to changes in the pH and temperature, besides the recovery capacity due to its intrinsic magnetic properties. However, not restrict to it, their benefits need to be further studied, mainly in concern to the use of magnetic hyperthermia.

### 3.3.3 Magnetic hyperthermia assay

In order to investigate the effects of an alternating magnetic field (AMF) on MCLEA activity a factorial design (2x2) with two variables (frequency and amplitude) at two levels (-1 and +1) was used. The Fig 5 shows a comparison between the MCLEA activity observed at

optimal condition (control) and the observed in the hyperthermia assay with different states of frequency and amplitude. AMF application decreased the MCLEA activity to around 50% when at least one variable was set at -1 level of the factorial design and to 40% when both frequency and amplitude were set at +1 level. These results diverge from those reported by Liu and co-workers and Xia and co-works. The firsts observed an increase of almost 25% in the lipase activity immobilized on MNP under application of a AMF of 0.8 kA $m^{-1}$ at 600 Hz, while the second observed an increase in 16% of laccase activity immobilized on polymer-coated MNP at the same AMF conditions. However, it is worth mentioning that these authors made use of AMF frequency with an order of magnitude at least 300 times lower than the applied in this work. In ferrofluids at low frequency, the rotation arise as result to a small permanent magnetic moment in MNP, while at high frequency (kHz-MHz), the phase lag between the applied AMF and the induced magnetic moment results in a torque, which implies that in the high frequency range, the magnetization is not able to follow the field instantaneously [45]. In such conditions, have been shown that the rotation of the magnetic moment or physical rotation of MNP depends on AMF amplitude [46]. In addition, the rapid change of magnetic field direction at high AMF frequency can prevent the MNP from aligning with the field direction [47], which can lead to a decrease in both MNP diffusion rate and their collision with the substrate and, consequently, in the enzymatic activity as observed in this work.

**Fig. 5.** Effects of AMF frequency and amplitude in MCLEA activity compared to control experiment.

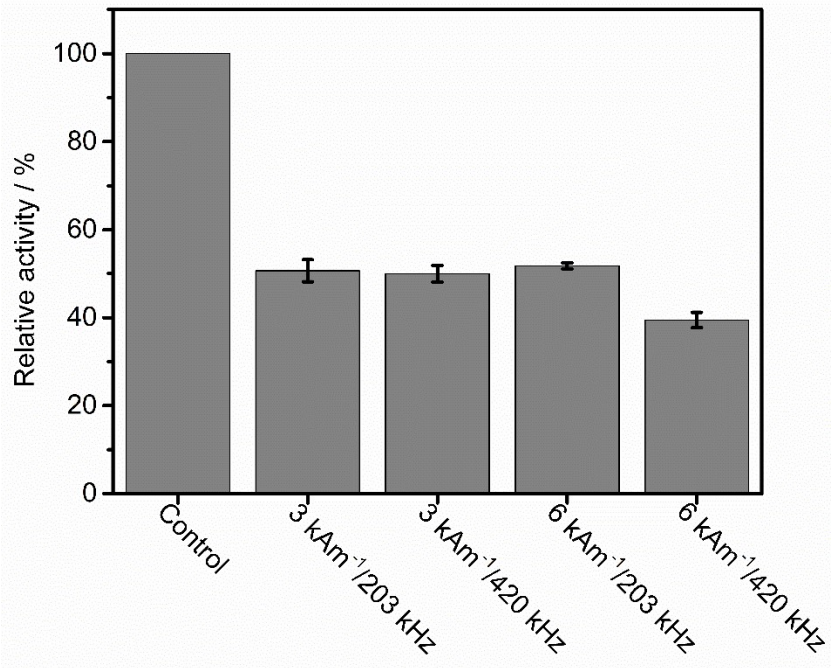

The Fig. 6 shows an effect size plot for AMF frequency and amplitude on MCLEA activity. As observed, frequency plays a higher effect when compared to amplitude and its respective interactions. Similar results were reported by Liu and co-workers studying the AMF effects on lipase immobilized MNP applied in the resolution of (*R,S*)-2-octanol [22]. The frequency level-shift from -1 until +1 decrease 6.5% of MCLEA activity, while the same level-shift of amplitude and interaction factor decrease by 4.7% and 5.81%, respectively. Thus, as a result if factorial design is desired that further investigations should started in conditions of lower AMF frequency.

**Fig. 6.** Effects size plot of the AMF frequency (f), amplitude (B) and interaction factor (fB) on MCLEA activity.

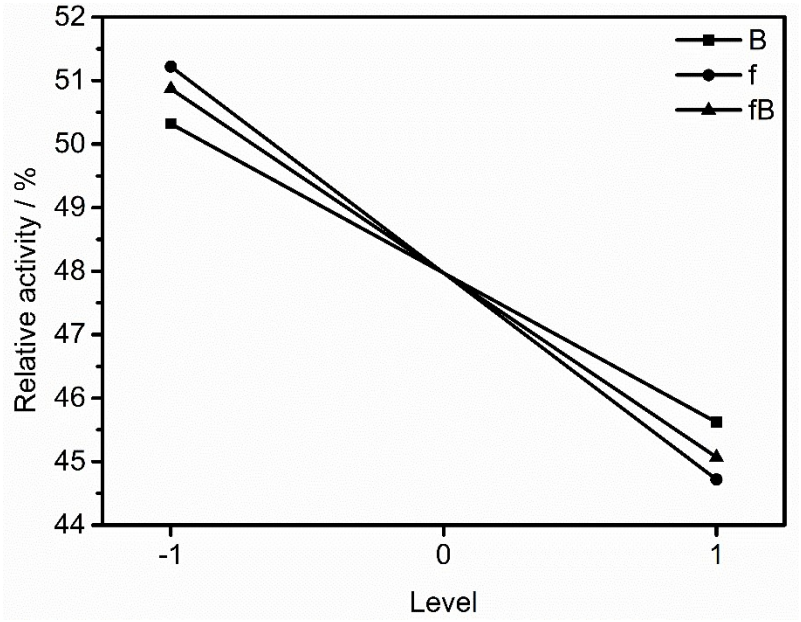


Lastly, an analysis of variance was carried out in order to determine the significance of the effects of AMF frequency and amplitude on MCLEA relative activity and the results are presented in Tab. 6. Both variables and their respective interaction show effects statistically significant on MCLEA activity (*F*-value > *F*-critical). In addition, the highest *F*-value confirm that frequency plays a more significative effect when compared to amplitude and interaction factor between the variables on MCLEA activity.

**Tab. 6.** Significance of effects of AMF frequency (f), amplitude (B) and its interaction (B x f) in MCLEA relative activity.

| Variable | Degrees of freedom | Sum of squares | Mean of squares | *F*-value | *F*-critical | *p*-value |
|---|---|---|---|---|---|---|
| **B** | 1 | 66.10 | 66.10 | 19.8498 | 5.3176 | 0.00212 |
| **f** | 1 | 127.07 | 127.07 | 38.1591 | 5.3176 | 0.0002 |
| **fB** | 1 | 101.17 | 101.17 | 30.3813 | 5.3176 | 0.0005 |
| **Error** | 8 | 26.64 | 3.33 | | | |

## 3.4 Conclusions

In this work was reported synthesis and characterization of unusual magnetic cross-linked enzyme aggregate (MCLEA) of cellulases with highest and stable catalytic activity at low temperatures. The MCLEA shows a high enzyme loading efficiency of 90%, as high as the demonstrated by its non-magnetic analogue. However, its higher enzymatic activity suggests a catalytic enhancement effect as a result of the magnetic nanoparticle presence in cellulase cross-linked aggregate structure.

Applying alternating magnetic field (AMF) on MCLEA leaded to a substantial decrease in its catalytic activity, particularly in the highest values of frequency and amplitude. As result of factorial design is desired that further studies should carried out in conditions of lower AMF frequency, because, in contrary, the existence of a torque will imply in the requirement of stronger fields.

Lastly, although the initial assumption in regard positive effect of the AMF application on catalyst activity of enzyme immobilized on magnetic support has not to be observed in this work, the data here presented can help to fill the gap of further study in this growing and essential approach that is the use of magnetic support for enzyme immobilization.

## Acknowledgments

The authors are grateful for the financial support provided by the Brazilian funding agencies: National Council for Scientific and Technological Development (CNPq, grant number 142288/2016-0) and Financier of Studies and Projects (FINEP, grant number 01.14.0151.00).

**References**

[1] S. Velasco-lozano, M. Knez, F. Lo, Coupling enzymes and inorganic piezoelectric materials for electricity production from renewable fuels, Acs Appl. Energy Mater. 1 (2018) 2032−2040. https://doi.org/10.1021/acsaem.7b00328.

[2] E. Ermis, Halal status of enzymes used in food industry, Trends Food Sci. Technol. 64 (2018) 69–73. https://doi.org/10.1016/j.tifs.2017.04.008.

[3] M. Kalantari, M. Yu, Y. Yang, E. Strounina, Z. Gu, X. Huang, Tailoring mesoporous-silica nanoparticles for robust immobilization of lipase and biocatalysis, Nano Res. 10 (2017) 605–617. https://doi.org/10.1007/s12274-016-1320-6.

[4] J. Chapman, A.E. Ismai, C.Z. Dinu, Industrial applications of enzymes: recent advances, techniques, and outlooks, Catalysts. 8 (2018) 238–263. https://doi.org/10.3390/catal8060238.

[5] R.A. Sheldon, S. van Pelt, Enzyme immobilisation in biocatalysis: why, what and how, Chem. Soc. Rev. 42 (2013) 6223–6235. https://doi.org/10.1039/c3cs60075k.

[6] N. Karaki, A. Aljawish, C. Humeau, L. Muniglia, J. Jasniewski, Enzymatic modification of polysaccharides: mechanisms, properties, and potential applications: a review, Enzyme Microb. Technol. 90 (2016) 1–18. https://doi.org/10.1016/j.enzmictec.2016.04.004.

[7] M. Bilal, Y. Zhao, T. Rasheed, M.N. Iqbal, Magnetic nanoparticles as versatile carriers for enzymes immobilization: a review, Int. J. Biol. Macromol. 120 (2018) 2530–2544. https://doi.org/10.1016/j.ijbiomac.2018.09.025.

[8] R.A. Sheldon, Cross-linked enzyme aggregates (CLEAs): stable and recyclable biocatalysts, Biochem. Soc. Trans. 35 (2007) 1583–1587.

[9] S.S. Nadar, A.B. Muley, M.R. Ladole, P.U. Joshi, Macromolecular cross-linked enzyme aggregates (M-CLEAs) of a-amylase, Int. J. Biol. Macromol. 84 (2016) 69–78. https://doi.org/10.1016/j.ijbiomac.2015.11.082.

[10] S. Velasco-lozano, F. López-gallego, J.C. Mateos-díaz, E. Favela-torres, Cross-linked enzyme aggregates (CLEA) in enzyme improvement - a review, Biocatalysis. (2015) 166–177. https://doi.org/10.1515/boca-2015-0012.

[11] H. Vaghari, H.J. Mojgan, Application of magnetic nanoparticles in smart enzyme immobilization, Biotechnol. Lett. 38 (2016) 223–233. https://doi.org/10.1007/s10529-015-1977-z.

[12] S. V Otari, S.K.S. Patel, S. Kim, J.R. Haw, V.C. Kalia, I. Kim, J. Lee, Copper ferrite magnetic nanoparticles for the immobilization of enzyme, Indian J. Microbiol. 59 (2019) 105–108. https://doi.org/10.1007/s12088-018-0768-3.

[13] C.C.S. Fortes, A.L. Daniel-da-silva, A.M.R.B. Xavier, A.P.M. Tavares, Optimization of enzyme immobilization on functionalized magnetic nanoparticles for laccase biocatalytic reactions, Chem. Eng. Process. Process Intensif. 117 (2017) 1–8 https://doi.org/10.1016/j.cep.2017.03.009.

[14] J. Feng, S. Yu, J. Li, T. Mo, P. Li, Enhancement of the catalytic activity and stability of immobilized aminoacylase using modified magnetic Fe3O4 nanoparticles, Chem. Eng. J. 286 (2016) 216–222. https://doi.org/10.1016/j.cej.2015.10.083.

[15] M. Reza, J. Mohammadi, M. Peyda, Covalent immobilization of Candida antarctica lipase on core-shell magnetic nanoparticles for production of biodiesel from waste cooking oil, Renew. Energy. 101 (2017) 593–602. https://doi.org/10.1016/j.renene.2016.09.022.

[16] S.S. Nadar, V.K. Rathod, Magnetic macromolecular cross linked enzyme aggregates (CLEAs) of glucoamylase, Enzyme Microb. Technol. 83 (2016) 78–87. https://doi.org/10.1016/j.enzmictec.2015.10.009.

[17] A. Awad, W. Adel, M. Özacar, Z. Ziyade, Evaluation of different saccharides and chitin as eco-friendly additive to improve the magnetic cross-linked enzyme aggregates (CLEAs) activities, Int. J. Biol. Macromol. 118 (2018) 2040–2050. https://doi.org/10.1016/j.ijbiomac.2018.07.075.

[18] S. Peirce, M. Elena, R. Isticato, R. Fernández, P. Salatino, A. Marzocchella, Structure and activity of magnetic cross-linked enzyme aggregates of bovine carbonic anhydrase as promoters of enzymatic CO2 capture, Biochem. Eng. J. 127 (2017) 188–195. https://doi.org/10.1016/j.bej.2017.08.014.

[19] W. Wu, Z. Wu, T. Yu, C. Jiang, W. Kim, W. Wu, Z. Wu, T. Yu, C. Jiang, Recent progress on magnetic iron oxide nanoparticles: synthesis, surface functional strategies and biomedical applications, Sci. Technol. Adv. Mater. 16 (2015) 23501–23544.

https://doi.org/10.1088/1468-6996/16/2/023501.

[20] I. Armenia, M. Valeria, G. Bonavia, L. De Matteis, P. Ivanchenko, G. Martra, R. Gornati, J.M. De, G. Bernardini, Enzyme activation by alternating magnetic field: importance of the bioconjugation methodology, J. Colloid Interface Sci. 537 (2019) 615–628. https://doi.org/10.1016/j.jcis.2018.11.058.

[21] N.L. Klyachko, M. Sokolsky-papkov, N. Pothayee, M. V Efremova, D.A. Gulin, N. Pothayee, A.A. Kuznetsov, A.G. Majouga, J.S. Riffle, Y.I. Golovin, A. V Kabanov, Changing the enzyme reaction rate in magnetic nanosuspensions by a Non-heating magnetic Field, Angew. Chemie - Int. Ed. 51 (2012) 12016–12019. https://doi.org/10.1002/anie.201205905.

[22] Y. Liu, C. Guo, C.-Z. Liu, Enhancing the resolution of (R,S)-2-octanol catalyzed by magnetic crosslinked lipase aggregates using an alternating magnetic field, Chem. Eng. J. 280 (2015) 36–40. https://doi.org/10.1016/j.cej.2015.05.089.

[23] G. Liu, J. Zhang, J. Bao, Cost evaluation of cellulase enzyme for industrial-scale cellulosic ethanol production based on rigorous Aspen Plus modeling, Bioprocess Biosyst. Eng. 39 (2016) 133–140. https://doi.org/10.1007/s00449-015-1497-1.

[24] N. Srivastava, M. Srivastava, P.K. Mishra, V.K. Gupta, G. Molina, Applications of fungal cellulases in biofuel production: Advances and limitations, Renew. Sustain. Energy Rev. 82 (2018) 2379–2386. https://doi.org/10.1016/j.rser.2017.08.074.

[25] F. Yazdani, M. Seddigh, Magnetite nanoparticles synthesized by co-precipitation method: The effects of various iron anions on speci fi cations, Mater. Chem. Phys. 184 (2016) 318–323. https://doi.org/10.1016/j.matchemphys.2016.09.058.

[26] M.M. Bradford, A rapid and sensitive method for the quantitation microgram quantities of protein utilizing the principle of protein-dye binding, Anal. Biochem. 254 (1976) 248–254.

[27] M. Tanaka, M. Taniguchi, R. Matsuno, T. Kamikubo, Purification and properties of cellulases from Eupenicillium javanicum, J. Ferment. Technol. 59 (1981) 177–183.

[28] A.R. Khataee, M. Fathinia, S. Aber, M. Zarei, Optimization of photocatalytic treatment of dye solution on supported TiO2 nanoparticles by central composite design: intermediates identification, J. Hazard. Mater. 181 (2010) 886–897.

https://doi.org/10.1016/j.jhazmat.2010.05.096.

[29] Z.M. Gao, T.. Wu, S.. Peng, Preparation and structural features of ultrafine spinel magnesium ferrites, ACTA PHYSICO-CHIMICA Sin. 11 (1995) 395–400. https://doi.org/10.3866/PKU.WHXB19950503.

[30] M. Ma, Y. Zhang, W. Yu, H. Shen, H. Zhang, N. Gu, Preparation and characterization of magnetite nanoparticles coated by amino silane, Colloids Surfaces A Physicochem. Eng. Asp. 212 (2003) 219–226. https://doi.org/10.1016/S0927-7757(02)00305-9.

[31] L.D. White, C.P. Tripp, Reaction of (3-Aminopropyl) dimethylethoxysilane with amine catalysts on silica surfaces, J. Colloid Interface Sci. 232 (2000) 400–407. https://doi.org/10.1006/jcis.2000.7224.

[32] J. Sánchez-Ramírez, J.L. Martínez-Hernández, P. Segura-Ceniceros, G. López, H. Saade, M.A. Medina-Morales, R. Ramos-González, C.N. Aguilar, A. Ilyina, Cellulases immobilization on chitosan-coated magnetic nanoparticles: application for Agave Atrovirens lignocellulosic biomass hydrolysis, Bioprocess Biosyst. Eng. 40 (2017) 9–22. https://doi.org/10.1007/s00449-016-1670-1.

[33] R. Saini, J.K. Saini, M. Adsul, A.K. Patel, A. Mathur, D. Tuli, R.R. Singhania, Enhanced cellulase production by Penicillium oxalicum for bio-ethanol application, Bioresour. Technol. 188 (2015) 240–246. https://doi.org/10.1016/j.biortech.2015.01.048.

[34] L. Zang, J. Qiu, X. Wu, W. Zhang, E. Sakai, Y. Wei, Preparation of magnetic chitosan nanoparticles as support for cellulase immobilization, Ind. Eng. Chem. Res. 53 (2014) 3448−3454. https://doi.org/10.1021/ie404072s

[35] J. Han, L. Wang, Y. Wang, J. Dong, X. Tang, L. Ni, L. Wang, Preparation and characterization of $Fe_3O_4$-$NH_2$@4-arm-PEG-$NH_2$, a novel magnetic four-arm polymer-nanoparticle composite for cellulase immobilization, Biochem. Eng. J. 130 (2018) 90–98. https://doi.org/10.1016/j.bej.2017.11.008.

[36] K. Saha, P. Verma, J. Sikder, S. Chakraborty, S. Curcio, Synthesis of chitosan-cellulase nanohybrid and immobilization on alginate beads for hydrolysis of ionic liquid pretreated sugarcane bagasse, Renew. Energy. 133 (2019) 66–76. https://doi.org/10.1016/j.renene.2018.10.014.

[37] J. Zdarta, A. Jedrzak, Ł. Klapiszewski, T. Jesionowski, Immobilization of cellulase on a functional inorganic-organic hybrid support: stability and kinetic study, Catalysts. 7 (2017) 374–390. https://doi.org/10.3390/catal7120374.

[38] M. Rastogi, S. Shrivastava, Recent advances in second generation bioethanol production: an insight to pretreatment , sacchari fi cation and fermentation processes, Renew. Sustain. Energy Rev. 80 (2017) 330–340. https://doi.org/10.1016/j.rser.2017.05.225.

[39] M. Ballesteros, J. Carrasco, C. Martin, M.J. Negro, F. Saez, R. Saez, Selection of thermotolerant yeasts for simultaneous saccharification and fermentation (SSF) of cellulose to ethanol, Applled Biochem. Biotechnol. 28 (1991) 307–315.

[40] W. Kopp, T.P. Da Costa, S.C. Pereira, M. Jafelicci, R.C. Giordano, R.F.C. Marques, F.M. Araújo-Moreira, R.L.C. Giordano, Easily handling penicillin G acylase magnetic cross-linked enzymes aggregates: catalytic and morphological studies, Process Biochem. 49 (2014) 38–46. https://doi.org/10.1016/j.procbio.2013.09.024.

[41] L. Cao, Immobilised enzymes: science or art?, Curr. Opin. Chem. Biol. 9 (2005) 217–226. https://doi.org/10.1016/j.cbpa.2005.02.014.

[42] L. Betancor, A. Hidalgo, G. Ferna, C. Mateo, M. Guisan, Preparation of a stable biocatalyst of bovine liver catalase using immobilization and postimmobilization techniques, Biotechnol Prog. 19 (2003) 763–767.

[43] J. Cleiton, S. Santos, O. Barbosa, C. Ortiz, A. Berenguer-murcia, Importance of the support properties for immobilization or purification of enzymes, ChemCatChem. 7 (2015) 2413–2432. https://doi.org/10.1002/cctc.201500310.

[44] R. Ahmad, M. Sardar, Enzyme immobilization: an overview on nanoparticles as immobilization matrix, Biochem. Anal. Biochem. 4 (2015) 2–8. https://doi.org/10.4172/2161-1009.1000178.

[45] X.J.A. Janssen, A.J. Schellekens, K. Van Ommering, L.J. Van Ijzendoorn, M.W.J. Prins, Controlled torque on superparamagnetic beads for functional biosensors, Biosens. Bioelectron. 24 (2009) 1937–1941. https://doi.org/10.1016/j.bios.2008.09.024.

[46] G. V. Kurlyandskaya, M.L. Sánchez, B. Hernando, V.M. Prida, P. Gorria, M. Tejedor,

Giant-magnetoimpedance-based sensitive element as a model for biosensors, Appl. Phys. Lett. 3053 (2015) 3053–3055. https://doi.org/10.1063/1.1571957.

[47] T. Xia, W. Lin, C. Liu, C. Guo, Improving catalytic activity of laccase immobilized on the branched polymer chains of magnetic nanoparticles under alternating magnetic field, J. Chem. Technol .Biotechnol. (2018) 88–93.

## General conclusions

Considering the current demand for renewable raw materials, lignocellulosic biomass shows as an essential low-cost biomaterial for several areas of financial and environmental interest. Faced it, many approaches have been studied and applied out in a variety of biomass conversion processes.

In summary, this thesis aimed to modify magnetic nanoparticles with cellulase enzymes and applied it in a biomass conversion process. For this purpose, different MCLEAs were synthesized and showed potential for obtention of value-added chemicals from lignocellulosic biomass. Essentiality, their showed potential for cello-oligosaccharides production, an important class of glucose oligosaccharides with prebiotics properties of food and pharmaceutical industry interest. Besides that, cross-linking reaction between cellulases and magnetic nanoparticles leaded to production of MCLEAs with some enhanced properties when compared to free enzymes, among which can be cited thermal stability and recovery and recycle capacity. Thus, such enhancement in catalytic properties suggests a positive effect of the magnetic nanoparticles in the cellulase cross-linked structure.

Further studies have carried to increase the knowledge in regard some physical-chemistry properties of the MCLEAs. Thus, was showed that as increases in colloidal stability can avoid the thermal denaturation of enzymes and that high frequency of alternating magnetic field can decrease its respective catalytic activity. In addition, such studies can be explored to assess physical-chemistry behavior of other systems involving different enzymes and support.

Lastly, it is expected that this work can contribute with current and future advances in the use of magnetic nanoparticles as support for enzyme immobilization. But, not restricted to only it, is expected that can help in changes of paradigms of current industrial manufacture toward more sustainable industrial processes.

## Attachments

### Attached file 1:

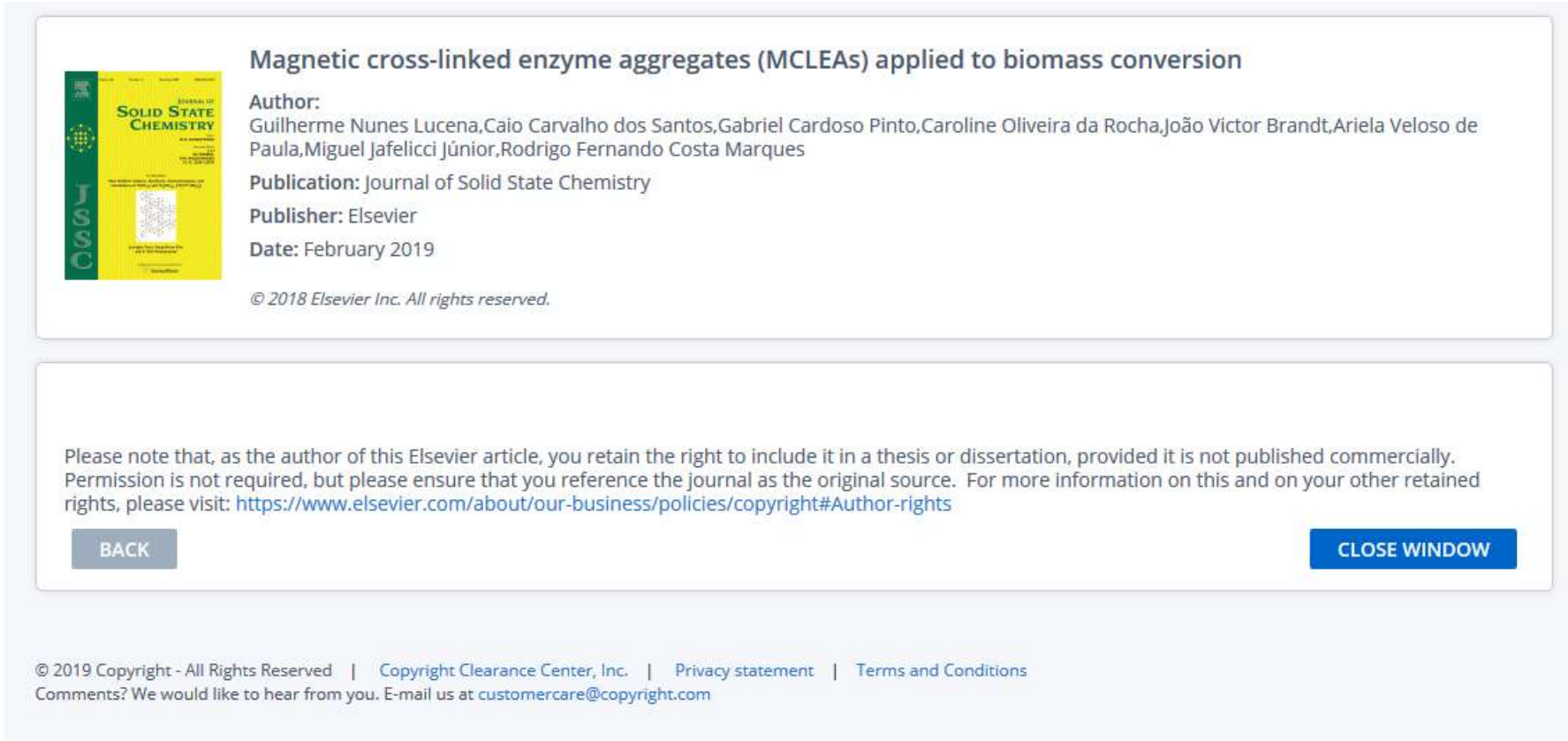

Magnetic cross-linked enzyme aggregates (MCLEAs) applied to biomass conversion

Author:
Guilherme Nunes Lucena,Caio Carvalho dos Santos,Gabriel Cardoso Pinto,Caroline Oliveira da Rocha,João Victor Brandt,Ariela Veloso de Paula,Miguel Jafelicci Júnior,Rodrigo Fernando Costa Marques

**Publication:** Journal of Solid State Chemistry

**Publisher:** Elsevier

**Date:** February 2019